CLINICAL IMPLEMENTATION OF LUNG STEREOTACTIC BODY RADIATION THERAPY (SBRT)

This thesis/dissertation is submitted to the University of Ghana, Legon, in partial fulfilment of the requirement for the award of **MPHIL in MEDICAL PHYSICS Degree**.

BY

ABIGAIL NAA MOMOEDE QUAYE

(10804981)

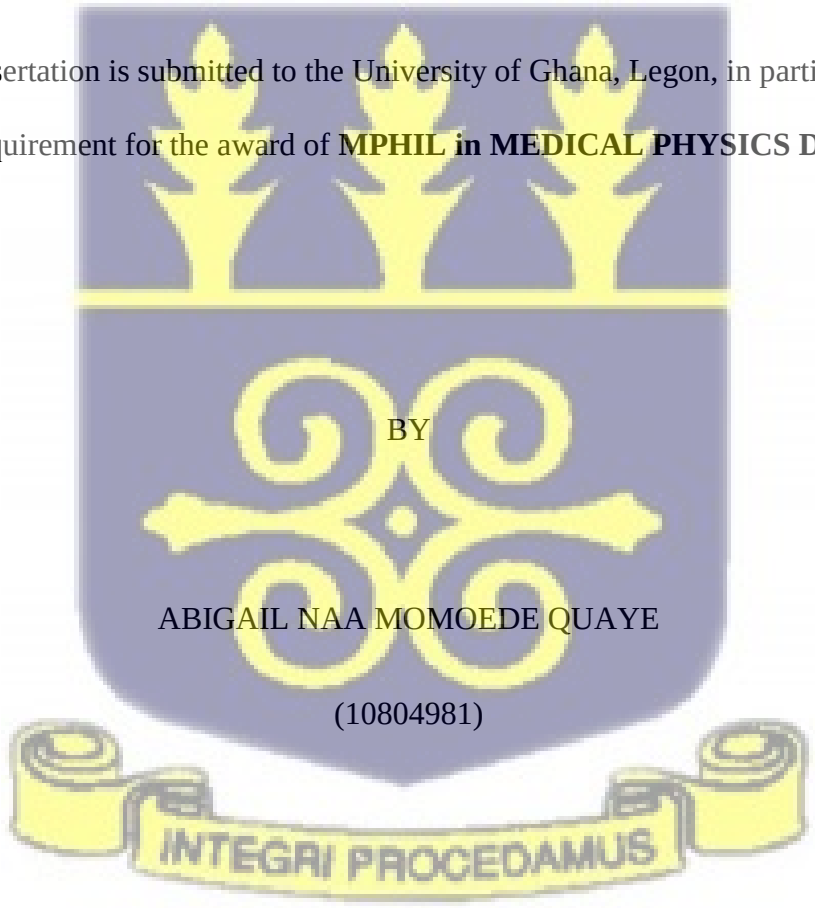

DECEMBER, 2021

DECLARATION

This thesis results from the research work undertaken by Abigail Naa Momoede Quaye in the Department of Medical Physics, University of Ghana, supervised by Mr Eric C. D. K. Addison, Dr Mark Pokoo-Aikins and Prof. Ernest Osei.

To the best of my knowledge, it contains no material previously published by any person or material accepted for the award of any degree of the university, except due acknowledgement has been made in the text.

.....

Abigail Naa Momoede Quaye
(Student)

Date: 15/12//2021

.....

Mr. Eric C. D. K. Addison
(Principal Supervisor)

Date: 15/12/2021

.....

Dr. Mark Pokoo-Aikins
(Co-Supervisor)

Date: 16/12/2021

.....

Prof. Ernest Osei
(Co-Supervisor)

Date: 16/12/2021

DEDICATION

This research work is dedicated to my parents, Mr Napoleon Darko Quaye and Mad. Patience Yaaley Adjei and my sisters, Francisca Korkor Quaye and Roberta Naa Karley Quaye.

ACKNOWLEDGEMENTS

First, uttermost gratitude to Almighty Father for the grace and resources He gave to go through the programme and successfully undertake this research study. Secondly, I sincerely appreciate the supervisors for their immense support and instructions throughout the study to ensure successful work. Again, special thanks to the Komfo Anokye Teaching Hospital for allowing this study to be performed at their institution, specifically the Oncology Directorate. Sincere gratitude to the Medical Physics staff for the access to their systems and equipment, massive support, and guidance in carrying out this study.

Again, special thanks to Samuel Ona-Adu of the Kwame Nkrumah University of Science and Technology for his expertise and assistance in the fabrication of the lung phantom; Mr Saheed Ganiyu for his support in developing the motion platform.

Profound gratitude to my parents and siblings; Mr Napoleon Darko Quaye, Mad. Patience Yaaley Adjei, Francisca Korkor Quaye and Roberta Naa Karley Quaye for their love and support in diverse ways.

Finally, a special thanks to Mrs Valerie Fumey Nassah and her family, the Addison family, Mr Kingsley Akosah, Ms Juliana Adu-Gyamfi, and Ms Wilhemina Aniagyei for their enormous encouragement and support in diverse ways.

TABLE OF CONTENT

LIST OF FIGURES

LIST OF TABLES

ABBREVIATIONS

2DCRT	Two Dimensional Conformal Radiation Therapy
3-D CT	Three-Dimensional Computed Tomography
4-D CT	Four-Dimensional Computed Tomography
AAA	Analytical Anisotropic Algorithm
AAPM	American Association of Physicists in Medicine
ABC	Active Breathing Control
AC	Abdominal Compression
AIDS	Acquired Immune Deficiency Syndrome
AJCC	American Joint Committee on Cancer
AP	Anterior-Posterior
BED	Biological Effective Dose
CBCT	Cone-beam Computed Tomography
CI	Conformality Index
CIRS	Computerized Inspection Reporting System
CO_2	Carbon Dioxide
COPD	Chronic Obstructive Pulmonary Disease
CT	Computed Tomography
CTV	Clinical Target Volume
DIBH	Deep-Inspiration Breathe Hold
D_{max}	Maximum Dose
D_{min}	Minimum Dose
DNA	Deoxyribonucleic Acid
Dp	Prescription Dose
DVH	Dose Volume Histogram
EBUS	Endobronchial Ultrasound
ECBAS	Ethics Committee for Basic and Applied Sciences
EPA	Environmental Protection Agency

EPIDs	Electronic Portal Imaging Devices
GLOBOCAN	Global Cancer Observatory
GI	Gradient Index
GTV	Gross Tumour Volume
HCAs	Heterocyclic amines
HI	Homogeneity Index
HIV	Human Immune Virus
HU	Hounsfield Unit
ICRP	International Commission on Radiological Protection
ICRU	International Commission on Radiation Units and Measurements
IGRT	Image-guided Radiation Therapy
ITV	Internal Target Volume
KATH IRB	Komfo Anokye Teaching Hospital Institutional Review Board
LINAC	Linear Accelerator
MIBH	Mid-inspiration breath-hold
MU	Monitor Unit
MV	Megavolt
NSCLC	Non-Small Cell Lung Cancer
OAR	Organs at Risk
OBI	On-Board Imager
OS	Overall Survival
PMMA	Polymethyl methacrylate
PTV	Planning Target Volume
QA	Quality Assurance
RED	Relative Electron Density
RFA	Radiofrequency Ablation
ROI	Region of Interest
RPM	Real-time Position Management System

RT	Radiation Therapy
RTOG	Radiation Therapy Oncology Group
RTOG	Radiation Therapy Oncology Group
SALT	Saint-Anne, Lariboisiere and Tenon
SBRT	Stereotactic Body Radiation Therapy
SCLC	Small Cell Lung Cancer
SI	Superior Inferior
TMP	Thermoplastic masks
TPS	Treatment Planning System
TV	Target Volume
TVPIV	Target Volume covered by the prescribed dose
UICC	Union for International Cancer Control
VCS	Vacuum cushions
VPIV	Volume covered by the prescribed dose
WHO	World Health Organisation

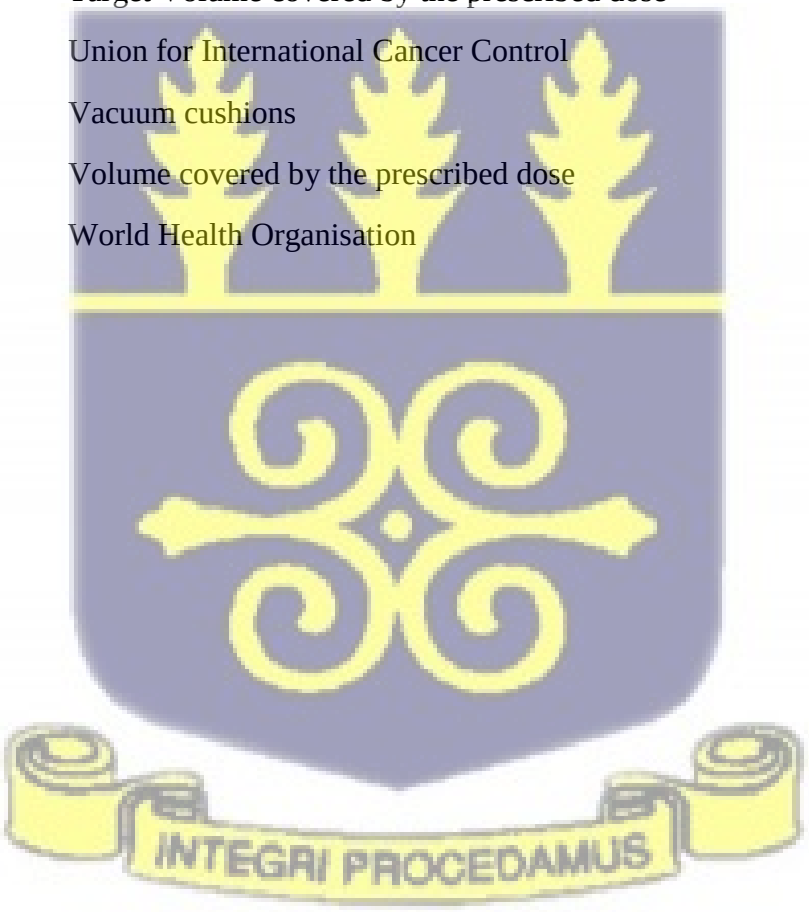

ABSTRACT

The stereotactic Body Radiation Therapy (SBRT) technique was developed to treat lung cancers at the Komfo Anokye Teaching Hospital without a four-dimensional computed tomography (4-D CT) scanner to account for motion in treatment planning and delivery. A tank-type water lung phantom was designed and developed from locally available materials, including wood, perspex and acrylic filled roll-on ball implanted in the wood to simulate the lung field, body, and tumour. A motion platform was developed to mimic breathing. The lung phantom underwent a standard and a slow CT scan to account for motion (0.5 cm and 1 cm). Radiation treatment plans were generated according to the Radiation Therapy Oncology Group (RTOG) 0915 protocol for lung SBRT and delivered with a Varian Clinac iX linear accelerator to the phantom for dosimetric verification with a dose prescription of 50 Gy in five fractions. Clinical tumour sizes of 1 cm and 3 cm were used as case studies to demonstrate the dose to organs at risk (OARs). Average measured doses were compared to treatment planning calculated doses for the phantom with and without motion. Dose deviation for treating static mimicked tumour was 8.43%, -4.31% for phantom in 0.5 cm motion, and -25.96% for phantom in 1 cm motion. Phantom dosimetric analysis for PTV $V_{100\%}$, $V_{99\%}$, $V_{90\%}$ at 50 Gy/5 without motion were 86.77%, 91.19% and 99.96%; with 0.5 cm motion were 98.60%, 99.61% and 100%; and with 1 cm motion were 72.72%, 90.47% and 99.65%, respectively. Clinical analysis for PTV $V_{100\%}$, $V_{99\%}$, $V_{90\%}$ at 48 Gy/5 were 101.10%, 102.62% and 100.49%, respectively. For a tumour size of 3 cm at 50 Gy/5 were 98.10%, 99.68% and 100%, respectively; and for 1 cm tumour size were 97.36%, 99.19% and 100 %, respectively. SBRT treatment planning and delivery were feasible without 4-D CT from phantom studies at the study site. The statistics propose that the target was sufficiently covered with the dose for all

scenarios, thereby achieving the primary radiotherapy goal without excessively dosing OARs to minimise toxicity.

CHAPTER ONE

INTRODUCTION

1.1 BACKGROUND

Abnormal cell growth is an oncogene. Cancer cells proliferate fast as they have no volume constraints, no resources shared by extra cells, and no signals from the body to stop them from reproducing. (Hanahan & Weinberg, 2000; Hanselmann & Welter, 2022). Cancer cells are often structured differently from healthy cells, do not function correctly, and may spread to many places of the body. Tumours, or irregular tissue development, are collections of cells capable of uncontrollably expanding and distributing; their growth is unregulated (Baba & Câtoi, 2007; Hanahan & Weinberg, 2000). Tumours may be noncancerous (benign) or cancerous (malignant). Benign tumours propagate gradually without spread, but malignant tumours mature fast, may infiltrate into neighbouring normal tissues, and spread to other parts of the body (Baba & Câtoi, 2007; Hanahan & Weinberg, 2000; Lambert et al., 2017). Locally invasive cancer occurs when malignant tumours extend into nearby normal tissues, and metastatic cancer occurs when the tumour spreads to distant tissue (Cady, 2007; I. J. Fidler, 1989). The original tumour is the primary tumour, and metastatic tumours are those malignant cells that advance to other parts of the body. Cancerous cells utilise the circulatory (Dong et al., 2013; Plaks et al., 2013) and lymphatic systems (Alitalo & Detmar, 2011; Leong et al., 2011; Padera et al., 2016; H. Zhou et al., 2021) to migrate to other body areas and form secondary tumours (Figure 1.1). The lymphatic system oversees flushing waste, poisons, and other undesired material from cells and tissues so that they may be evacuated out of the body. The lymphatic system comprises lymphatic veins, lymph nodules, lymph liquid, and lymphocytes, all of which work together to protect the body against infection

and illness (Alitalo & Detmar, 2011). Cancer cells may detach from the tumour and enter the lymphatic vessel and subsequently travel from the local site to a distant part of the body (metastasis) (Cady, 2007; Hanahan & Weinberg, 2000; Lambert et al., 2017; Leong et al., 2011; Padera et al., 2016; H. Zhou et al., 2021). In cancer patients, lymph nodes are the primary route for metastasis (Hoshida et al., 2006). Cancer is considered to have metastasised when it has spread from its initial location to other sections of the body. Cancer may spread to practically any body region, while some forms of cancer are more likely than others to migrate to specific sites, such as the bone, liver, and lung.

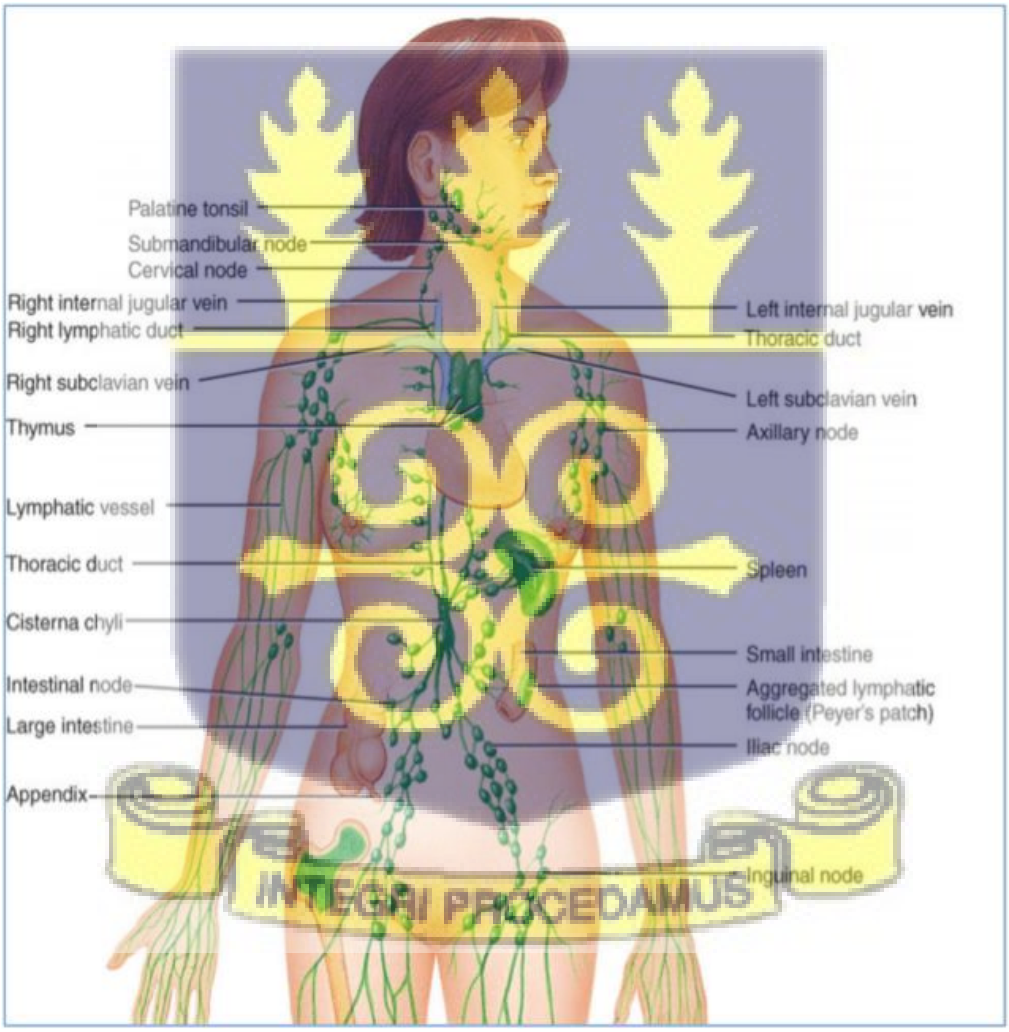

Figure 1.1: Lymphatic system showing the network of lymph nodes (photo credit: Edwards, 2019).

1.1.1 CANCER EPIDEMIOLOGY

Cancer is the world's second-largest cause of death. According to the World Health Organization, approximately 70% of cancer fatalities occur in poor and middle-income nations, where late-stage presentation and diagnosis are frequent and a lack of access to treatment. (GLOBOCAN, 2020b) estimated about 19.3 million new cancer cases worldwide and around 10 million cancer-related deaths in 2020. Breast cancer incidence has exceeded lung cancer incidence worldwide, accounting for 11.7 per cent of all cancer cases, while the latter accounts for 11.4 per cent.

Conversely, lung cancer is the leading cause of mortality, accounting for 18% of all fatalities in 2020 for both sexes and all ages. Cancer incidence and death rates vary across areas and nations (Fidler et al., 2016). Cancer incidence and mortality are rising globally for intricate reasons. However, they may be attributed to ageing, a growing population, late-stage presentation, and inaccessibility to early diagnosis and treatment. Along with an increase in cancer incidence and mortality, one of the causes of the rise in cancer incidence and mortality in economically developing countries is an increase in the adoption of cancer-causing behaviours such as obesity, physical inactivity, reproductive activities, and smoking (Becher & Winkler, 2011).

A cancer diagnosis is usually low in Africa, with most cases presenting in late stages. Developing nations, including Ghana, accounted for 63 per cent of the anticipated 12.7 million new cancer cases globally in 2020. Access to cancer data is restricted due to the absence of accurate cancer registries in most cancer centres in Africa. Cancer data problems in most developing countries have been documented by (Becher & Winkler, 2011; Bray et al., 2018; Laryea et al., 2014). The availability of population-based cancer statistics differs by country. In 2012, Ghana launched the Kumasi Cancer Registry, the country's first population-based cancer registry, to make data on cancer cases registered in Kumasi public. Laryea et al. (2014) examined the 2012 data from the

Kumasi Cancer Registry and determined that women accounted for most cancer diagnoses, accounting for 69.6 per cent of all registered cases. In 2015, the total cancer incidence in Kumasi was 46.1 per 100,000 people. A 54.1 per 100,000 occurrence rate was predicted for women, whereas men had a 37.1 per 100,000 incidence rate (Laryea et al., 2014). Breast and cervical cancers were common among Ghanaian women, with incidence rates of 16.1 and 13.7 per 100,000, respectively. In Ghanaian males, prostate cancer had the highest incidence rate of 10.5 per 100,000 (Amoako et al., 2019). Most malignancies are now preventable via evidence-based preventative techniques and early detection programmes. According to Mensah & Mensah (2020), 30–50% of all cancer cases are avoidable by avoiding identified risk factors. Again, early identification reduces the death rate of the remaining 50% of all cancer patients.

1.1.2 AETIOLOGY FOR CANCERS

Cancer has no one origin, but experts think the interaction of various elements, some of which are environmental, hereditary, or constitutional. Mutations in the cell's deoxyribonucleic acid (DNA) cause cancer. DNA is a genetic substance containing biological instructions for growth, survival, and reproduction that makes every individual unique. DNA informs the cell of its function and how to grow and spread. Various interactions with the DNA can lead to either single or double DNA strand breaks, which could lead to either DNA repair, death or miss-repair, and it is the miss-repair of the DNA that can lead to cancer induction. Mutations may instruct a healthy cell to enable fast growth, fail to halt uncontrolled cell growth, or produce errors while fixing DNA errors, resulting in malignant cells. Childhood malignancies often develop from cell changes or mutations in stem cells (Lupo et al., 2019; Lupo & Spector, 2020). Leukaemia, Hodgkin lymphoma, medulloblastoma, retinoblastoma, and Wilms tumour are only a few examples of pediatric cancers. However, there is a crowning in the incidence of bone and soft-tissue sarcomas in mid-adolescence

and an increased incidence of lymphoma and other solid tumours that continues well into adulthood (Fidler et al., 2018; Lupo & Spector, 2020; Schonfeld et al., 2019). Epithelial cells are the sort of cells that become malignant in adulthood. These cells would have been exposed to various environmental factors throughout time. Most adults who have survived childhood cancers have an increased risk of experiencing late cancer or therapy effects (Fidler et al., 2018; Schonfeld et al., 2019).

Adult malignancies have been associated with risk factors that raise an individual's chances of developing a disease. Risk factors also describe cancer recurrence. Risk variables might not always imply causation. Therefore, some individuals with several risk factors never get cancer, while others with no known risk factors do. Common risk factors for cancer include age, lifestyle (tobacco use, obesity, and alcohol consumption), family history, genetic disorder, environmental exposures, exposure to certain viruses such as the human papillomavirus (HPV), and prior radiation therapy, and exposure to specific chemicals. Some risk factors, such as smoking, being overweight, and drinking alcohol, can be avoided by abandoning the harmful behaviours involved, while others, such as becoming older, cannot be avoided.

1.1.2.1 ENVIRONMENTAL EXPOSURE

The environment in which a person lives may raise his or her chance of acquiring cancer. Carcinogens are any chemical or exposure that can cause cancer development, and such may be present in our surroundings, including our homes, workplaces, and outdoor spaces. Cancer incidence also increases by exposure to substances such as asbestos and high levels of benzene (Hang et al., 2020; Jemal et al., 2010; UNSCEAR, 2006).

1.1.2.2 RADIATION EXPOSURE

Radon gas is a carcinogen which may be found in the air or accumulates in rooms from the earth (Conrath, 2012; Hunter et al., 2015). Radiation exposure for therapeutic or diagnostic reasons increases one's risk of developing cancer (Ali et al., 2020; Andersson et al., 2017; DeLaney et al., 2020; Dracham et al., 2018; Journy et al., 2017; Linet et al., 2012). Other radiation exposures that are cancer risk factors include radioactive fallout from nuclear weapons testing, Chornobyl and Fukushima accidents that are risk factors (Cardis et al., 2006; Land et al., 2010; Walsh et al., 2014).

1.1.2.3 INFECTIONS

Among cancer risk factors is infections, though its association is controversial. Infections boost cancer risk in a variety of ways. Some viral infections cause malignant alterations in the DNA directly. Hepatitis B (HBV) and C viruses (HCV), Epstein-Barr virus (EBV), human papillomavirus (HPV), human immunodeficiency virus type 1 (HIV-1), Helicobacter pylori (H. pylori), and Streptococcus bovis (S. bovis) are involved in the development of around 5% of all malignancies. (De Flora & La Maestra, 2015; Ohshima & Bartsch, 1994). Other infections may cause lasting irritation, increasing one's risk. Other diseases, such as HIV, impair the immune system, making it incapable of protecting against cancer progression (Kirk et al., 2007; Sigel et al., 2012). The human papillomavirus (HPV) raises the chances of cervical, anal, vulvar, or vaginal cancer development. According to research, HPV may play a role in various head and neck malignancies (Barta et al., 2019; M. Fidler et al., 2016; Jonathan M. Samet et al., 2009).

1.1.2.4 AGE

Cancer may strike at any age, and the typical age for a cancer diagnosis, depending on the kind, is between 65 and 74 years (NCI, 2021). After being exposed to carcinogens and inflammatory processes, the human body becomes less effective in detecting and destroying malignant and precancerous cells. Cancer is considered an age-related disease because most cancers increase with age, and some investigations showed that age is related to cancer (SMETANA et al., 2016; White et al., 2014). Nevertheless, old age does not necessarily lead to cancer.

1.1.2.5 LIFESTYLE

Individual lifestyle and personal choices contribute to many cancer developing risk factors (Ferlay et al., 2015; Khan et al., 2010). That is to say; people have control over their exposure to such risk factors as smoking, alcoholism, obesity and diet (Freisling et al., 2020; Katzke et al., 2015; McKenzie et al., 2016). Smoking harms the lungs and raises the risk of numerous cancers (Hecht, 1999, 2012; L. Jacob et al., 2018; Kispert & McHowat, 2017; McKenzie et al., 2016; O'Keeffe et al., 2018). Quitting smoking lowers the risk of cancer development (Dryden, 2016; Rogotti, 2022; US Department of Health and Human Services, 2020). Alcohol is an irritation that may harm cells and encourage the formation of carcinogenic substances in the colon. Limiting the quantity of alcohol consumed daily lowers cancer risk (Deng et al., 2021). Obesity is one of the primary causes of cancer and increases the risk of breast cancer, colorectal cancer, endometrial cancer, oesophageal cancer, pancreatic cancer, and kidney cancer. Excess fat cells create more oestrogen and insulin, which encourage cancer development. Maintaining or achieving a healthy body weight may lower cancer risks. Several foods and nutrients may be associated with cancer risk factors (Agudo et al., 2018; Bertuccio et al., 2019). However, refrigerator usage was associated with a reduced risk of gastric cancer (Yan et al., 2018). Unsafe sex practices may increase the chance of HPV, HIV, and hepatitis B and increase cancer risk.

1.1.2.6 GENETICS

Certain gene types have contributed to cancer, and these genetic changes are present in most malignancies (Knudson, 2002; Mendiratta et al., 2021; Van Cott, 2020). Oncogenes, tumour suppressor genes, and mismatch-repair genes are three categories of genes that may regulate cell proliferation and change (mutated) in some malignancies (Tomasetti et al., 2015; Yarbro, 1992; Zingde, 1993). Some genetic changes are inherited, while others occur sporadically acquired (Kuchenbaecker et al., 2017; Priedigkeit et al., 2021). Sporadic cancers are those that occur sporadically due to environmental exposures. Hereditary breast and ovarian cancer (HBOC) is an example of cancer caused by an inherited mutation in either the BRCA1 or BRCA2 gene (Feuvret et al., 2006a; Kuchenbaecker et al., 2017; Pallonen et al., 2022).

1.1.3 SIGNS AND SYMPTOMS OF CANCER

Cancer can manifest itself in various ways, each symptom cancer-specific and dependent on the affected body part (Holtedahl et al., 2021). Benign tumours or other disorders cause the majority of such symptoms. Early cancer and some types of cancer may not exhibit any symptoms. On the other hand, some symptoms may result from cancer or a less severe condition. Cancer patients experience a variety of symptoms, including pain, dyspnea, fatigue, depression, cough, cognitive impairment, neurological problems, abnormal lumps, weight loss, bleeding, and changes in the skin, breast, bladder, and bowel (Holtedahl et al., 2018, 2021; Laird et al., 2011). These symptoms negatively impact patients' daily functioning and quality of life (Dodd et al., 2001; S. Y. Wang et al., 2008). A persistent symptom or screening test result indicating the presence of cancer necessitates additional research to confirm that the ailment is cancer-related. If a condition persists for more than a few weeks, it is critical to consult a doctor.

1.1.4 DIAGNOSIS OF CANCER

Despite the vital role of prevention in reducing the enormous burden of cancer on the world's population, screening and early diagnosis are integral in setting up timely therapeutic management to save many lives. A comprehensive assessment of a person's history, physical examination, and diagnostic tests is required to diagnose cancer correctly. Effective diagnostic testing confirms or rules out the presence of sickness, monitors the disease process and is sometimes a basis to prepare for and assess treatment success. The doctor may obtain a patient's personal and family medical history to begin the diagnosing procedure. A cancer diagnosis may entail imaging, laboratory tests, tumour biopsy, endoscopic examination, surgery, or genetic testing. These investigations are required based on the severity of the symptoms.

Because cancer symptoms include high or low quantities of chemicals in the body, laboratory testing for these compounds may assist physicians in making a diagnosis. These compounds are measured in laboratory tests of blood, urine, tissue samples, or other bodily fluids for tumour markers or other body fluids. However, abnormal laboratory findings are not a reliable indicator of cancer. Most tumour markers are generated by both normal and cancer cells, but cancer cells produce them in considerably more significant quantities (M. J. Duffy et al., 2007; Michael J. Duffy, 2013; Kabel, 2017).

Imaging techniques represent internal body components that help clinicians determine if a tumour is present. In recent years, diagnostic radiography has evolved significantly, owing to the introduction of new strategies and techniques that may identify cancer earlier and help patients avoid surgery (Beyer et al., 2020; Kourou et al., 2015; Lloyd & McHugh, 2010; Martinelli et al., 2019; Pucci et al., 2019). X-rays, ultrasound scans, computed tomography (CT) scans, magnetic resonance imaging (MRI), positron emission tomography (PET) scans, and nuclear medicine scans

are the imaging modalities used for diagnosis, staging and monitoring of cancer (Auweter et al., 2014; Bandyopadhyay et al., 2019; Burglin et al., 2017; Campos & Diaz, 2018; Capalbo et al., 2015; Eary, 1999; Frega et al., 2020; Guo et al., 2018; Hernando et al., 2010; Hochhegger et al., 2015; Husband, 1985; Kapoor & Kasi, 2021; Khiewvan et al., 2016, 2017; Kiratli et al., 2016; Luining et al., 2022; McCarten et al., 2019; Mendhiratta et al., 2016; Otoni et al., 2017; Paydary et al., 2019; Prado et al., 2009; Rao & Grigsby, 2018; Rix et al., 2018; Salmanoglu, 2021; Serrano et al., 2010; Sureshkumar et al., 2020; Tedesco et al., 2019; Wu et al., 2021; Zaucha et al., 2019; Y. Zhang & Yu, 2020).

X-rays use low doses of radiation to photograph the intended body part. Ultrasound examination produces a sonogram (picture) of the bodily part by using high-intensity soundwaves (not in the hearing range). A CT scan generates a sequence of pictures that provide a three-dimensional (3-D) representation of the area of interest exposed to X-rays from various angles. Before scanning, patients may be given a contrast substance to emphasise certain body regions in the picture. An MRI employs a strong magnet and radio waves to generate comprehensive images of the body's interior, which may highlight the difference between healthy and sick tissue. A contrast agent is sometimes used during an MRI scan to make tumours seem brighter in the pictures. A nuclear medicine scan uses radioactive material to create images of the body's interior. Before the scan, a small amount of radioactive material is injected into the bloodstream, accumulating in bones and other organs. A scanner creates images of bone or other organs using radioactivity detected and quantified in the body. The radioactive material in the body degrades over time and may pass through urine or stools. This type of nuclear medicine scan examines the bones for damage or abnormalities. It may be used to detect metastatic bone tumours. The intravenous injection of

radioactive material causes hot spots in the bone. The PET scan is another nuclear medicine scan that produces complete 3-D pictures of inside body areas where glucose is taken up.

PET scanning is an imaging modality used primarily in oncology. It uses radiotracers to assess the body's metabolic processes. Commonly used tracers include 18F fluoro-deoxyglucose (FDG), or [18F] FDG PET. The cells use 18F-FDG instead of glucose for metabolism. Oncogenic sites have high metabolic activity and thus high glucose uptake. These areas are very well taken up by 18F-FDG, which is a bright spot on the PET scan (Kapoor & Kasi, 2021). This aids in metastasis detection. If any of these tests reveal that a person has cancer, another testing may be necessary to help the doctor plan therapy. This test is done to define the cancer stage since understanding the grade of the tumour is critical for deciding on the appropriate therapy.

1.1.5 CANCER STAGING

Staging determines the location, growth rate, and spread of cancer to other organs. Cancer staging helps determine prognosis and treatment options. Physical exams, blood tests, and imaging tests like MRI, CT, and ultrasound are used to stage patients. Biopsies are sometimes conducted to analyze microscopic tissue samples from the suspected tumour site. If surgery is performed, pathologists can determine the operative stage by examining the excised tissue. Different malignancies, including the brain, spinal cord, and blood cancers, have distinct staging procedures. Most staging systems, such as the Tumour Node Metastasis staging system, consider the tumour's location, cell type, size, lymph node metastasis, and grade. (Brierley et al., 2017).

Following testing, practitioners use TNM staging to determine a patient's stage and treatment options. After that, the TNM method is used to classify cancer into stages (0-IV), with 0 being the least advanced. The TNM technique is used to stage most cancers and considers tumour size, number, vascular invasion, lymph node involvement, and metastasis. The primary tumour is

denoted by the letter 'T'. This grouping can be a letter or a number in Table 1.1 (Brierley et al., 2017; UICC, 2016).

Table 1.1: Primary Tumour classification.

Classification	Description
TX	Primary tumours cannot be measured
T0	No indication of the primary tumour
Tis	Cancer cells only grow in a layer of cells without advancing into deeper layers. This may be termed *in situ* or pre-cancer.
T1, T2, T3 or T4	Describes the tumour's size and/or spread to nearby organs. The T number indicates the tumour's size and/or metastasis into neighbouring tissues.

'N' is the lymph node involvement based on number and location. Classifications in N can be assigned to a letter or number Table 1.2. (Brierley et al., 2017; UICC, 2016)

Table 1.2: Regional Lymph nodes classification.

Classification	Description
NX	No information about nearby lymph nodes
N0	Neighbouring lymph nodes do not have cancer
N (N1, N2, or N3)	The size, location, and/or the number of neighbouring lymph nodes affected by cancer. The higher the N number, the more significant cancer spreads to nearby lymph nodes.

'M' stands for any spread to other organs from the primary tumour and is termed metastasis. Description of distant metastasis grouping in Table 1.3 (Brierley et al., 2017; UICC, 2016).

Table 1.3: Distant Metastasis

Classification	Description
M0	No distant spread found
M1	The cancer advance to distant organs

Each form of cancer has its TNM classification, with distinct descriptions of letters or numbers allocated to TNM groups.

The grade of a tumour is often considered in staging. The grade influences the growth and spread of cancer. Well-differentiated cancer cells appear normal and grow slowly, while poorly differentiated cells appear abnormal and develop rapidly. However, grading impacts cancer therapy (Rakha et al., 2010; van Dooijeweert et al., 2021).

Cell type (such as oesophageal cancer), tumour location, tumour marker levels in the blood (such as prostate cancer), test results on cancer cells (such as breast cancer), and patient age (for example, thyroid cancer) are additional variables that affect cancer staging (American Cancer Society, 2020; Buranaruangrote et al., 2014; Canadian Cancer Society, 2021; National Cancer Institute, 2015).

1.1.6 TREATMENT OVERVIEW AND MODALITIES

Cancer therapy is situation-dependent and may be administered alone or with other therapeutic modalities. The most often used cancer treatment treatments include radiotherapy, chemotherapy, and surgery, all of which aim to cure, reduce, or prevent cancer progression. Primary, adjuvant, and palliative care are possible treatment alternatives. The primary goal of treatment is the cure; adjuvant therapy is used to remove remaining cancer cells following primary treatment to prevent a recurrence, and palliative therapy is used to reduce treatment-related side effects or disease-related signs and symptoms. There are many ways to treat cancer, such as surgery, chemotherapy,

radiotherapy, hormone therapy, and immunotherapy. The best one is chosen based on the type and stage of cancer, the patient's overall health, and preferences. After the patient and doctor weigh the pros and cons of each option, a treatment modality is chosen (Abbas & Rehman, 2018; Diwanji et al., 2017; Ezer et al., 2015; Kumar et al., 2017; Z. Wang et al., 2018; S. Yang et al., 2019; Zappa & Mousa, 2016).

Childhood cancer is distinct from adult cancers in diagnosis, treatment, and prognosis, especially survival rate and illness origin. Children have a five-year survival rate of more than 80%, while adults have a rate of 68%. The disparity could be explained by the increased sensitivity of paediatric cancer to treatment and children's tolerance for more aggressive therapy

(Akinkuotu et al., 2021; Jensen et al., 2021; Siegel et al., 2021; Ward et al., 2014).

1.1.6.1 SURGERY

Surgery assists in treating cancer by physically removing the tumour from the body. Subject to the tumour site and other considerations, this treatment is performed openly or via minimally invasive incisions. Surgery may be curative (removal of all cancer), debulking (removal of a portion of the tumour when removal of the entire tumour would cause harm to adjacent organs), or palliative (done to alleviate pain and impairment) (Abbas & Rehman, 2018). When medication fails to manage pain, palliative surgery may be utilised. Reconstructive surgery is used to enhance a patient's outlook after surgery.

In contrast, preventive surgery involves the removal of tissues that are likely to become malignant even if no evidence of cancer is present. Surgery is a mechanical method of temporarily removing a large tumour resistant to chemotherapy and radiation treatment. Nonetheless, several aspects of surgery are challenging and ineffective for subclinical metastases. Surgery has certain limitations, including the inability to eradicate cancer cells.

1.1.6.2 CHEMOTHERAPY

Chemotherapy is a cancer treatment that uses chemicals to destroy rapidly developing cancer cells. Chemotherapy may help slow cancer progression, halt its spread, or prevent recurrence. Chemotherapy may be used alone or in conjunction with other therapeutic options (Curran et al., 2011; MacHtay et al., 2012; Seike et al., 2021; van Dooijeweert et al., 2021). Hair loss, weariness, mouth sores, and stomach issues may occur due to the treatment and must be controlled (Abbas & Rehman, 2018). Chemotherapy is the delivery of anticancer medications that rapidly travel throughout the body, destroying cancer cells on the spot. It inhibits primary tumour development and dissemination and metastasis, and subclinical metastases. Chemotherapy destroys not just malignant cells but also normal cells, shortening patients' lives over time.

1.1.6.3 RADIOTHERAPY

Radiotherapy uses high-energy radiation such as photons or X-rays to destroy cancer cells. Radiotherapy damages DNA and other essential biological molecules directly and indirectly through the creation of free radicals. Radiotherapy may be delivered based on the type of cancer, the size, and location of the tumour, its proximity to healthy and radiosensitive tissues, the overall health of the patient, the patient's age, and past cancer treatments. Radiotherapy is either curative or palliative. Radiotherapy is a painless procedure that does not require anaesthesia. Radiotherapy is effective and is used to treat many cancers; however, it has risks and side effects. Radiation therapy can affect nearby tissues depending on their proximity to the tumour. Radiotherapy can cause diarrhoea, tiredness, nausea, and anorexia, although such effects are transitory (Dilalla et al., 2020). Long-term treatments have more negative effects than short-term ones (Brook, 2020; Majeed & Gupta, 2021). Radiation has long-term side effects like shortness of breath and narrowing the gullet. Lung diseases like radiation pneumonitis can be caused by radiation.

Radiation pneumonitis occurs in 5–15% of lung cancer patients getting radiotherapy(Arroyo-Hernández et al., 2021; Hanania et al., 2019; Rahi et al., 2021).

Before treating a patient in Radiation Oncology, a CT simulation of the treatment site is conducted. Computed tomography creates images of the patient to target radiation therapy precisely. It also helps avoid overdosing normal tissues around the tumour, lowering unwanted effects. The photographs are placed into a treatment planning system. The radiation therapy delivery technique, beam energy, number of treatment fields, and treatment angles are chosen at this step. Medical physicists ensure treatment plans meet radiation oncologists' specifications. The presence of normal tissue in the beam path during therapy determines radiation side effects. After examining the treatment plans, the radiotherapist delivers them to the patient. X-rays are frequently taken before therapy to ensure appropriate posture. External beam radiotherapy (EBRT) and interstitial radiotherapy (brachytherapy) are two types of radiation therapy that can be used to treat cancer. Brachytherapy is a type of radiotherapy used to treat small oral and oropharyngeal tumours. External beam radiation is the most common type of radiotherapy, targeting the tumour and surrounding tissues with X-rays or electrons. The treatment course is usually once or twice a day for 4 – 7 weeks.

Radiation therapy has evolved to better treat cancer by targeting the tumour while sparing normal tissues. External beam radiotherapy can use a range of methods and radiation types. Stereotactic radiosurgery (SRS), stereotactic radiation therapy (SRT), stereotactic body radiation therapy (SBRT), and proton therapy are examples of EBRT.

One of the problems with radiotherapy for small tumours that move a lot when people breathe is that there is much uncertainty related to substantial tumour motion (Atkins et al., 2015; Langen & Jones, 2001; Liu et al., 2007; Mageras et al., 2004; Shirato et al., 2004; Torshabi & Dastyar, 2017;

S. Yoganathan et al., 2017; Yu et al., 2012). Several studies applied diverse motion management techniques such as abdominal compression, active breathing control and respiratory gating adept at limiting or decreasing target motion or tracing the target motion during treatment (Giraud & Houle, 2013; Keall, Mageras, et al., 2006; Langen & Jones, 2001; Van Gelder et al., 2018; S. Yoganathan et al., 2017). Due to target coverage ambiguity, the impact of respiratory motion on lung tumour treatment has been questioned. Mageras et al. (2004) used four-dimensional CT (4DCT) to quantify lung tumour motion and found that in seven of twelve patients, tumour motion exceeded 1 cm. According to Yu et al. (2012), early-stage non-small cell lung cancer patients showed more than 50% greater tumour mobility than locally advanced patients. They found a relationship between diaphragm motion and tumour movement.

1.2 PROBLEM STATEMENT

Radiation therapy for lung cancers is administered using several modalities such as 3DCRT, IMRT, VMAT, and, more recently, SBRT (Abbas & Rehman, 2018; Lemjabbar-Alaoui et al., 2015). SBRT is an advanced unique technique that accurately administers highly focused escalated radiation doses (five fractions or less) to treat malignant target volumes. SBRT has been employed to treat some cancers, including lung, spine, liver, pancreas, kidney and adrenals (Atkins et al., 2015; Benedict et al., 2010; Diwanji et al., 2017; Kumar et al., 2017; Stumpf et al., 2016). SBRT has been delivered using either 3DCRT, VMAT or IMRT. One of the challenges associated with the radiotherapy of minor tumour sizes sited inside organs in motion due to respiration (i.e. lung) is the significant target coverage uncertainty related to substantial tumour motion (Atkins et al., 2015; Langen & Jones, 2001; Liu et al., 2007; Mageras et al., 2004; Shirato et al., 2004; Torshabi & Dastyar, 2017; S. Yoganathan et al., 2017; Yu et al., 2012). Several studies applied diverse motion management techniques such as abdominal compression, active breathing control and

respiratory gating adept at limiting or decreasing target motion or tracing the target motion during treatment (Giraud & Houle, 2013; Keall, Mageras, et al., 2006; Langen & Jones, 2001; Van Gelder et al., 2018; S. Yoganathan et al., 2017).

The Oncology Directorate of the Komfo Anokye Teaching Hospital (KATH) currently treats lung malignancies as static tumours without motion management strategies. Thus, comparatively more significant margins are used to account for tumour motion during treatment planning, resulting in the irradiation of relatively larger healthy tissue sizes around the tumour and leading to relatively high toxicity in the lungs and radiation injuries such as radiation pneumonitis. Consequently, this study aims to develop an approach for lung cancer radiotherapy at KATH that considers tumour motion. This technique can significantly conform the dose to the target volume for tumour management. It could result in improved biochemical degeneration-free survival, cancer progression-free survival, and cancer-specific survival. Consequently, it will significantly affect the care offered to lung cancer patients at KATH. In addition, irradiating less healthy lung tissue will reduce treatment toxicities and potentially improve patients' quality of life.

1.3 OBJECTIVES

The main objective is to develop a treatment technique for lung cancers using the Stereotactic Body Radiation Therapy method at the Oncology Directorate of the Komfo Anokye Teaching Hospital (KATH) that considers the target motion and minimises treatment toxicity. The specific objectives include:

1. To design and develop lung phantom for SBRT dosimetric verification
2. To develop SBRT treatment planning and treatment delivery protocols.
3. To maximise target coverage while minimising dose to normal tissue.

1.4 RELEVANCE AND JUSTIFICATION

The influence of respiratory motion on treating thoracic tumours has been challenged with target coverage uncertainty connected with significant tumour motion. Mageras et al. (2004) used four-dimensional CT (4DCT) to look at lung tumour movement. In seven out of twelve patients, they found that tumour movement could be more than 1 cm, especially in the craniocaudal direction. (Yu et al., 2012) investigated lung tumour motion characteristics in non-small cell lung cancer patients and reported that early-stage lung cancer patients had more than 50% higher tumour motion than the locally progressed patients cohort. They also observed a link between tumour movements and location, volume, and diaphragm motion.

The success of radiotherapy is dependent on the total radiation dosage to the target, but the dose prescribed for lung cancer treatment is limited by the radiation tolerances of surrounding normal tissues and organs. In recent years, various treatment methods have been developed to help escalate the dose to targets leading to tumour control while at the same time reducing the dose to normal tissue surrounding the target leading to fewer toxicities. In the absence of motion management techniques for lung cancer radiotherapy, there is the potential for geometrical misses due to respiratory-induced tumour movements and anatomical changes during radiation administration, potentially leading to local control failures. Further, relatively large volumes of normal lung tissue are usually included in the treatment field to ensure adequate target coverage, leading to high incidence and severity of normal tissue damage and potentially life-threatening to patients.

Consequently, this study aims to develop an approach for lung cancer radiotherapy at KATH that takes into consideration the tumour motion. This approach has the potential to extremely conforming doses close to the target volume related to tumour control, leading to enhanced biochemical degeneration-free survival, cancer progression-free survival, and cancer-precise

survival. Thus it will have a very high impact on the care provided to lung cancer patients at KATH. Furthermore, irradiating less healthy lung tissue will lessen treatment toxicities and potentially increase patients' quality of life.

SBRT also allows for shorter treatment times, greater comfort, and convenience. SBRT is especially beneficial to Ghana, as most patients now commute from remote areas to Accra or Kumasi, the country's only metropolis with radiation facilities. Komfo Anokye Teaching Hospital (KATH) welcomes patients from 12 of Ghana's 16 regions and Burkina Faso and Ivory Coast. Most patients, particularly those coming from remote locations outside the region for radiation therapy, must find lodging in Kumasi for many weeks. These fees are in addition to therapy, which most patients cannot afford. Finally, some patients stop therapy to go back to work to pay the remaining bills. Radiotherapy gaps affect treatment outcomes, although only marginally. As a result, the use of SBRT at KATH and throughout Ghana would reduce patient and staff costs without compromising treatment outcomes.

This technology could be expanded to additional cancer sites to improve the therapeutic ratio for patient benefit.

1.5 SCOPE OF THE STUDY

The scope of the study is limited to the lung phantom studies and a clinical case study of a patient CT data set at the Oncology Directorate, Komfo Anokye Teaching Hospital (KATH).

1.6 ORGANIZATION OF THESIS

The first chapter of this thesis introduces cancer, the research issue, and the problem studied.

Chapter 2 discusses lung cancer. The chapter first explains the forms of lung cancer, symptoms, diagnosis, risk factors, and treatment techniques. Further, stereotactic body radiation treatment (SBRT) is discussed in the chapter. This chapter's final portion discusses radiation.

Chapter 3 discusses the study's methodologies and equipment. A lung phantom and motion platform were fabricated to test SBRT treatment plans. A motionless phantom received several treatment plans. An experimental investigation was done to compare the planned and delivered doses.

Chapter 4 discusses the findings from the study.

Chapter 5 summarises the findings and addresses recommendations and future research objectives. Finally, the appendices provide the study's ethical clearances.

CHAPTER TWO

LITERATURE REVIEW

2.1 LUNG – ANATOMY AND FUNCTION

Every cell in the body requires oxygen to survive and expel carbon dioxide produced by cell processes. The lungs are thoracic organs that allow people to breathe by inhaling oxygen and exhaling carbon dioxide. This gas exchange occurs in alveoli within the lungs. Besides this fundamental role, the lungs also regulate the blood pH by increasing or decreasing CO2 levels.

The lungs filter microscopic gas bubbles from the blood and convert angiotensin I to angiotensin II, which helps regulate blood pressure. The right and left lungs each have three lobes. The trachea, the tube that transports air into and out of the lungs, ends here. The bronchus connects the lungs to the trachea. The bronchi divide into bronchioles, which are even smaller tubes. Every lung has 30,000 bronchioles, some as thin as hair. Each bronchiole tube ends in a cluster of alveoli, which resemble small grape clusters. The lungs contain around 600 million typical alveoli, each with a surface area comparable to a tennis court. The interstitium is a thin layer of cells that supports the alveoli and contains blood vessels. The pleura surrounds the lungs. Each breath lubricates the lungs, allowing them to expand and contract freely. The lungs are shown in Figure 2.1. Any organ in the body might be harmed by diseases that produce abnormal lung function.

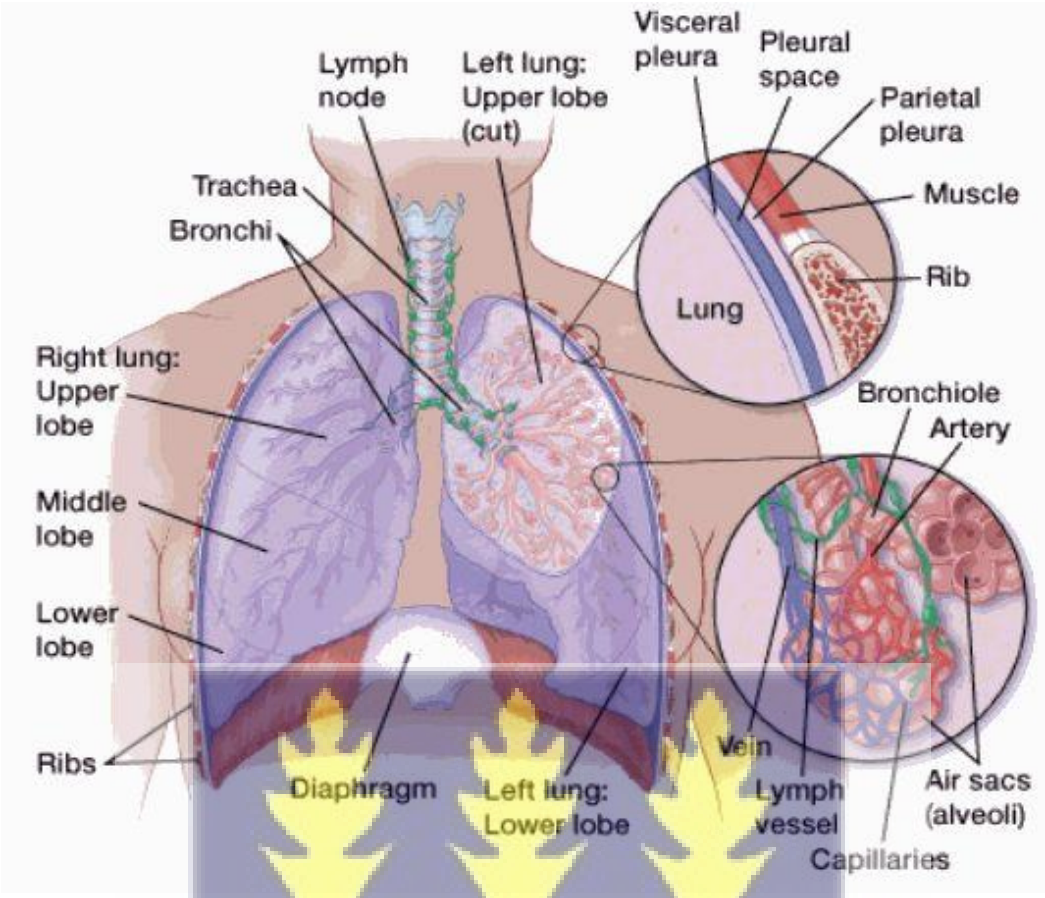

Figure 2.1: Structure of the Lung (American Cancer Society, 2019).

2.2 LUNG CANCER

Lung cancer is a lung disease in which normal lung cells transform into harmful abnormal cells known as cancer cells. Lung cancer begins in the lungs, most commonly in the cells that line the bronchi and other lung structures such as the bronchioles or alveoli. Cancer cells multiply to form clusters known as tumours, which grow and destroy lung tissue. Figure 2.2 depicts a cancerous mass in the lung.

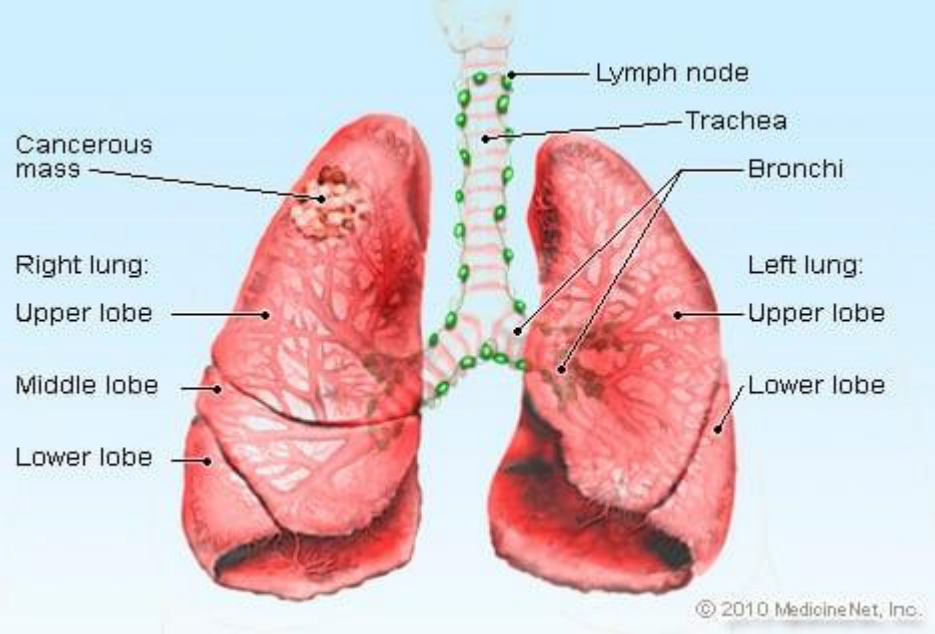

Figure 2.2: Lung with cancerous mass (MedicineNet, 2010).

Lung cancer may progress to other body areas through the blood or lymph fluid (a natural liquid that aids in the collection of undesired waste material from the body), resulting in a condition known as lung cancer metastasis. Lung cancer metastases can progress to lymph nodes near the lungs and other organs via the bloodstream via the bloodstream, such as bones, the adrenal glands, and the brain (Figure 2.3). Cancer can begin in other organs before spreading to the lungs and is referred to as metastasis of the initial form of cancer, not lung cancer. Lung cancer is the only cancer that starts in the lungs (NCCN, 2021).

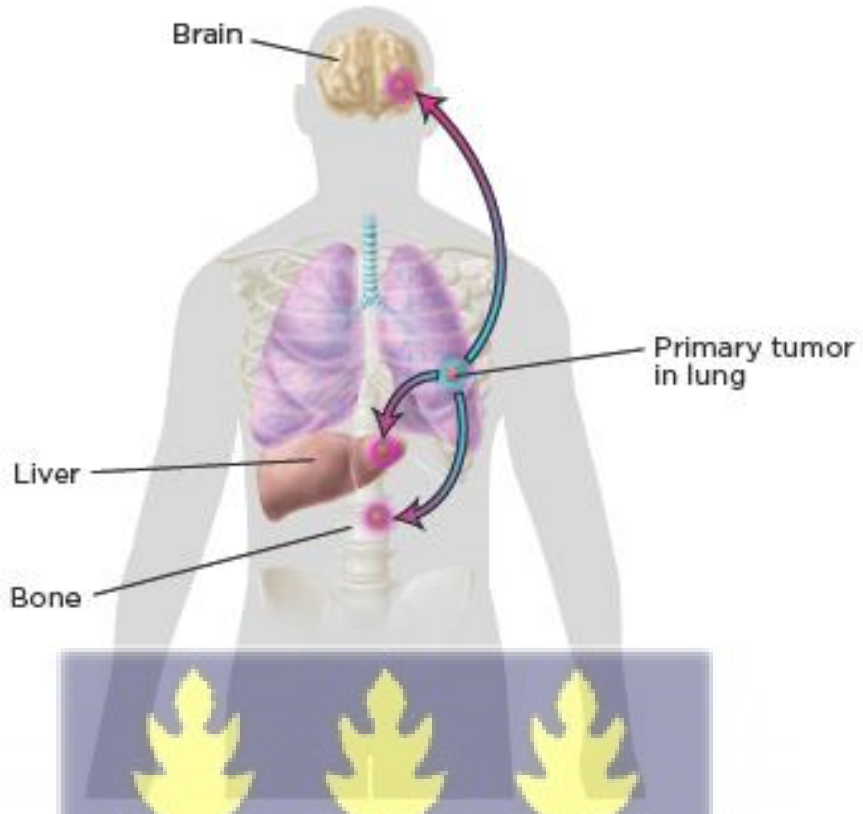

Figure 2.3: Lung cancer metastasis to other organs in the body (LUNGEVITY, 2021).

2.3 LUNG CANCER EPIDEMIOLOGY

Lung cancer is the most typical disease in males and the third commonest cancer in women, with 2 million new cases documented in 2020 (GLOBOCAN, 2020b). Lung cancer is the leading cause of cancer mortality in both genders (Barta et al., 2019; Bray et al., 2018; GLOBOCAN, 2020c; Malhotra et al., 2016). According to WHO (2020), lung cancer is one of the most typical cancers, accounting for 2.26 million cases, and it is the leading cause of cancer death, accounting for 1.8 million deaths in 2020. According to GLOBOCAN (2020c), lung cancer is placed eighth, with 478 deaths out of 535 new cases, or almost 50% of new cases.

Globally, lung cancer is most frequent in older people. People mostly diagnosed with lung cancer are 65 years or older, with only a small number of people diagnosed younger than 45 years. (NCI,

2021). The typical age at diagnosis is approximately 70 years. Overall, the lifetime chance of lung cancer is approximately 1 in 15 for men and 1 in 17 for women. These numbers include both smokers and nonsmokers. The risk is significantly higher for smokers and much lower for nonsmokers (Barta et al., 2019; Malhotra et al., 2016).

Increased understanding of the dangers of smoking and other risk factors has led to significant declines in lung cancer mortality rates in high-income countries (Gaafar & Aly Eldin, 2005). In contrast, incidence and mortality rates for lung cancer have increased in some low- and middle-income nations (Huerta & Grey, 2007). In industrialised countries, women had a higher lung cancer mortality rate than men. In contrast, lung cancer death rates are low in developing countries. In industrialised nations, lung cancer mortality has reduced considerably due to a greater understanding of lung cancer risk factors, particularly the harmful effects of smoking. Additionally, early detection contributes to this decline (Jemal et al., 2010).

According to GLOBOCAN (2020b), females have a lower incidence rate. However, lung cancer is currently the third most prevalent disease among women (8.4 per cent of all cancers) and the leading cause of cancer mortality globally (18 per cent of the total). In Western Africa, the incidence rates among males and women were 11.1 per cent and 5.7 per cent, respectively. Cancer kills more than half of all people in low- and middle-income countries (Barta et al., 2019; Bray et al., 2018; GLOBOCAN, 2020c; Hamdi et al., 2021; Malhotra et al., 2016; L. A. Torre et al., 2016).

In 2011, at the 18th Union Conference of the African Region on Lung Cancer and Tuberculosis Awareness, it was reported that 67% of lung cancer cases worldwide occur in men aged 50 to 69. Africa had 4,525 lung cancer deaths in 2006 (AFRO UNION Conference, 2011; Bello et al., 2011).

GLOBOCAN (2020c) estimated the incidence rate of lung cancer in various African regions and reported that men had a higher incidence rate than women. Furthermore, the incidence of lung

cancer was lower in the East, Middle, and West African regions than in the Southern and Northern parts of Africa. Urman et al. (2016) attributed the low incidence in Africa to a lack of research studies on the aetiology of lung cancer and a lack of cases or detection biases. GLOBOCAN (2020c) has the lowest lung cancer mortality rate in Sub-Saharan Africa, excluding South Africa. The population-based data on lung cancer incidence and mortality are unavailable, and the GLOBOCAN relies on local registries to estimate these figures (Becher & Winkler, 2011).

Lung cancer is increasing in Northern and Southern Africa in both men and women, according to Hamdi et al. (2021), with a 3 to 5 fold increase in males compared to females. Southern Africa has twice the IR of North Africa. Southern Africa's heavy cigarette, cannabis, and alcohol consumption may explain this. In 2018, less than 3 cases per 100,000 people in the Eastern, Central, and Western regions.

In 2018, the WHO (2020b) reported 250 lung cancer cases in Ghana. Lung cancer incidence and mortality are ranked eighth in Ghana, with 2.2 and 3.1 per cent of the total, respectively. Males had an age-standardised world incidence rate of 3.8, while females had an incidence rate of 2.8 (GLOBOCAN, 2020a). Lung cancer accounts for 1.6% of all cancers in Ghana, according to Laryea et al. (2014). In 2014, lung cancer was the third most common malignancy in males (5.3%) but not among the top five in women. Based on Ghana's cancer profile, the WHO (2020b) predicted 348, 250, and 511 lung cancer cases in 2012, 2018, and 2040. (Kitson-Mills et al., 2019) studied cancer prevalence in an Accra neighbourhood and found uranium deposits in particular areas increase the risk of lung cancer.

2.4 LUNG CANCER AETIOLOGY

Lung cancer rarely affects those under 40 but primarily affects the elderly. Lung cancer can strike anyone at any age, and age is a risk factor (Dela Cruz et al., 2011). Many risk factors for lung cancer can be addressed, such as smoking cessation and family history. Some people with many risk factors never get lung cancer, whereas others do. This phenomenon is still being studied.

In Africa, smoking is responsible for 90% of lung cancers; nevertheless, HIV/AIDS is also a cause of lung cancer (Kirk et al., 2007; Malhotra et al., 2016; Sigel et al., 2012; Urman et al., 2016; Winstone et al., 2013). Africa is the most affected region by HIVAIDS (Kharsany & Karim, 2016). The incidence of lung cancer in the HIV-infected population is more comparable to that of the general population (Sigel et al., 2012, 2017).

Geographic location and occupational setting are significant risk factors for lung cancer in Ghana (Laryea et al., 2014). Even though smoking is not part of the Ghanaian culture, it has been established as a risk factor for cancer.

A person's age, specific illnesses and treatments (previous radiotherapy), family history of lung cancer, and exposure to cancer-causing substances (radon, asbestos, arsenic, beryllium, cadmium, chromium, nickel) are all risk factors for lung cancer (Barta et al., 2019; Clark & Alsubait, 2020; NCCN, 2021; NCI, 2021; Zappa & Mousa, 2016).

2.4.1 SMOKING

Smoking is the leading cause of lung cancer, and around 85 per cent of lung cancer patients have smoked at some time in their life (L. A. Torre et al., 2016). The risk increases with the number of cigarettes smoked daily and decreases with the duration of smoking. Additionally, the risk grows with smoking duration and initiation age. There are approximately 70 recognised carcinogens in cigarette smoke (Dela Cruz et al., 2011; Malhotra et al., 2016). Smoke also contains hazardous,

radioactive chemicals, such as radon and decay products (Malhotra et al., 2016; L. Torre et al., 2015; L. A. Torre et al., 2016; Urman et al., 2016).

Secondhand smoking involves breathing smoke from other people's cigarettes, which is akin to cigar smoking and causes lung cancer. (Fukumoto et al., 2015; Hang et al., 2020; A. S. Kim et al., 2018; Li et al., 2016; Naeem, 2015; Sheng et al., 2018; Sun et al., 2017).

Thirdhand smoke (THS) is a newly identified tobacco smoke danger that has been a public issue recently due to its widespread indoor presence and considerable unfavourable biological and physiological impacts (Hang et al., 2019; Thomas et al., 2014). There is evidence that third-hand smoking (THS) can cause cancer (Hang et al., 2018, 2020; P. Jacob et al., 2017). Infants and children living in a smoking household are susceptible to THS and secondhand smoke, and exposure has been associated with an increased risk of lung cancer later in life (Sarker et al., 2020; Thomas et al., 2014).

Never smokers are individuals who have never smoked and have never smoked more than 100 cigarettes in their lives. Globally, the fraction of lung cancers unrelated to cigarette smoking is around 15% in males and 53% in women (A. S. Kim et al., 2018; Jonathan M. Samet et al., 2009; Toh & Tan, 2017; Wakelee et al., 2016). Never smokers account for 25% of lung cancer cases, and adenocarcinoma is the most often diagnosed cell type of lung cancer among them (Dubin & Griffin, 2020; Malhotra et al., 2016; Parker, 2019; Jonathan M. Samet et al., 2009; Toh & Tan, 2017; Wakelee et al., 2016).

2.4.2 RADON EXPOSURE

Radon-222 is a byproduct of the decay of radium-226, whereas radium is a byproduct of the decay of uranium-238. Uranium and radium are present in varying amounts in the earth's crust, including soil, rock, and stone. Radon is a naturally occurring radioactive gas that is colourless, odourless, and tasteless and has a half-life of 3.82 days. Radon is a well-known carcinogen and a source of ionising radiation exposure in the environment (Bissett & McLaughlin, 2010; O'Keeffe et al., 2018). Radon is harmless, but its breakdown products, termed radon daughters, are solid radioactive particles that can attach to surfaces like dust or lung epithelium, causing DNA damage and perhaps lung cancer (Eidy & Tishkowski, 2021; Garcia-Rodriguez, 2018; Laughlin, 2012).

Radon is the world's second-largest cause of lung cancer after smoking (Lorenzo-González et al., 2019). Radon causes roughly 20,000 lung cancer cases every year, according to the EPA in the US. They suggest testing indoor radon levels in households and applying mitigation measures to mitigate excessive radon concentration levels (Conrath, 2012).

Although Ghana does not have a geologic radon potential reference level, some study has been done on radon levels in Ghana. (Badoe, 2007) measured radon gas levels in the Ashanti Region for six years to create a vulnerability map for Ghana. The radon concentrations were within the United States Environmental Agency's tolerance range. In addition, Akortia (2010) and Kitson-Mills et al. (2019) have evaluated the indoor radon levels in some Ghanaian communities. Akortia (2010) observed that the effective dosage equal to the population was two to three times lower than the 1 mSv indicated by the ICRP, while Kitson-Mills et al. (2019) discovered that the average indoor concentration was below the WHO's globally recommended level. These researches' low levels and outcomes do not rule out the need for radon gas evaluations in Ghana, notwithstanding

the low amounts measured. Radon gas is widely recognised as a critical lung cancer risk factor; thus, a national geologic radon potential evaluation is recommended.

2.4.3 EXPOSURE TO HAZARDOUS CHEMICALS

Occupational exposures cause 3 – 15% of lung cancer cases. Some proven and suspected compounds that cause lung cancer are arsenic, asbestos, chromium, mustard gas, nickel, silicon, iron ore, wood dust and acrylonitrile. The danger of asbestos exposure varies depending on the exposure type. Occupational exposure is far riskier than environmental exposure.

Cooking and other fumes are significant danger concerns, especially in developing nations like Ghana (Barta et al., 2019; Dela Cruz et al., 2011; Malhotra et al., 2016; Urman et al., 2016). The type of coal utilised affects the results. Smoky coal enhances the risk of lung cancer. Diesel exhaust causes lung cancer (Attfield et al., 2012; Silverman et al., 2012).

2.4.4 CANCER TREATMENTS

Some cancer treatments increase the risk of lung cancer. The risk rises after receiving radiotherapy to the chest, particularly in smokers. Amadori & Ronconi (2005), Seike et al. (2021) and Wang et al. (2021) from their studies, observed radiation-induced solid tumours, including lung cancer, in individuals treated with radiotherapy for thoracic malignancies. Radiotherapy uses high-energy radiation that can damage DNA and cause cancer. Regardless of radiotherapy delivery modality, critical chest structures get considerable radiation resulting in radiation-induced damage. These injuries may be treatable or irreparable. According to research on Hodgkin's disease and breast cancer, irradiating the lungs triples the chance of lung cancer later in life (Kaufman et al., 2008; Wennstig et al., 2021).

2.4.5 DIETARY FACTORS

Some chemicals found in food, such as Heterocyclic amines (HCAs) in high-protein foods, have been carcinogenic (Rizwan Khan et al., 2017). Arsenic is a carcinogen, and its presence in drinking water may increase the risk of lung cancer(Roy et al., 2018; Q. Zhou & Xi, 2018).

2.4.6 GENETIC PREDISPOSITION AND FAMILY HISTORY OF LUNG CANCER

Lung cancer in nonsmokers appears to have a distinct genetic profile, tumour microenvironment, and epidemiology (de Alencar et al., 2020). It has been linked to several risk factors, including hereditary propensity (Benusiglio et al., 2021; de Alencar et al., 2020). Researchers have discovered a genetic predisposition within the bronchial epithelium of the lung that has yet to be resolved (Kanwal et al., 2017; I. A. Yang et al., 2013). Some researchers have linked specific genetic mutations to lung cancer, and having these genes may be the reason for never smokers developing lung cancer (Ankathil, 2010; Koeller et al., 2018). If a person's parent, sibling, or child has had lung cancer, developing lung cancer increases (Benusiglio et al., 2021; Osann, 1991; J. M. Samet et al., 1986). Suppose lung cancer occurs at a younger age or in multiple relatives, the risk increases.

2.4.7 OTHER DISEASES

Two lung diseases linked to lung cancer are chronic obstructive pulmonary disease (COPD) and pulmonary fibrosis. COPD makes it difficult to breathe because the lung tissue is damaged or too much mucus. Pulmonary fibrosis is severe scarring of lung tissue that makes breathing difficult. COPD history increases the risk of lung cancer and pulmonary fibrosis (Yoo et al., 2019).

HIV infected persons have a greater risk of developing lung cancer than the universal populace (Chaturvedi et al., 2007; Shiels et al., 2010; Sigel et al., 2017). The HIV patient's weakened

immune system increases inflammation, and chronic lung problems may contribute to increased cancer risk. Nonetheless, HIV treatment does not result in lung cancer.

2.5 LUNG CANCER PATHOPHYSIOLOGY (SYMPTOMS)

Lung cancer does not typically exhibit symptoms in its early stages, but advanced malignancies do. The most common symptoms include chronic cough, coughing with blood, chest discomfort, persistent breathlessness, aching when breathing or coughing, unexplained weariness and weight loss, hoarseness, lack of appetite, and face or neck swelling. Cough occurs in 50–70% of individuals with primary lung lesions due to a mass that irritates the cough receptors in the airway (Latimer, 2018; NCCN, 2021; Ruano-Raviña et al., 2020; Siddiqui et al., 2021). Squamous cell carcinoma and small cell lung cancer have this symptom. Weight loss affects 46% of people, while pleuritic chest discomfort affects roughly 20% (NCCN, 2021; Siddiqui et al., 2021). Patients often arrive with advanced illness due to the lack of symptoms in the early stages of cancer. Lung cancer is often revealed due to symptoms and is less frequently seen in X-rays before symptoms appear. Lung cancers may be discovered as part of a cancer screening programme or in an X ray by coincidence.

2.6 LUNG CANCER DIAGNOSIS

Some lung cancers may be discovered through screening; however, most lung cancers are discovered because they are causing issues. As a result, people with an increased risk of lung cancer in the United States and other developed countries may consider annual lung cancer screenings with low-dose CT scans. Lung cancer screening is typically provided to older adults who have smoked heavily for many years or quit smoking within the last 15 years. On World Cancer Day 2015, Ghana's Ministry of Health unveiled its National Cancer Control Strategy with the theme "Not Beyond Us." The goal was to reduce the rising number of cancer cases through

primary prevention, effective screening, and early detection. (Mensah & Mensah, 2020) noted in their narrative review that despite establishing a national cancer control plan, there is still an increasing incidence of cancers due to a lack of cancer control preparedness.

If a doctor believes a patient has lung cancer, numerous tests must be performed to ensure that the signs and symptoms are caused by cancer and not by another condition. X-rays, MRI, CT, and PET scans provide better information and detect tiny lesions in suspected lung cancer patients. Sputum cytology can also detect cancerous cells in the patient's phlegm. Bronchoscopy, mediastinoscopy, or needle biopsy may detect whether tumour cells are malignant. The accurate diagnosis of lung cancer is made in the laboratory by examining a sample of lung cells. Body tissue and fluid testing are required for diagnosis. A patient's malignant cells are sampled to establish the kind of lung cancer cell. Samples are taken from the fluid surrounding the lungs, a lung tissue sample known as a biopsy, or a sputum sample. The samples are taken to the lab, magnified, and a diagnosis is made based on the cells' characteristics.

Lung cancer may spread to lymph nodes and cause them to enlarge (Figure 2.4), and a physical examination can be performed. Lung cancer often spreads to lymph nodes in the chest and neck. Body temperature, breathing rate, weight, blood pressure, lung, heart, and gut sound, pulse, look of the eyes, skin, nose, ears, mouth, organ size and amount of discomfort when touched are assessed during this examination.

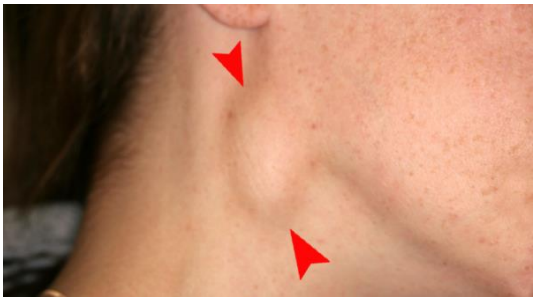

Figure 2.4: Lung cancer metstasised to lymphatic systems causing cervical lymphadenopathy (Anath, 2021)

The initial test performed to identify lung cancer is generally a chest X-ray. Most lung tumours look like a white-grey mass in X ray images (Figure 2.5). On the other hand, chest X-rays cannot provide a conclusive diagnosis since they often fail to discriminate between cancer and other illnesses, such as lung abscesses. If a chest x-ray indicates that a person has lung cancer, more tests are performed to determine the existence of lung cancer and, if present, what kind it is and how far it has progressed.

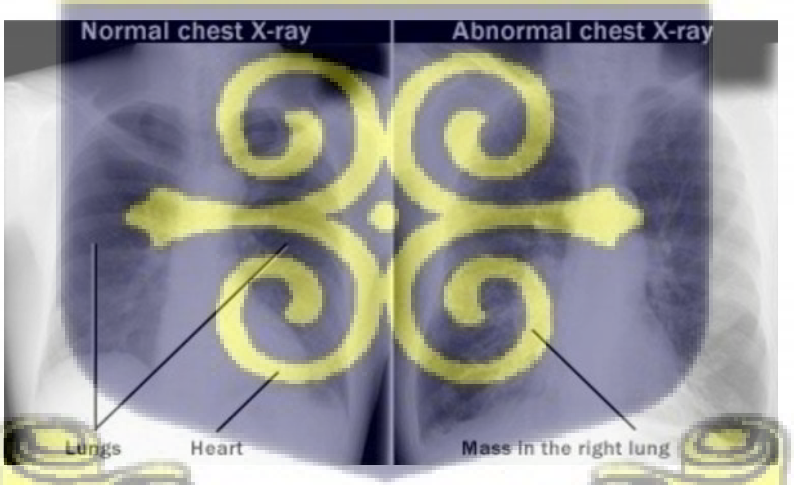

Figure 2.5: Chest X-ray of normal lungs against cancer affected lungs (Mayo Clinic, 2020)

Following a chest X-ray, the next test is generally a CT scan. CT scans are more diagnostic than ordinary chest X-rays, particularly in detecting lungs (Figure 2.6). A CT scan s an X-ray does not

combine a computer and X-rays to produce three-dimensional pictures of the interior of the patient's body. A contrast medium is provided before a CT scan to increase picture quality.

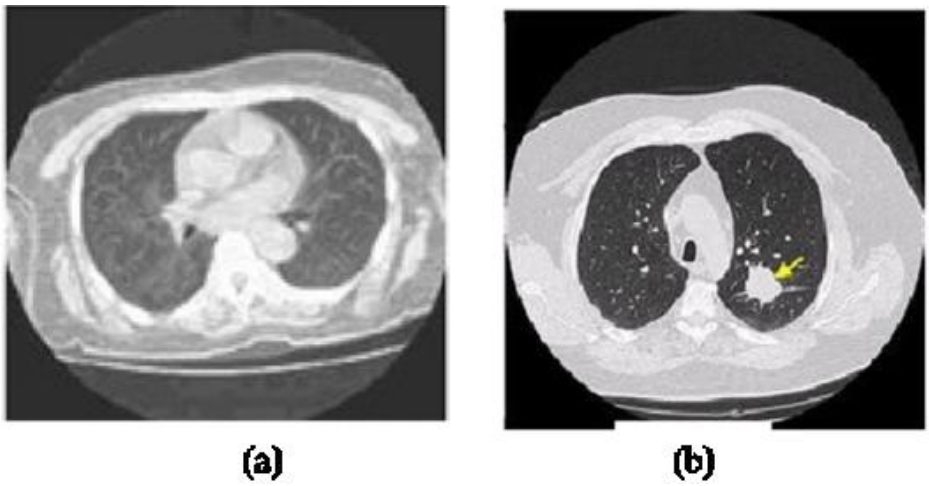

Figure 2.6: Lung CT image showing (a) normal lung and (b) lung cancer with an arrow pointing at the tumour (Anifah et al., 2018)

If a CT scan reveals that a patient has cancer at an early stage, a PET-CT scan may be performed. PET-CT can show where active cells are in the body (as shown in Figure 2.7), aiding diagnosis and treatment selection. A radiopharmaceutical is injected into the person before the scan. PET/CT enables the fusion of functional and anatomical information about the lung, allowing for more accurate disease staging (Hochhegger et al., 2015).

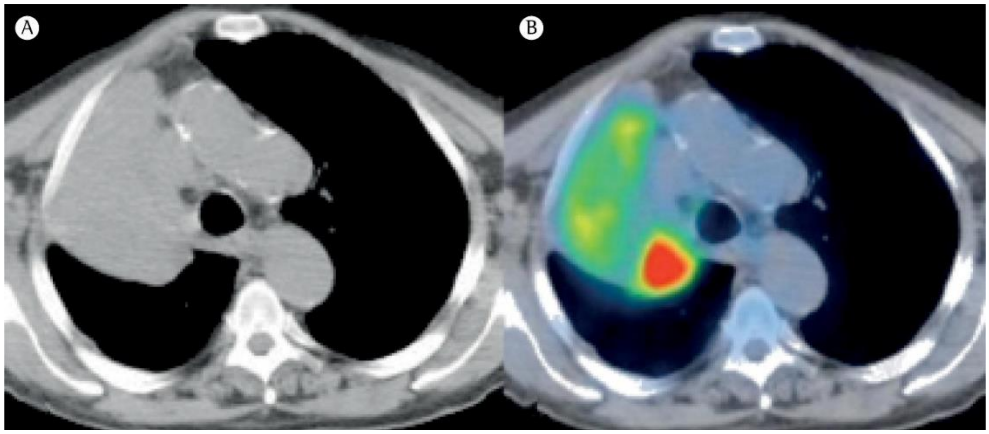

Figure 2.7:PET/CT images showing the difference between normal surrounding tissue and tumour with active cancer cells coloured. (a) CT image (b) PET/CT image (Hochhegger et al., 2015)

A biopsy is a procedure that removes tissue or fluid from the body for examination. Biopsies for lung tumours come in a variety of forms. When a CT scan reveals the risk of cancer in the central area of the chest, a bronchoscopy is recommended. A bronchoscopy is a technique that enables a doctor to examine a person's airways and extract a tiny sample of cells. A narrow tube with a camera at the end, known as a bronchoscope, is pushed through the mouth, nose, throat, and airways. Endobronchial ultrasound scan (EBUS) is a novel method that combines bronchoscopy with an ultrasound scan. EBUS enables lymph nodes in the centre of the chest for biopsy and the capacity to view within the airways. A lymph node biopsy may reveal whether or not malignant cells form in the node and what sort they are.

Other biopsy modalities include thoracoscopy, mediastinoscopy, and cutaneous biopsy using a needle (Figure 2.8). The CT image aids the clinician in seeing where the abnormal tissue is in the lung. A needle is inserted through the chest wall and into the abnormal lung tissue to remove a small piece of the tissue (NCCN, 2021). Tissue obtained during a biopsy is submitted to a pathologist to analyse and classify the illness. The pathology report indicates whether cancer began

in the lung or elsewhere. If the disease began in the lungs, the report would specify the kind of lung cancer.

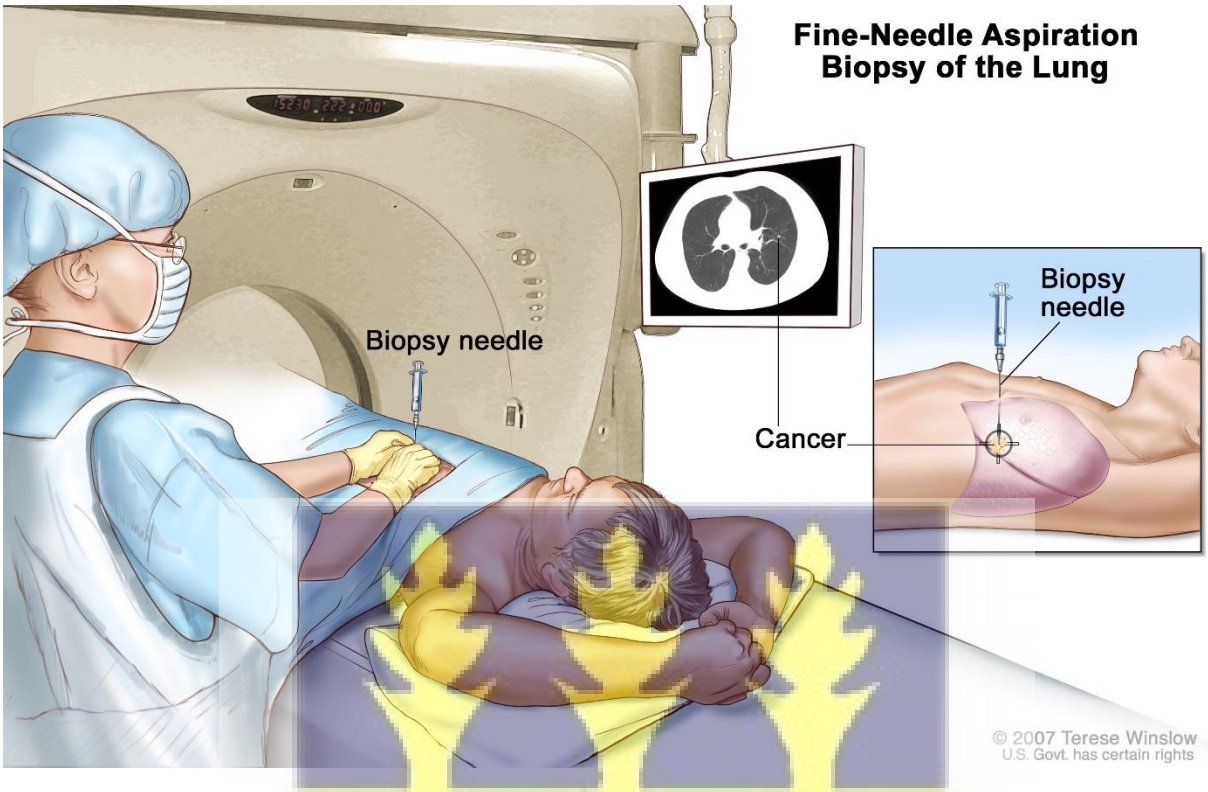

Figure 2.8: CT-guided biopsy (NCCN, 2021).

2.7 CLASSIFICATION OF LUNG CANCER

There are several forms of lung cancer, and the only way to establish which type a patient has is by sampling. It is critical to determine the kind of cancer since it influences treatment choices and prognosis.

Lung cancer is categorised into small cell lung cancer (SCLC) and non-small cell lung cancer (NSCLC). These categories are so-called for the sort of cancer cells and how they look under a microscope.

2.7.1 SMALL CELL LUNG CANCER (SCLC)

As the name implies, small cell lung cancer (SCLC) is composed of microscopic cells that have not grown entirely. SCLC is predominant among women who have a lengthy history of smoking. It is the top cause of cancer death in men and the second-highest cause of cancer death in women worldwide. Small cell lung cancer, which often begins in the bronchi and rapidly spreads to other body regions and lymph nodes, is divided into limited and extensive stages. It is the most aggressive lung cancer, growing and spreading faster. Usually, it would have spread to other body regions when it is identified. SCLC accounts for around 15% of all lung malignancies (Yang et al., 2019; Zhao et al., 2018).

2.7.2 NON-SMALL CELL LUNG CANCER (NSCLC)

Non-small cell lung cancer is the most recurrent type of lung cancer, accounting for 85 per cent of all cases (Z. Chen et al., 2014). NSCLC consists of large mature cells, and the respiratory tract has many mature cells. So, depending on whether the mature cell has turned malignant, this category of lung cancer includes subcategories (Clark & Alsubait, 2020; Society, 2019; Zappa & Mousa, 2016). less common types of NSLC include as carcinoid tumour, salivary gland carcinoma, pleomorphic carcinoma, and unclassified carcinoma. Carcinoids are found in about 5% of all NSCLCs. Both men and women are equally at risk of getting carcinoid cancers, although smoking is no apparent relation.

2.7.2.1 ADENOCARCINOMA

Mucin is vital for maintaining the lungs wet and is generated in the lung by particular lung gland cells. When these cells become cancerous, they are referred to as adenocarcinoma, where “adeno” means "from a gland," and glands generate mucin. Adenocarcinoma accounts for 40% of all NSCLCs, mainly affecting women, although it may afflict smokers and non-smokers (Zappa &

Mousa, 2016). Adenocarcinoma develops slowly and has a better chance of being detected early before spreading to other organs.

2.7.2.2 SQUAMOUS CELL CARCINOMA

Matured cells are also seen in the normal lung, but they are flatter than adenocarcinoma cells and are held together by proteins that form a desmosome. Desmosomes assist cells in forming an obstruction between the airways and the rest of the body. When these cells become malignant, they are referred to as squamous cell carcinoma, which happens around 30% of the time and is prevalent in men who have a history of smoking. Squamous cell carcinoma has the most substantial relation to smoking (Zappa & Mousa, 2016).

2.7.2.3 LARGE CELL CARCINOMA

Large cell carcinoma does not have many distinguishing features other than that, thus its name. It occurs in 10% of all NSCLCs and is more common among male smokers (Zappa & Mousa, 2016). This kind of lung cancer is closely linked to smoking and often begins in the core area of the lungs before spreading to surrounding lymph nodes, the chest wall, and distant organs.

2.8 LUNG CANCER STAGING

Staging is done to define the location of the lung cancer cells, the size of the lung tumour, and the degree to which the lung cancer has spread. Lung cancer procedures for medical practice are subject to staging models, which are essential for predicting prognosis and determining therapy options. However, it does not specify the number of years of survival. The findings of tests and tissue samples aid in determining the stage of lung cancer.

The Tumour, Node, Metastasis (TNM) staging approach, which is used to grade distinct regions of cancer development, has been approved by the Union for Worldwide Cancer Control (UICC), the American Joint Committee on Cancer (AJCC), and many other international cancer centres

(UICC, 2016). The letter T in TNM stands for the size and extent of the primary tumour. The letter N denotes whether or not the tumour has spread to the lymph nodes. The letter M in the TNM acronym stands for metastasis, which indicates the degree to which cancer has spread throughout the body. Each letter has a number in the system that indicates the amount of tumour development: the greater the number, the more dangerous the increase. The TNM staging method for lung cancer from the 8th edition of the TNM staging handbook for staging and directing lung cancer therapy in multidisciplinary centres is shown in Table 2.1.

Table 2.1: Lung cancer staging using TNM system 8th edition (Kay et al., 2017).

Primary Tumour	
Tx	Cannot be assessed; Tumour in sputum/bronchial washings not in imaging/bronchoscopy
T0	No evidence
Tis	Carcinoma in situ
T1	≤ 3 cm surrounded by lung/visceral pleura, not involving the main bronchus
T1a (mi)	Minimally invasive adenocarcinoma
T1a	≤ 1 cm
T1b	> 1 to ≤ 2 cm
T1c	> 2 to ≤ 3 cm
T2	> 3 to ≤ 5 cm or Involves the main bronchus without carina involvement or Visceral pleural invasion or atelectasis/post obstructive pneumonitis extending to the hilum
T2a	> 3 to ≤ 4 cm
T2b	> 4 to ≤ 5 cm
T3	> 5 to ≤ 7 cm or Separate tumour in the same lobe or Direct invasion of the chest wall (includes parietal pleura and superior sulcus)/parietal pericardium/phrenic nerve
T4	> 7 cm or
	Separate tumour in different lobe of ipsilateral lung or Invasion of heart/ great vessels/diaphragm/mediastinum/trachea/carina/oesophagus/ recurrent laryngeal nerve/vertebral body
	Regional lymph node
Nx	Cannot be assessed
N0	No involvement
N1	Ipsilateral peribronchial and/or hilar nodes and intrapulmonary nodes
N2	Ipsilateral mediastinal and/or subcarinal nodes
N3	Contralateral mediastinal or hilar; ipsilateral/contralateral scalene/supraclavicular
	Distant metastasis
M0	No distant metastasis
M1	Distant metastasis is present
M1a	Tumour (s) in contralateral lung; pleural/pericardial nodule/malignant effusion
M1b	Single extrathoracic metastasis
M1c	Multiple extrathoracic metastases in one/ more organs

Figures 2.9 to 2.14 are the illustrations for the various TNM categories.

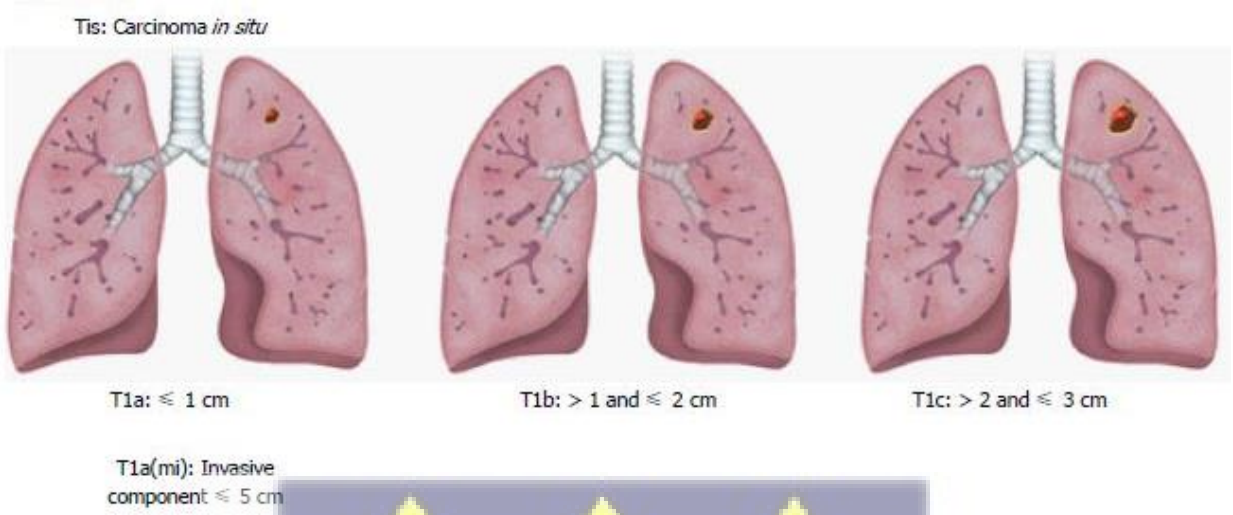

Figure 2.9: Lung cancer primary tumour T1 illustration (Kay et al., 2017).

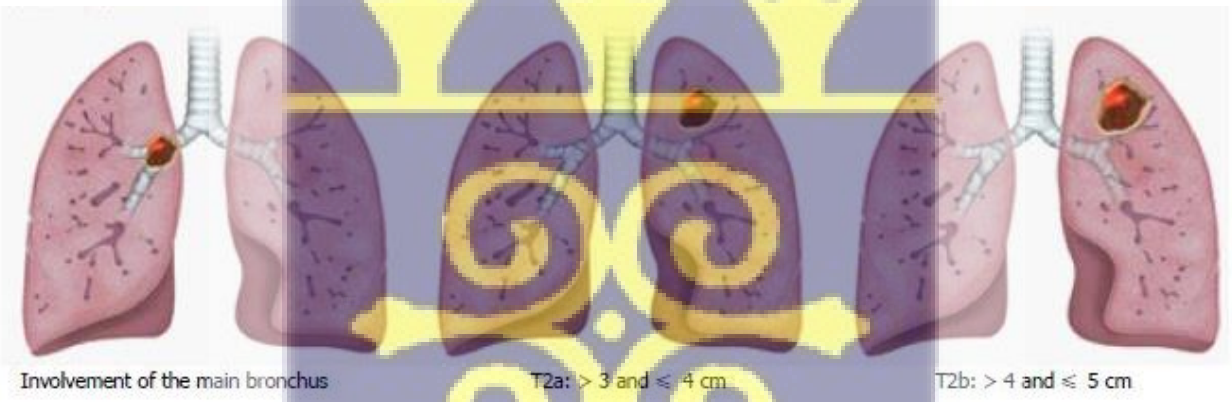

Figure 2.10: Lung cancer primary tumour T2 illustration (Kay et al., 2017).

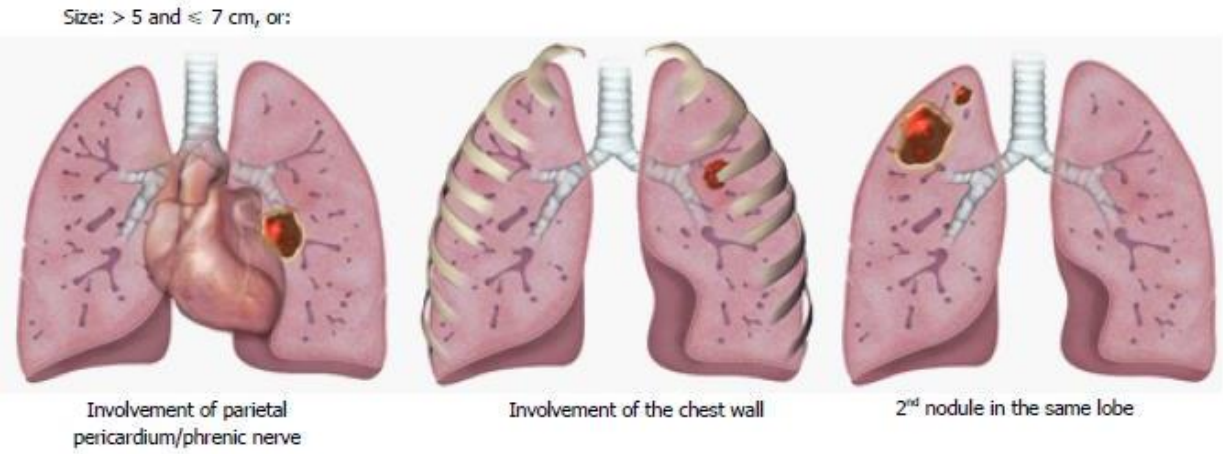

Figure 2.11: Lung cancer primary tumour T3 illustration (Kay et al., 2017).

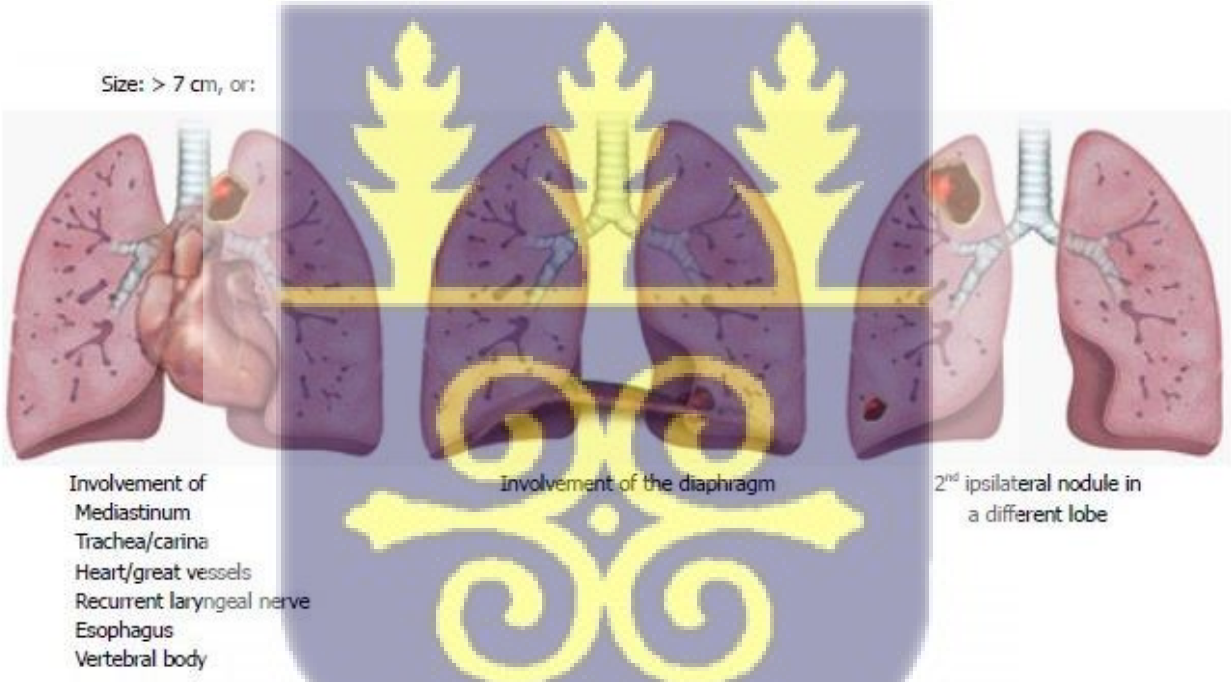

Figure 2.12: Lung cancer primary tumour T4 illustration (Kay et al., 2017).

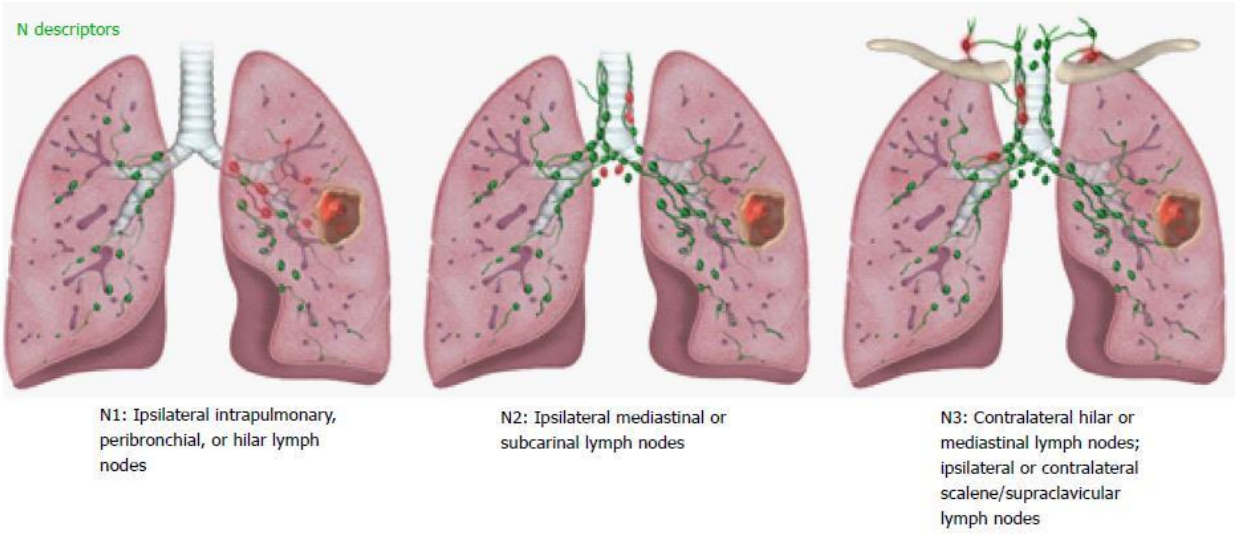

Figure 2.13: Lung cancer regional lymph node illustration (Kay et al., 2017).

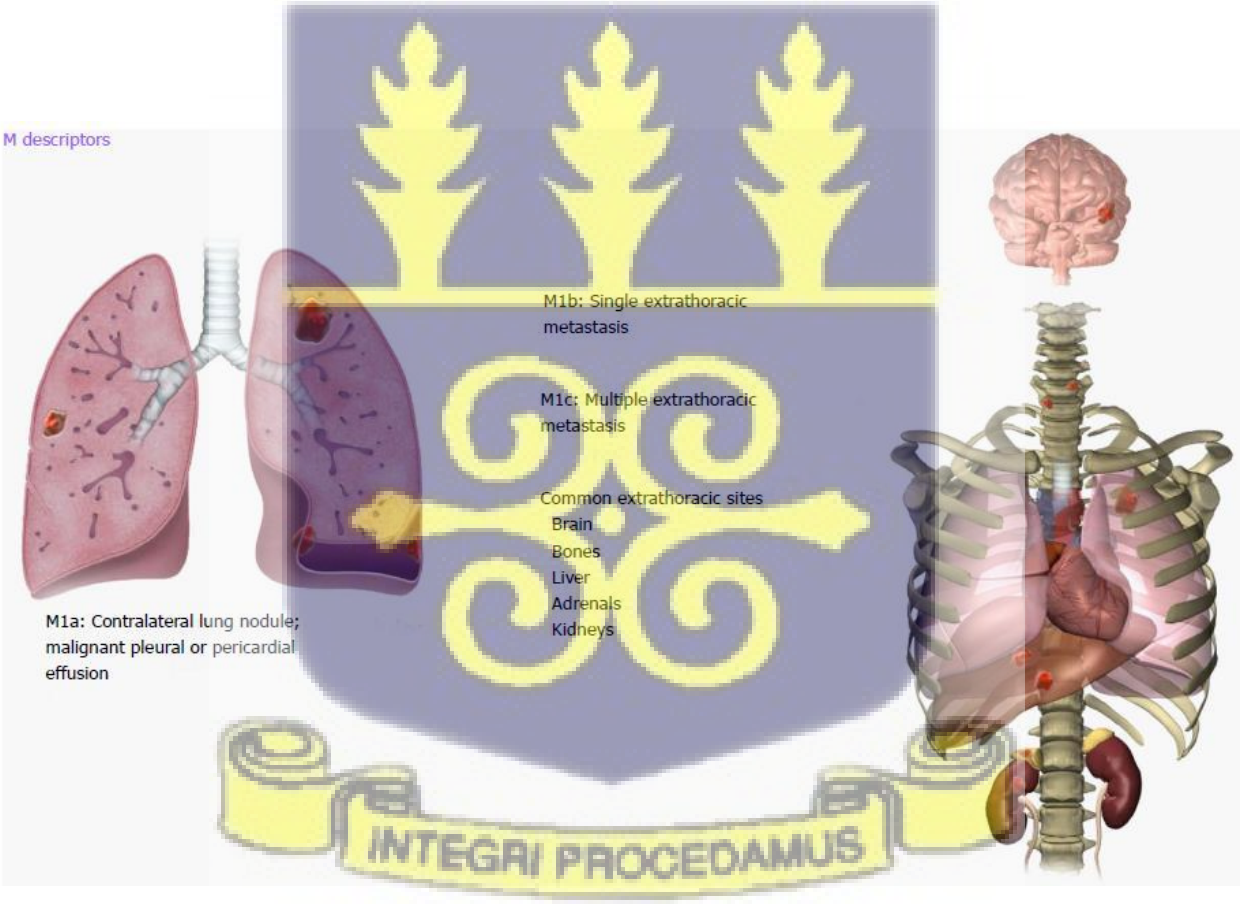

Figure 2.14: Lung metastasis illustration (Kay et al., 2017).

Cancer stages are determined by a combination of TNM classifications and prognosis. Although occult carcinoma and stage 0 are uncommon diagnoses, there are four (4) significant stages of cancer, as detailed in Table 2.2 and represented in Figure 2.15.

Table 2.2: Tumour staging

Stage	Meaning
Stage 0	cancer cells are found in the lining of the airways
Stage I	a small tumour is found inside the lung
Stage II	Cancer grows and spreads to nearby lymph nodes or non-lung tissues.
Stage III A	The tumour grows into any size and is found in lymph nodes on the same side of the chest or nearby organs.
Stage III B	This is similar to stage III-A, but in this case, cancer cells are found in lymph nodes on the opposite side of the chest. Cancer may also be found in lymph nodes above the collarbone.
Stage IV	Tumours might be found in both lungs. Additionally, cancer may have spread to distant organs such as the brain, liver, skin, and other distant tissues.

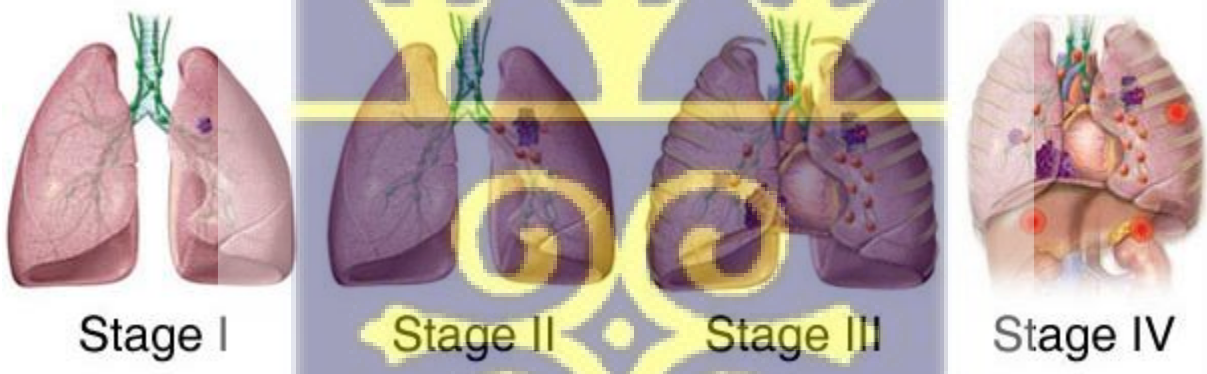

Figure 2.15: Lung cancer stages (St. Stamford Modern Cancer Hospital Guangzhou, 2019).

SCLC has fewer components than NSCLC, and most doctors use a two-stage technique, restricted and expanded. On one side of the chest, cancer can be treated with a single radiation field. Cancercancer may have spread to the other side of the chest or distant organs.

Cancer staging is performed twice for some individuals: before treatment (clinical stage) and after surgery (pathologic stage).

2.9 LUNG CANCER TREATMENT AND MANAGEMENT

Early identification of lung cancer is essential for achieving a cure; regrettably, many patients seek medical assistance after the illness has progressed. Lung cancer therapy is determined by the kind of cancer mutation, the level of dissemination, and the patient's overall health. A team of Radiation Oncologists, Radiation Therapists, and Medical Physicists collaborate to provide the best therapy for each patient. The doctor also talks with the patient about the treatment choices available for their cancer kind and stage, including the advantages, dangers, and side effects of each modality.

Surgery, radiation, chemotherapy, targeted therapy, or a combination of these therapies may be used to treat non-small cell lung cancer. Radiotherapy and chemotherapy are the most often used treatments for small cell lung cancer. Radiofrequency ablation (RFA), targeted medication therapy, immunotherapy, and palliative operations are some of the additional therapeutic possibilities.

2.9.1 SURGERY

Surgery is a typical therapy for lung cancer; however, the technique varies from person to person. Lung cancer surgery entails removing a piece or the complete lung. A surgeon performs the operation, which includes one of the following procedures: wedge resection, segmental resection, lobectomy, and pneumonectomy, as illustrated in Figure 2.16. Lobectomy and pneumonectomy are the most prevalent. The excision of a piece of the lung containing the tumour and a margin of healthy tissue is known as a wedge resection. Segmental resection removes a more considerable volume of the lung but not the whole lobe. A lobectomy removes one whole lung lobe, while a pneumonectomy is the removal of the entire lung. Surgical resection for resectable and operable early-stage cancer might be used as a treatment for NSCLC, depending on the feasibility of the cure (Lemjabbar-Alaoui et al., 2015).

However, patients may refuse surgery or be inoperable, in which case the malignancy may be treated with radiation.

Wedge Resection Segmentectomy Lobectomy Pneumonectomy

Figure 2.16: Lung cancer surgical treatment options and resected specimen in dark red (Hu, 2016).

2.9.2 CHEMOTHERAPY

Chemotherapy employs the use of medications to destroy cancer cells. One or more medicines may be delivered intravenously or consumed orally in cycles. Lung cancer chemotherapy chemicals are injected into the veins and circulate throughout the body, treating cancer. Adjuvant chemotherapy or concomitant chemo-radiation are often used to destroy remaining malignant cells in patients. Chemotherapy may help individuals with metastatic cancer relieve pain and other symptoms (Nakamura & Maeda, 2022; S. Yang et al., 2019). The rationale for treating lung cancer with concurrent chemo-radiation is to enhance regional and systemic cancer control, which has resulted in increased overall survival for NSCLC (Curran et al., 2011; Postmus et al., 2017).

Cancer cell death is caused by targeted medication treatment, which focuses on particular defects inside cancer cells. Immunotherapy uses the immune system of patients to combat cancer. Palliative care is a kind of supportive care offered to patients to help them cope with the signs, symptoms, and side effects of cancer therapy. The care provides patients comfort before and after

cancer treatment and has been shown to enhance patient mood and quality of life(Melin-Johansson et al., 2010; Nottelmann et al., 2021).

2.9.3 RADIOTHERAPY

Radiotherapy employs high-energy X-rays or particles to treat lung cancer. Radiotherapy is often used as the primary treatment before surgery to decrease the tumour volume and then as the secondary treatment after surgery to kill any cancer cells that may remain in the treated region or treat lung cancer that has spread to other areas of the body. In other circumstances, radiation is the primary treatment, either alone or in conjunction with chemotherapy. Radiotherapy is used in conjunction with surgery for NSCLC and chemotherapy for SCLC. Radiotherapy is also utilised when a patient is inoperable or refuses surgery. In advanced cancer patients, radiotherapy may be used to ease discomfort.

External beam radiation treatment is the most often utilised approach for conforming radiation beams from an external source to the tumour contour. The goal is to send the highest amount of radiation to the tumour while giving the least amount of radiation to the surrounding normal tissues. Three-dimensional conformal radiation treatment (3D-CRT), intensity-modulated radiation therapy (IMRT), stereotactic body radiation therapy (SBRT), and proton therapy are some of the procedures used to treat lung cancer.

Three-dimensional conformal radiation treatment (3D-CRT) produces an x-ray beam that fits the geometry of the target; however, it is not as focused as IMRT.

Intensity-modulated radiation treatment (IMRT) uses x-ray beams tailored to the target's form while sparing normal tissue. It takes roughly six weeks to complete treatment.

Stereotactic body radiation treatment (SBRT) uses high-dose X-ray beams to treat cancer. High radiation dosage is provided for each treatment, but only for a fraction of the time. Treatment typically takes approximately a week and a half.

Proton therapy uses proton beams to treat cancer. Proton beams administer radiation primarily inside the tumour, and therapy takes around six weeks.

A multidisciplinary team of radiation oncology experts creates the treatment plan and administers it to lung cancer patients. A radiation oncologist, a medical physicist, a thoracic surgeon, a radiologist, a histopathologist, an oncology nurse, and a palliative care representative are all part of the team.

Currently, most patients with small inoperable lung cancer are treated with stereotactic body radiation treatment (SBRT). Inoperable patients include the elderly, those with chronic heart failure, and those who are in danger of postoperative haemorrhage because they are using blood-thinning medications (Keall, Balter, et al., 2006; Keall, Mageras, et al., 2006; Robert Timmerman et al., 2010; Zappa & Mousa, 2016).

2.10 STEREOTACTIC BODY RADIATION THERAPY (SBRT)

2.10.1 OVERVIEW

Stereotactic Body Radiation Therapy (SBRT) is a cutting-edge procedure used to treat primary and metastatic tumours in various anatomical areas. SBRT uses cutting-edge technology to target deep-seated tumours inside the body with high doses of radiation. It is a non-invasive technique since it is utilised when surgery is either impossible or complicated. In contrast to conventional fractionated therapy, which is provided in relatively moderate doses over 5 - 6 weeks, SBRT

includes administering high-dose radiation treatment, often up to five sessions. Each therapy session lasts between 30 and 60 minutes. SBRT has the potential to be utilised to treat malignancies of the liver, lung, abdomen, lymph nodes, and spine.

SBRT treats extracranial malignancies with highly conformal radiation in 5 fractions. The administration of a very high dosage in a short period results in a high biologically effective dose (BED). SBRT is also more convenient for patients and more cost-efficient due to the short total treatment period. As scientifically proven, patients treated at the centre with SBRT will have superior cosmetic treatment results than those treated with surgery (Ezer et al., 2015; Grills et al., 2010; Shaverdian et al., 2015; X. Wang et al., 2018; Yamamoto et al., 2014). Nonetheless, centrally placed tumours need extra caution in radiotherapy delivery since their placement implies a high potential of typical tissue damage, which might have adverse clinical effects (Bahig et al., 2016; Haseltine et al., 2016; Kang et al., 2015; Modh et al., 2014; Thompson & Rosenzweig, 2019; Yamashita et al., 2014). As a result, SBRT necessitates a high degree of precision and accuracy throughout the treatment delivery procedure. The American Association of Physicists in Medicine (AAPM), as well as the ACR-ASTRO, have made recommendations on the use of SBRT, including safety, treatment planning, setup, and therapy delivery, among other things, to ensure safe and quality SBRT (Benedict et al., 2010; Halvorsen et al., 2017). These therapies have been administered effectively utilising the respiratory gating approach (Diwanji et al., 2017; Giraud et al., 2011; Nagata & Kimura, 2018; Saito et al., 2014; Videtic et al., 2017). KATH presently features a Varian CLINAC iX with SBRT and gating capabilities. Respiratory gating approaches were chosen for this investigation because they have a high potential for improving irradiation of tumour areas influenced by respiratory motion, namely the lung. The adoption of this approach minimises pulmonary toxicity at large dosages. Gated Stereotactic Body Radiation Therapy

(SBRT) will be investigated in this case study of lung malignancies to counteract the respiratory generated motion effect since there is more clinically verified evidence of greater local control(Aparicio et al., 2019; Lagerwaard et al., 2008; Mahadevan et al., 2018; Nagata & Kimura, 2018; Singh et al., 2014; Robert Timmerman et al., 2010; Yeung et al., 2017). Timmerman et al. (2010) assessed the effectiveness and toxicity of SBRT in 55 medically inoperable patients with early-stage lung cancer. After three years, the research found a patient survival rate of 55.8 per cent, excellent rates of local control, and modest treatment-related morbidity.

SBRT also offers patients the logistical benefit of a substantially shorter radiation schedule without sacrificing results. The benefits of geometric accuracy and dosimetric improvements are predicted; however, this work focuses on employing respiratory gating.

Bromgren, Lax, and co-workers at Karolinska University Hospital pioneered stereotactic radiation to treat lung and liver tumours in 1991 (Blomgren et al., 2004; Lax et al., 1998). SBRT was developed and successfully deployed in Japan for lung tumours in 1994 (Uematsu et al., 1997). Following this novel invention, several centres in Japan, Europe, and America utilised SBRT, with remarkable outcomes recorded (Blomgren et al., 2009; Robert Timmerman et al., 2003; Uematsu et al., 1997). In instances where treatment choices were previously restricted, stereotactic body radiation therapy is now employed. It is primarily employed when there are a limited number of recurring locations to give an ablative dosage of radiation, such as lymph nodes, lungs, spine, and liver. It has been the therapy of choice for many persons with low-volume tumours for whom surgery may not be the best option. SBRT is distinguished by patient immobilisation, the limitation of average tissue exposure to high-dose radiation, the prevention or accounting for organ movements such as respiratory motion, the use of stereotaxy, and the delivery of doses with subcentimeter precision. Target delineation, treatment planning, and radiation administration are

the three main components of an SBRT therapy. A radiation oncologist, medical physicist, radiation therapist, and, depending on the body location and indication, a diagnostic radiologist, nurse, anesthesiologist, and dosimetrist are all part of the therapy team. Surgeons and other medical experts may also be part of the treatment team.

SBRT differs from other forms of external beam radiation therapy (EBRT) in that it uses high-dose radiation, delivers one to five fractions within a few days, is non-invasive, reduces overall treatment time, has high effectiveness, accuracy, and improved treatment response, and is available as an outpatient service. SBRT employs image-guided technology with millimetre-scale precision and the capacity to protect healthy tissue while increasing the radiation dosage. SBRT has a sizeable local control rate ranging from 60% to 90%, which is a significant advantage over other modalities (Aparicio et al., 2019; Janssen et al., 2016; Lee et al., 2021; Singh et al., 2015; von Reibnitz et al., 2018). Some multicentre studies have been conducted to support the use of SBRT. Local immune function is often intact, particularly when compared to conventional radiation. SBRT obtained a 98 per cent local control rate in the phase II RTOG 0236 experiment (Nyman et al., 2016a; R Timmerman et al., 2014). SBRT gave a total dosage of 60 Gy to the tumour in three fractions for one week. In NSCLC patients with proven comorbidities such as emphysema, heart disease, and stroke, three-year overall survival (OS) was 56% (R Timmerman et al., 2014). SBRT does not require hospitalisation due to the short duration of the treatment course, giving patients more freedom in their busy lives, even if they are travelling from a distance, resulting in little or no interruption of their treatment schedule. Standard fractionated radiotherapy (2D-CRT, 3D-CRT, and intensity-modulated radiation treatment (IMRT)) is commonly administered in 25–50 fractions over five days per week for 5 to 10 weeks. SBRT has a significant drawback in that it requires reasonable motion control and an image guiding system, which may not be accessible in

all departments or health care institutions. Again, SBRT is not appropriate for many situations; it is only appropriate for tiny, well-defined tumours that can be observed on imaging such as CT or MR scans.

Furthermore, if the cancer is adjacent to a fine, typical structure, such as the spinal cord or intestine, the quantity of radiation that may be safely supplied may be restricted. SBRT may sometimes induce side effects ranging from minor tiredness and temporary oesophagitis to catastrophic occurrences like pneumonitis or bleeding. SBRT is less hazardous than standard radiation since it does not need surgical incisions. Some general side effects and complications of radiation may occur, including weariness, nausea, and oedema.

2.10.2 LUNG SBRT

Lung SBRT/SABR is a well-established therapeutic option for individuals with early-stage non-small cell lung cancer and those with one or more lung metastases (secondary). For the treatment of non-small cell lung cancer, it is considered that exceptionally high radiation doses are required (Kumar et al., 2017; Newman et al., 2019; Robert Timmerman et al., 2010). Lung SBRT was initially utilised for peripheral lung tumours (tumours on the lung's margins). However, it is now being employed for more central tumours (tumours towards the middle of the lungs and deeper in the lungs). The movement of the patient's breathing may be controlled, allowing for extremely high and targeted radiation doses to be delivered. In several clinical studies, patients with a minor amount of metastatic lung disease (secondary tumours from other cancers that have spread to the lung) may also benefit from lung SBRT (Chinniah et al., 2017; Lindberg et al., 2015; Miyakawa et al., 2017; Navarro-Martin et al., 2016; Nyman et al., 2016a, 2016b; Ricardi et al., 2010; Shibamoto et al., 2015; R Timmerman et al., 2014).

SBRT delivery has been made feasible by various technical developments, including the ability to comfortably immobilise patients during treatment, tumour movement monitoring, improved tumour identification, and more precise and accurate radiation therapy administration. IMRT, image-guided radiotherapy (IGRT), and volumetric-modulated arc treatment (VMAT) are advanced approaches used. The SBRT process comprises patient positioning for comfort, CT image capture (potentially with respiratory information to reconstruct tumour movement), verification imaging before treatment, and radiation administration using a linear accelerator.

2.11 LUNG SBRT IMPLEMENTATION PROCESS

The patient is immobilised, the lung and target are defined, and advanced techniques like IMRT, IGRT, and VMAT are used to tailor the dosage to the target. Using lung SBRT in an oncology centre requires several technical and clinical issues. Dahele et al. (2008) addressed patient evaluation, simulation and treatment planning, tumour and organ at risk characterisation, trial setup before treatment, online image guiding, and patient follow-up.

In most cases, SBRT begins with simulation. Using immobilising devices during CT simulation guarantees that the patient's posture is reproducible during therapy delivery. Due to mobility, particularly in lung tumours, a four-dimensional (4-D) scan is conducted to incorporate time in the CT scan. Treatment planning takes about a week after the 4-D scan. The treatment plan includes identifying the target organs and orienting the radiation beam to provide the recommended dose. The patient is then immobilised and scanned to determine the tumour's position and account for any changes that day. Daily personalised therapy for a patient is generated.

2.12 TREATMENT AND SIMULATION

SBRT requires determining each organ's radiation tolerance. This simulation procedure includes marking up for set up and target motion systematic and random errors. Image-guided radiotherapy

uses numerous imaging modalities before or during radiation treatments to align and evaluate the structural agreement between the simulation anatomy, radiotherapy treatment plan, and patient (IGRT).

2.12.1 TARGET MOVEMENT

The role of respiratory-generated motion has hampered the accuracy and precision of dose distribution to cancers while sparing normal tissues. According to Mageras et al. (2004), 7 out of 12 patients had tumour motion of more than 1 cm craniocaudally. Yu et al. (2012) discovered that early-stage non-small cell lung cancer patients had more than 50% greater tumour mobility than locally advanced individuals. Tumour movement is linked to location, volume, and diaphragm motion.

Respiration is semi-periodic and predictable for each patient. Since respiratory motion patterns vary between fractions and even within a fraction, no common respiratory motion patterns can be anticipated for a single patient. Lung tumour motion was linked to diaphragm motion, superior-inferior lung tumour implantation, GTV, and illness T stage (Liu et al., 2007). It has been reported that the range of respiratory motion is up to 50 mm, with the lower lung demonstrating the most significant tumour movement (Harada et al., 2016; Jan et al., 2015; Keall, Balter, et al., 2006; Liu et al., 2007; Seppenwoolde et al., 2002; Shimizu et al., 2001; Shirato et al., 2004). Similarly, Langen & Jones (2001) and Liu et al. (2007) found that tumour motions are highest superior-inferior, with critical parts anterior-posterior and left-right. However, when studying lung tumours in general, the tumour mobility is generally less than 5 mm (Liu et al., 2007). According to (Liu et al., 2007), only 40% of lung tumours migrate 5 mm or more, and only 12% migrate 10 mm or more.

Torshabi & Dastyar (2017) studied the effects of tumour motion on treatment quality and irradiation of thoracic tumours and compensating strategies. Using a correlation model to observe the amount of tumour mobility revealed ways that may increase precise targeting of dynamic tumours for high tumour control and minimal normal tissue problems, Yoganathan et al. (2017) investigated the prevalence, effect, and management of respiratory-induced target motion in radiation treatment using a correlation model to assess the amount of tumour movement. Their findings suggest that respiration-induced motion affects radiotherapy. Respiratory motion, for example, adds dosimetric error. Tracking, motion encompassing, and gating are three strategies for managing respiratory motion.

Respiratory-induced lung tumour mobility has affected imaging and radiation treatment (Mageras et al., 2004; Shimizu et al., 2001; Yu et al., 2012). Respiratory motion affects picture capture for radiation, generating artefacts when ignored. They distort the target volume and produce inaccurate positional and volumetric data. Artefacts are frequent in thoracic CT images.

There are imaging and treatment planning methods to address the issue of tumours moving due to respiratory activity. Since tumour mobility occurs during imaging and medication administration, it is essential to account for tumour movement in imaging and planning.

2.12.2 IMMOBILISATION AND POSITIONING

SBRT for lung cancer patients requires a precise, repeatable, and comfortable immobilisation device. Lung cancer immobilisation devices mimic the patient's posture during simulation and radiation. Ideal immobilisation methods and technologies reduce intrafraction motion, restrict beam attenuation, and do not interfere with patient localization systems (Molitoris et al., 2019). Thermoplastic masks (TMPs) and vacuum cushions (VCs) are two standard SBRT immobilisation

devices (Chen et al., 2019). Furthermore, abdominal compression strategies have been utilised to restrict respiratory tumour mobility during the simulation and subsequent radiation treatments.

2.12.3 RESPIRATORY MOTION ASSESSMENT AND CONTROL

In SBRT, mobility is a significant issue, especially in lung cancer, as the tumour moves a lot while the patient breathes. If there is little mobility, it is integrated into the desired volume. If the motion is significant, a large quantity of normal lung tissue may be treated to account for it. This condition demands motion management. Several malignancies, most often lung, liver, and abdominal tumours, require accurate computed tomography (CT) studies in the presence of respiratory activity.

2.12.3.1 EVALUATION OF MOTION

Managing tumour mobility during simulation and therapy is accomplished after placement and immobilisation. The phases of this exercise are evaluation and control. Motion assessment measures the time-dependent 3-D displacements of a tumour target or a reliable surrogate. Most motion evaluations use 4-D CT but can be done with real-time fluoroscopy or slow CT.

2.12.3.1.1 COMPUTED TOMOGRAPHY IN FOUR DIMENSIONS (4-D CT)

The 4-D scan is used during simulation to help locate tumour movements, which is employed in treatment planning and therapy. Incorporating time and motion into a three-dimensional computed tomography scan creates a unique volumetric data set of the human body. That depends on the CT scan series. For better diagnosis and therapy, a 4D CT scan delivers exact information about moving interior organs (Ford et al., 2003; Hugo & Rosu, 2012; Hutchinson & Bridge, 2015; Pakela et al., 2022; Vedam et al., 2003; W. J. Wang et al., 2018). Unlike a 3D CT scan, a 4D CT scan requires the body part to be stationary. 4D visuals show breathing, tumour movement, and how surrounding organ movement affects tumour position. Using 4D CT, radiation can be delivered at

a specific time in the respiratory cycle, reducing treatment-side effects (Atkins et al., 2015; Harada et al., 2016; Hof et al., 2009; Wang et al., 2009). Despite the benefits of 4D CT, variability in breathing patterns limits collecting. Artefacts can be visible even with breathing instruction. As well as higher patient radiation exposure and increased clinician work in delineating the target, 4DCT has its drawbacks.

2.12.3.1.2 SLOW CT SCAN

Currently, 4D-CT is used to remove the effects of respiratory motion to reduce tissue toxicity and ensure implementation accuracy. No four-dimensional computed tomography (4D-CT) machine is currently available in Ghana's three radiation oncology centres. Before 4-D CT, most European cancer centres employed slow CT, which proved beneficial (Chinneck et al., 2010; Lagerwaard et al., 2001; Van Sörnsen De Koste et al., 2001, 2003; S. A. Yoganathan et al., 2017). As a result, this study will utilise a slow CT scan. Slow CT scanning is performing many CT scans throughout numerous breathing cycles. A slow CT scan is performed with a slow gantry rotation speed to capture the entire spectrum of tumour movement within each slice. A slow CT scan produces a volume that encapsulates the tumour.

2.12.3.2 MOTION CONTROL TECHNIQUES

2.12.3.2.1 ABDOMINAL COMPRESSION

Abdominal compression (AC) is a systematic method for controlling respiratory motion in lung cancer patients receiving SBRT. Several studies have demonstrated its usefulness in reducing the amplitude of respiratory-induced tumour movements (Heinzerling et al., 2008; Negoro et al., 2001; Qi et al., 2021). However, it is difficult to replicate the compressive effects of AC throughout an SBRT treatment due to changes in the patient's anatomy, girth, and breathing patterns. Due to these

modifications, the likelihood of underdosing and overdose of neighbouring normal tissues may increase.

2.12.3.2.2 INHALATION AND EXHALATION BREATH-HOLD CT

Breath-hold CT scans are done twice during the breathing cycle, at the end of the inspiration and the expiration. Breath-hold is linked to a duty cycle in which the beam is turned on and off based on how well the tumour's location is known at all times.

2.12.3.2.3 GATING

The therapy beam may be 'gated' or administered only during specified respiratory phases or amplitudes set during treatment planning. During treatment, an external surrogate is employed to assess the breathing cycle. The association between surrogate gesture and tumour motion must be evaluated regularly to verify that there is no geographical miss. Gating may be done in two ways: by phase or amplitude, although phase-based gating is more prevalent. Respiratory gating has been explored, and many motion approaches have been used as surrogates for tumour placement (Giraud et al., 2011; Giraud & Houle, 2013; Kraus et al., 2021; Saito et al., 2014).

2.12.3.2.4 TRACKING

Tumour tracking techniques are enhanced motion management that enables real-time tumour position tracking while continually irradiating the tumour (Giraud & Houle, 2013; Seppenwoolde et al., 2002; Shimizu et al., 2001).

2.12.3.3 TUMOUR AND OAR DELINEATION

For effective and safe lung stereotactic body radiation therapy planning, accurate identification of the tumour and surrounding organs at risk is crucial (SBRT). SBRT utilises the target criteria established by the International Commission on Radiation Units and Measurements in its Reports 50 and 62 (ICRU 50, 1993; ICRU 62, 1999). The clinical target volume (CTV) and the position

may change due to respiratory movements or organ dynamics in specific locations. Respiratory motion is often compensated for by increasing the CTV by an internal motion margin, resulting in an internal target volume (ITV) volume. Because the demarcation of an ITV implicitly includes the CTV under the premise that microscopic disease expansion is integrated within the zone of internal motion, the CTV is often left undefined in these instances. Stable locations may not need the use of an ITV.

2.12.4 TREATMENT PLANNING

The planning CT is imported into the Treatment Planning System (TPS). A treatment plan employing the optimal combination of radiation beams to the target while sparing normal tissues is developed. Treatment Planning System (TPS) is specialised software used to produce patient-specific treatment plans. Before treating patients, these systems primarily enable clinicians to anticipate the dose delivered to each voxel in the patient for a particular orientation of the radiation beams and other factors. The ideal treatment plan with the highest therapeutic ratio is selected.

Simple non-overlapping beams or arcs covering a sizeable angular range are used to achieve rapid dose fall-off in SBRT. Assuring that the PTV dose coverage is adequate, the radiation oncologist checks dose/volume statistics. The volume of nearby normal tissues exposed to high and medium doses is reduced. An optimised 3-D design eliminates excessive prescription dosage levels within normal tissues. Dose/volume statistics for surrounding tissues and organs ensure that volume-based restrictions are not exceeded.

PTV margins can be estimated utilising enhanced treatment planning methods that account for image guidance's improved positional precision and thoracic tissue density fluctuations. Treatment planning options include 3-D CRT, IMRT, VMAT, and ARC.

Before treatment plan approval, evaluation occurs. There are numerous evaluation techniques available for radiation plans. In general, the evaluation of a treatment plan is conducted on two levels: the treatment portals and the isodose distribution. On five different levels, the isodose distribution can be examined: isodose curves, orthogonal planes and isodose surfaces, dose distribution statistics, differential dose-volume histogram, and cumulative dose-volume histogram. In radiotherapy treatment planning, dose-volume histograms (DVHs) connect radiation dose to tissue volume and are commonly utilised. Differential and cumulative DVHs are two often employed forms. Differential DVH represents the proportion or absolute volume (depending on the mode of the display) receiving dosage in the corresponding dose bin.

In contrast, cumulative DVH reflects the percentage or absolute volume getting a value greater than or equal to the corresponding dose bin's value. These DVHs are also utilised to construct additional radiobiological plan parameters, including tumour control probability (TCP) and normal tissue complication probability (NTCP) (NTCP). Cumulative DVH is employed at the research centre to evaluate treatment plans. It is the conversion that determines which volume receives which dose. It offers dose distribution statistics over a three-dimensional matrix of points representing the patient's anatomy as a quantitative evaluation tool.

2.12.5 SBRT QUALITY ASSURANCE PROGRAMME

SBRT needs higher precision and accuracy criteria than traditionally fractionated radiation therapy or intensity-modulated delivery because of the high radiation doses used per fraction. Several task groups and studies exist to aid in the commissioning and quality assurance of SBRT delivery devices (Lambrecht et al., 2019; Moustakis et al., 2020; Solberg et al., 2012; Xia et al., 2020).

2.12.6 TREATMENT DELIVERY AND VERIFICATION

Each therapy requires accurate patient positioning, radiation beam placement, and stereotactic localisation of the target, which is achieved by imaging and implanting a fiducial marker (s). The projected effects are identical whether delivery systems use room-mounted or on-board x-ray or CT-based localisation for image guidance. Visible tumours, fiducial markers, or pertinent anatomic landmarks are utilised for any localisation strategy. Imaging can also confirm the localization or preceding filling/emptying (i.e. full bladder treatments) of critical normal structures. Image-guided stereotactic surgery aims to confirm or modify the patient's position relative to the anticipated image data collection.

The inability of motion assessment methodologies to effectively account for changes in breathing patterns between the time of image capture and therapy is a disadvantage. Researchers have considered respiratory gating to mitigate this drawback, which includes using a trigger to activate and deactivate therapy. Some tumour mobility management techniques may be required for SBRT to reduce lung tumour migration. This will reduce the extent of the radiation field, hence decreasing the amount of healthy tissue exposed to a high radiation dose. Four-dimensional imaging (4-D MRI and 4-D CBCT), gating, monitoring, and breath-hold techniques are some of the tumour motion control measures performed in the room before therapy administration.

2.12.7 IMAGE-GUIDANCE RADIOTHERAPY (IGRT)

Image-guided therapy administration is a crucial aspect of stereotactic treatment administration. The primary objective of IGRT is to improve treatment precision by accurately matching the patient and his or her tumour before radiation administration. Improved image guidance may result in shorter PTV margins and lower doses to OARs while preserving optimal target coverage. Multiple studies have demonstrated that image-based verification of the target location has the

most significant impact on improving the precision of lung SBRT. Therefore, daily pre-treatment imaging is performed with online correction of set-up errors and baseline shifts; imaging must reveal the lung tumour directly or implanted markers as proxies for cancer location. During or after SBRT, imaging serves as a quality control measure. Kilovolt (kV)/megavolt (MV) orthogonal X-rays or cone-beam (CB) kV/MV CT scans may give precise alignment.

Electronic portal imaging systems were used after using planar film for image guiding (EPIDs). Verifying the treatment field via MV imaging is still common. While MV imaging is suitable for soft tissue contouring, it is inferior for bone. The addition of kV imaging arms to linear accelerators and EPID data collection have been widely used due to lower patient dosage and improved image quality. The EPID has limitations in imaging dosage, fiducial requirements, volumetric spatial resolution, and directional beam entrance. CBCT enables patient placement modification based on 3D soft tissue architecture, unlike the planning scan.

2.12.8 FOLLOW-UP AND OUTCOMES ASSESSMENT

All treated patients should be monitored for local control, survival, and normal tissue damage. In addition to participating in medical follow-up, radiation oncologists should review post-SBRT diagnostic imaging for possible post-treatment sequelae. Subacute or late toxicities can arise months or even years after radiation therapy. A legislative or regulatory peer-review method should be used to acquire confidential peer-review data.

CHAPTER THREE

MATERIALS AND METHODS

3.1 ETHICAL STATEMENT

The research protocol was reviewed and approved by the Ethics Committee for Basic and Applied Sciences (ECBAS) of the University of Ghana (ECBAS 05/20-21) and Komfo Anokye Teaching Hospital Institutional Review Board (KATH IRB) (KATH IRB/AP/095/21) in Appendix A.

3.2 STUDY SITE

The study was carried out at the Oncology Directorate of Komfo Anokye Teaching Hospital (KATH). There are only three radiotherapy centres in Ghana, two public (Komfo Anokye Teaching Hospital and Korle Bu Teaching Hospital) and the other private (Sweden Ghana Medical Centre). Komfo Anokye Teaching Hospital is a 1200-bed facility located in Kumasi, the Regional Capital of the Ashanti Region, with a total projected population of 4,780,380 (2010 Ghana population census). KATH's geographical location, the country's road network, and the commercial nature of Kumasi make the hospital accessible to all the areas that share boundaries with the Ashanti Region and Ghana. The Hospital serves patients from twelve out of the sixteen administrative regions in Ghana. It also receives patients from neighbouring countries, including Ivory Coast and Eastern Faso. The Hospital is made up of thirteen clinical Directorates and two non-clinical Directorates. The oncology Directorate is part of the clinical Directorates.

KATH Oncology Directorate provides outpatient services: radiation oncology, medical oncology, and haematology. The oncology Directorate is resourced with a medical linear accelerator, cobalt 60 teletherapy unit, X ray simulator, LDR brachytherapy, and 3D and 2D treatment planning systems to provide cancer care to patients in areas ranging from primary, secondary and tertiary

care. The centre treats all cancers, with over 1200 patients treated yearly. Lung malignancies referred to as KATH are treated as static tumours without the use of any motion management strategies. Thus, comparatively more significant margins are used to account for tumour motion during treatment planning, resulting in the irradiation of relatively larger healthy tissue sizes around the tumour and leading to relatively high toxicity in the lungs and radiation injuries such as radiation pneumonitis. Therefore, it is imperative to develop and implement an approach for lung cancer radiotherapy at KATH that considers the tumour motion. The medical linear accelerator used in KATH for external beam radiotherapy is equipped to deliver SBRT treatment. However, such has not been done. This approach can significantly conform dose tightly to the target volume related to tumour control and could lead to enhanced biochemical degeneration free survival and cancer advancement free survival. Thus, it will have a very high impact on the care provided to lung cancer patients at KATH. Furthermore, irradiating less healthy lung tissue will mean fewer treatment toxicities and a potential increase in patients' quality of life.

3.3 EQUIPMENT

3.3.1 LINEAR ACCELERATOR

A medical linear accelerator (LINAC) is a device used for external beam radiotherapy for patients with cancer. Varian Clinac iX is the linear accelerator used at the Oncology Directorate of KATH for cancer treatment. The Clinac iX™ linear accelerator (Figure 3.1) by Varian Medical Systems, Incorporation. is a customised external beam radiotherapy equipment for treating cancer with image guidance. The Clinac offers 3D CRT, IMRT, IGRT, VMAT, RapidArc™ and stereotactic radiosurgery treatments. Clinacs are usually equipped with On-Board Imager (OBI), high-intensity mode, RapidArc, RPM gating and motion management tools to deliver fast and effective patient treatments with accuracy. The Clinac iX installed at KATH for the treatment of cancer patients

has two-photon energies (6 MV and 16 MV) and four-electron energies (6 MeV, 9 MeV, 12 MeV and 16 MeV). The Clinac iX offers two photon beams (6 and 16 MV) and four-electron energies (6, 9, 12 and 15 MeV). The Clinac customizes high energy x-rays or electrons to conform to a tumour's shape and destroy cancer cells while sparing surrounding normal tissue. Clinac iX is used to treat all body sites using conventional techniques.

Figure 3.1: Varian Clinac iX.

3.3.2 COMPUTED TOMOGRAPHY (CT) SCANNER MACHINE

A CT scanner machine is medical diagnostic equipment that uses x rays to generate 3D images of the interior of patients for diagnostic purposes. The Siemens SOMATOM Perspective shown in Figure 3.2 is a computed tomography with a 128-slice configuration, 70 cm gantry aperture and a 50 cm scan field. The patient couch can hold patients' weights up to 200 kg and offers a reconstruction of 64 images.

Figure 3.2: Siemens Somatom Perspective CT scanner

3.3.3 DOSIMETRY EQUIPMENT

Dosimetry is a method for measuring, estimating, and evaluating absorbed doses of radiation. Medical physicists utilise dosimetry to ensure that radiotherapy equipment is calibrated appropriately and provides accurate radiation to patients. Figure 3.2 depicts the dosimetric equipment used for dose verification in this study.

(a) (b)

(c)

(d)

Figure 3.3: (a) Handheld Traceable barometer, (b) Siemens CT phantom, (c) Max 4000 Plus electrometer and (d) Exradin A19 ionisation chamber.

For dosimetry measurements, detectors are typically paired with a phantom. Dosimetry detectors include radiographic film, radio-chromic film, ionisation chambers, thermoluminescent detectors (TLDs) and optically-stimulated luminescent detectors (OSLDs), metal oxide semiconductor field-effect transistors (MOSFETs), diamond detectors, Alanine – Electron paramagnetic resonance and Gel dosimetry detectors. In this investigation, the ionisation chamber was chosen for dosimetry measurements. The Exradin® ion chamber is designed for clinical dosimetry measurements. Exradin® A19 ionisation chamber (Standard Imaging, Inc.) is a waterproof classic farmer type ion chamber characterised for absolute dosimetry.

A traceable digital barometer shows the barometric pressure trend and contains a stopwatch/timer and compass. A thermometer and altimeter are included. International dosimetry protocols require a temperature-pressure correction factor for vented ionisation chamber measurements. When measuring conditions comparable to reference conditions under which the ionisation chamber was calibrated, measurements are valid without adjustment considerations.

Max 4000 Plus electrometer is a display device for the radiation measurements done by the ionisation chamber. MAX 4000 Plus electrometer is designed for output measurements and data.

CT phantom is a highly specialised artefact used in medical imaging for quality control, equipment calibration, dosimetry, and education. CT phantom is a calibration phantom with known densities.

3.3.4 RADIOTHERAPY TREATMENT PLANNING SYSTEM (RTPS)

Eclipse Treatment Planning System (Varian Medical Systems, Palo Alto, CA; version 15.6) is a three-dimensional (3D) radiotherapy treatment planning system (Figure 3.4). The KATH Eclipse TPS features network connectivity for the automated transmission of image datasets and digital data interchange between workstations and other systems. Eclipse generates optimised treatment plans for patients undergoing external beam radiotherapy in the Directorate. Analytical Anisotropic Algorithm (AAA) is the dose algorithm for dose distribution computations now utilised at the study site. The AAA models the contributions of primary photons, extra-focal photons, and contaminated electrons individually and better accounts for the lateral flux. Additionally, AAA improves precision, particularly for dose estimations in heterogeneous media such as the lung.

Figure 3.4: Varian Eclipse™ treatment planning system user interface showing isodose distribution.

3.4 LUNG PHANTOM FABRICATION

3.4.1 TISSUE EQUIVALENCE OF WOOD AND TUMOUR SAMPLES

The tissue equivalence of locally accessible materials, such as wood and tumour-simulating samples, was evaluated. Some selected wood samples from a wood workshop were assessed to determine their lung tissue equivalence. To replicate the tumour, samples of chalk and perspex were created.

Computed tomography scans were performed on the Siemens Somatom Perspective CT at KATH's Accident and Emergency Unit shown in Figure 3.5.

Figure 3.5: Siemens Somatom Perspective CT scanner used in this study (Komfo Anokye Teaching Hospital, Kumasi).

First, the CT scanner was calibrated by scanning a Computed Tomography phantom with a known radiodensity to determine whether the scanner data provided the appropriate quantity of Hounsfield Units (HU) (Figure 3.6).

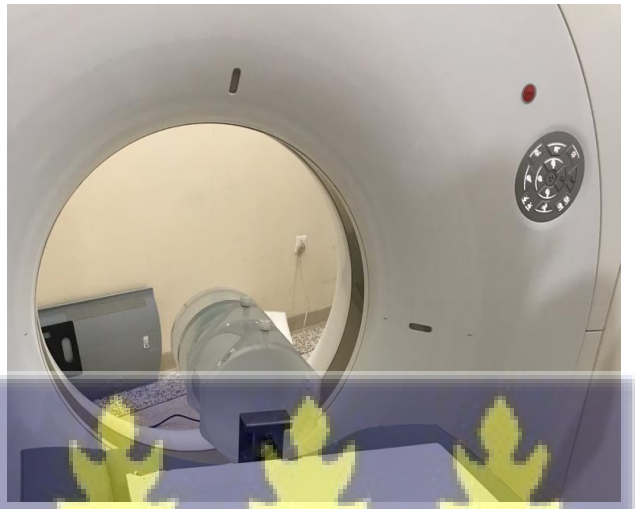

Figure 3.6: Setup for the determination of air and water CT numbers.

The prepared wood, chalk, sawdust plugs, and perspex samples were positioned on the couch (Figure 3.7) for CT scanning to assess their CT numbers and determine lung and tumour tissue equivalence. There were six wood samples, three sawdust plugs, two perspex plugs, and three chalk tumour samples.

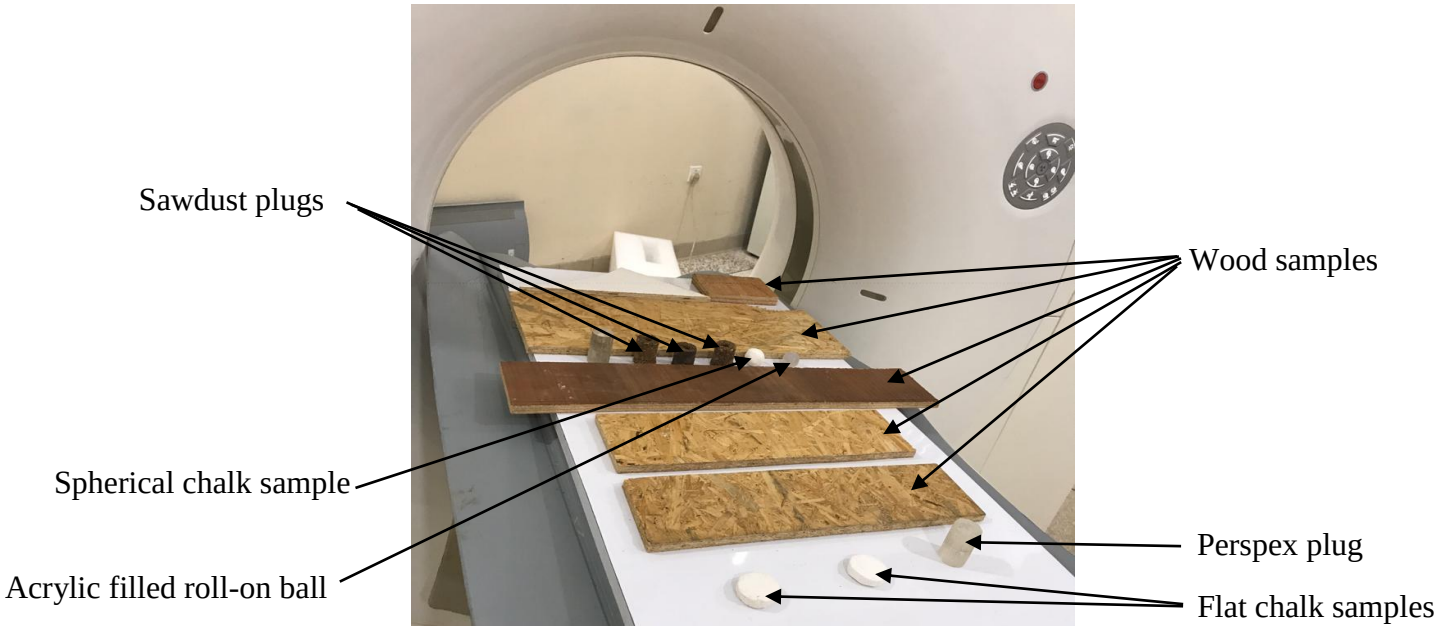

Figure 3.7: Lung and tumour simulating samples.

The adult CT procedure was employed for the scan, and the lung window was applied to see the wood samples. As shown in Figure 3.8, regions of interest were created to display the CT numbers on the pictures. Based on the CT scans, a suitable wood sample was chosen to create the lung field for the phantom.

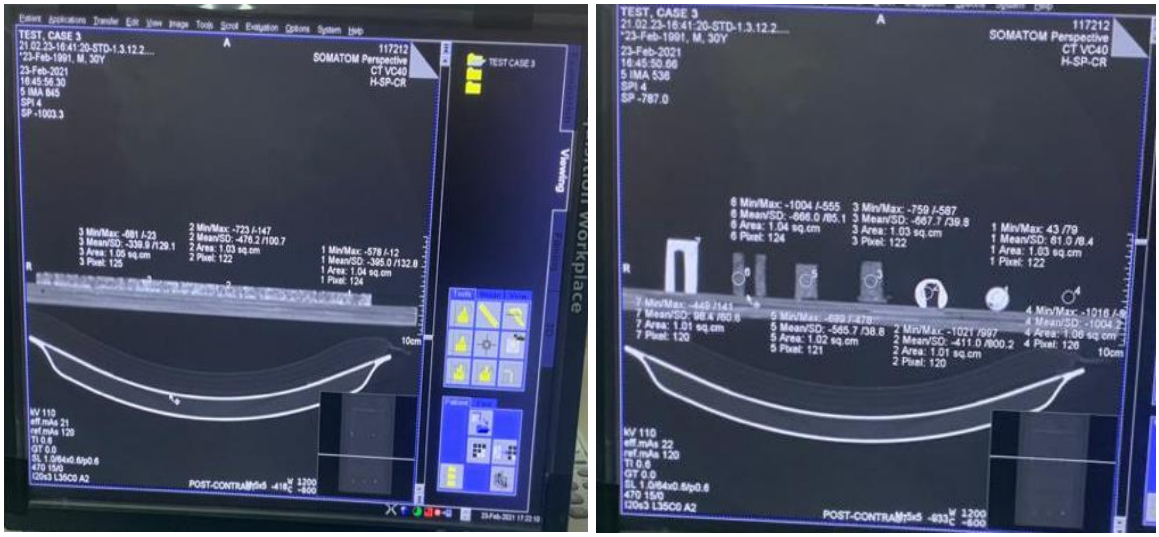

(a) (b)

Figure 3.8: CT scan images (a) wood sample; (b) perspex, chalk, and sawdust samples.

3.4.2 WATER TANK-TYPE LUNG PHANTOM DESIGN AND DEVELOPMENT

Phantoms are used in clinical and preclinical radiation dosimetry to study the effects of radiation on an organ or tissue. They can be made of water or more complicated materials and have definite shapes and sizes (Biglin et al., 2019). Following the design of Nishio et al. (2014), a lung SBRT phantom was built using locally accessible materials. These materials include PMMA, wood, and acrylic filled roll-on balls. Using the schematic diagram in Figure 3.9, an initial prototype, as shown in Figure 3.10, was built using locally accessible materials.

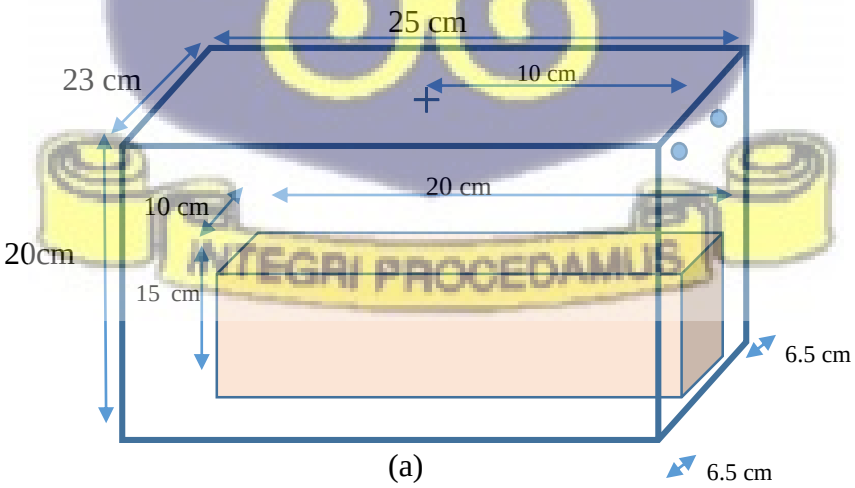

(a)

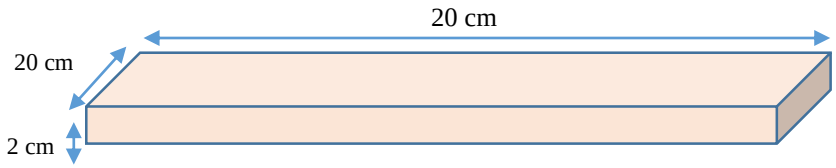

(b)

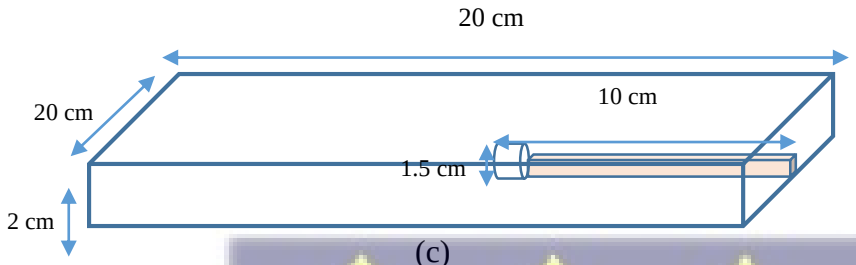

(c)

Figure 3.9: Schematic diagram of lung phantom. (a): phantom design; (b): schematic diagram of simulated lung field inserts; (c): diagram of the wood slab with indentation to accommodate simulated tumour and ionisation chamber cable.

(a) (b)

Figure 3.10: Prototype lung phantom (a) top view; (b) frontal view

As PMMA is extensively used in radiation dosimetry and was approved by the IAEA as a substitute for water, it was selected as the phantom material. Figure 3.11 depicts a generated heterogeneous lung phantom comprised of a 3 mm thick polymethyl methacrylate (PMMA), a lung field comprised of eight 2 cm wood slabs, and a simulated 2.9 cm spherical tumour buried in the lung field. The form and size of the phantom offer the possibility of simulating a human torso, and the PMMA tank can be filled with water, a tissue-equivalent material, via an opening on the front view.

(a) (b) (c)

Figure 3.11: Lung phantom; (a) frontal view (b) side view (c) top elevation.

As illustrated in Figure 3.12, the simulated tumour consisted of a roll-on ball filled with acrylic powder and a 1 cm hole in the centre to accommodate the effective length of the sensitive part of the ionisation chamber to detect the radiation. The tumour size was determined because most treated tumours are between 1.5 and 7.2 cm in diameter (Wolthaus et al., 2008). The two main wood slabs that sandwich the simulated tumour are a 0.5 cm semi-circular groove on each to house the ionisation chamber.

(a)

(b)

Figure 3.12: (a) Simulated tumour buried in wood slabs with groove (b) ionisation chamber inserted into the simulated tumour in the lung field.

3.5 MOTION PLATFORM

A motion platform was created to imitate the breathing effect. Sarudis et al. (2017) found that 95 per cent of the tumours in 126 individuals travelled 20 mm (2 cm) in the inferior-superior direction. The purpose of the motion platform was to enable the measurement of the real dosage distribution when the target is in motion. The movements were intended to be in the superior-inferior (SI) direction (z-axis), the long axis from the centre for distances between 0.5 cm and 1 cm. The SI direction was chosen because Liu et al. (2007) found that most of their individuals' tumours progressed more than 0.5 cm along the SI axes compared to the lateral and anterior-posterior (AP) axes. A motion platform with a car wiper motor installed as a variable displacement motor and a base trolley for the phantom, as depicted in Figure 3.13.

Figure 3.13: Motion platform with wiper motor connected to trolley.

3.6 SCANNING OF FABRICATED LUNG PHANTOM

The 4D CT scan is a novel image acquisition method that captures the tumour's position and mobility during distinct breathing phases. This allows investigation of the influence of intrafraction mobility on the tumour and adjacent tissue. However, in the absence of a 4D CT scanner at the study site, slow CT scanning was used to image moving targets in this study.

As shown in Figure 3.14, the phantom was scanned to determine the Hounsfield units of its constituent components. In this study, the adult chest protocol was used for all the CT scans

(a) (b)

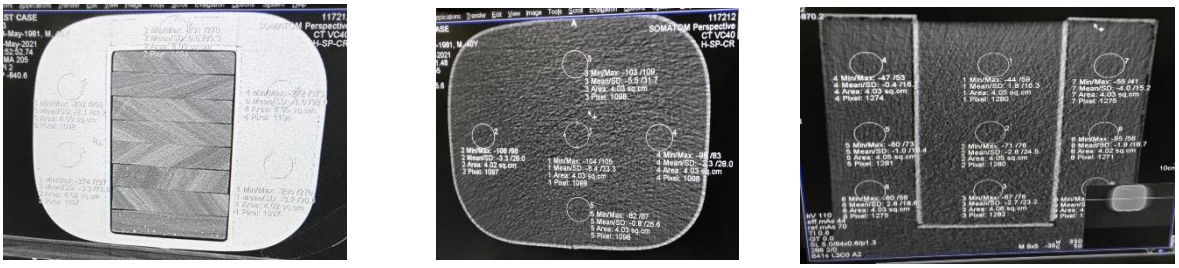

(c) (d) (e)

Figure 3.14: (a) and (b) set up for scanning fabricated lung phantom; (c), (d) and (e) are CT scan images of the fabricated lung phantom to assess the Hounsfield units of phantom components.

The lung phantom was set up as depicted in Figure 3.15 to obtain the standard and slow CT scans using the adult protocol with the following parameters: 110 kVp, 1 s gantry rotation time, 64 x 0.6 mm slice thickness, with a pitch of 0.4. A slow CT scan was performed, which portrays the spectrum of tumour movements more appropriately. Standard CT images were acquired at around 4s per slice, which is comparable to a typical breathing cycle. Slow CT scans of the moving phantom were taken using the same imaging approach as done for the standard CT, but with the longest available gantry rotation time of 0.6 s and the pitch reduced to 0.35 for 0.5 cm and 1 cm motions. Using a slice thickness of 1 mm, approximately 15 cm of the phantom containing the simulated tumour was scanned.

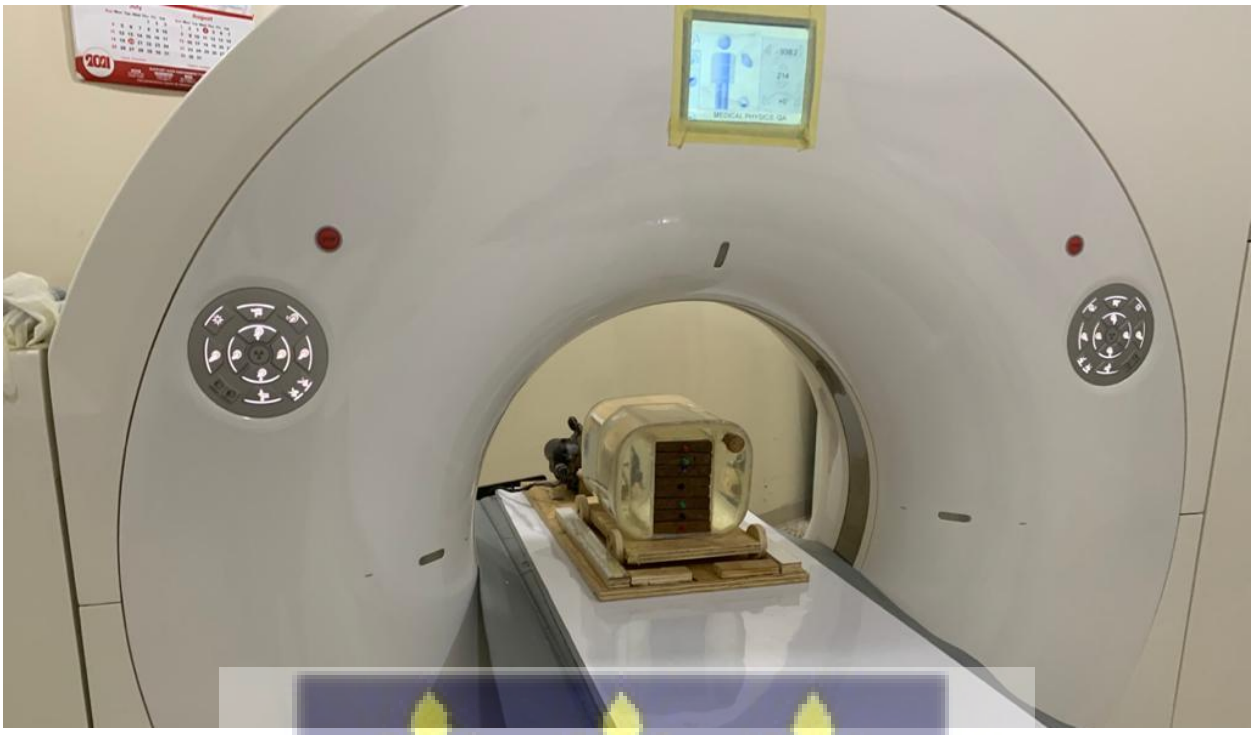

Figure 3.15: CT scan set-up of fabricated lung phantom on the motion platform.

A sample of CT images is presented in Figure 3.16.

Figure 3.16: CT scan user interface showing elevation and frontal view of the phantom.

3.7 CT SCANNER ELECTRON DENSITY CALIBRATION

The link between CT Hounsfield units and electron densities is critical for radiation treatment planning. To calibrate the treatment planning system's CT scanner, a CIRS electron density phantom was scanned to get Hounsfield units of tissue-equivalent materials (Figure 3.17). The phantom was aligned with lasers in the centre of a CT gantry and scanned using an adult abdominal imaging technique utilising kVp tube voltage. To calibrate the TPS, we used the CT numbers from the scan and the electron densities of the substitute tissues.

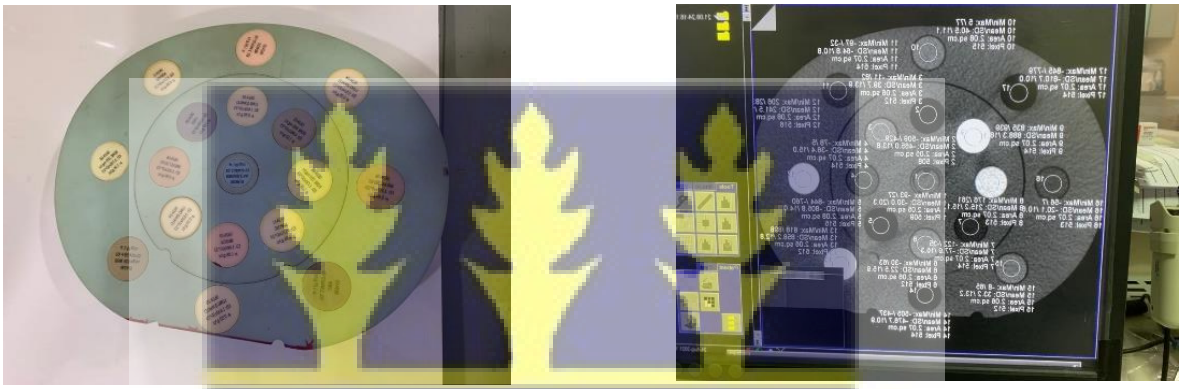

(a) (b)

Figure 3.17: (a) CIRS Electron Density Phantom 062M (b) CT scan image of CIRS Electron Density Phantom.

3.8 PHANTOM STUDY

3.8.1 CONTOURING OF VOLUMES

The lung phantom's standard and slow CT datasets were sent to the Eclipse TPS for treatment planning. Planning tumour volumes (PTVs) and organs at risk (OARs) were defined as recommended by ICRU 50 (1993), ICRU 62 (1999), and ICRU 83 (2010) reports.

As shown in Figure 3.18, only the PTV, lung, normal tissue, body of the phantom, and ionisation chamber cavity were outlined for the phantom experiments.

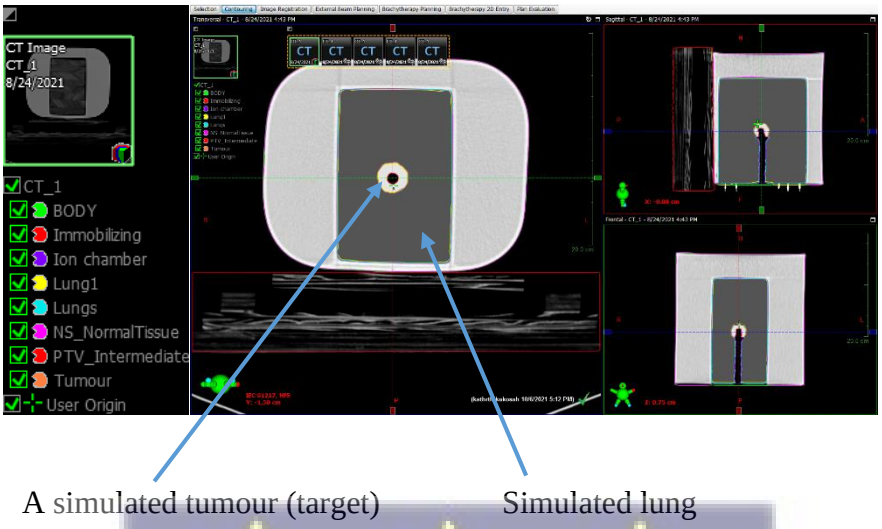

Figure 3.18: Contouring interface displaying transverse, sagittal and frontal views of the phantom CT image.

3.8.2 TREATMENT PLANNING

The Radiation Therapy Oncology Group (RTOG) lung protocol 0915 specifies the requirements for SBRT plans used in this study. Some clinical trials have shown improved local control rates and long term survival with these RTOG protocols (Chinniah et al., 2017; Hoffman et al., 2019; Osei et al., 2020; Videtic et al., 2015, 2019). RTOG prescription dose constraints for treatment planning and dose constraints employed in the treatment planning are in Table 3.1.

Table 3.1: RTOG planning dose-volume constraints (Bezjak et al., 2011; Videtic et al., 2014).

Volume/ OAR	Dose-volume constraints	
	48 Gy in 4 fractions	**50 Gy in 5 fractions**
PTV	$V_{100\%PD} \geq 95\%$	$V_{100\%PD} \geq 95\%$
	$V_{90\%PD} \geq 99\%$ maximum dose inside ITV	$V_{90\%PD} \geq 99\%$ maximum dose inside ITV
Bilateral lungs	$V_{11.6\ Gy} < 1500cc$	$V_{12.5\ Gy} < 1500cc$
	$V_{12.4\ Gy} < 1000cc$	$V_{13.5\ Gy} < 1000cc$
Spinal Cord	$V_{20.8\ Gy} < 0.35cc$, $V_{13.6\ Gy} < 1.2cc$	$V_{22.5\ Gy} < 0.25cc$, $V_{13.5\ Gy} < 0.5cc$
	Maximum point dose < 26 Gy	Maximum point dose < 30 Gy
Skin	$V_{33.2\ Gy}$ < 10cc maximum point dose < 36 Gy	$V_{30\ Gy}$ < 10cc maximum point dose < 32 Gy
Oesophagus	$V_{18.8\ Gy}$ < 5cc maximum point dose < 30 Gy	$V_{27.5\ Gy}$ < 5cc maximum point dose < 105% PD
Heart	$V_{28\ Gy}$ < 15cc maximum point dose < 34 Gy	$V_{32\ Gy}$ < 15cc maximum point dose < 105% PD
Great Vessels	$V_{43\ Gy}$ < 10cc maximum point dose < 49 Gy	$V_{47\ Gy}$ < 10cc maximum point dose < 105% PD
Trachea + bronchus	$V_{15.6\ Gy}$ < 4cc maximum point dose < 34.8 Gy	$V_{18\ Gy}$ < 4cc maximum point dose < 105% PD
Ribs	$V_{32\ Gy}$ < 1cc maximum point dose < 40 Gy	

3.8.2.1 FEASIBILITY TEST TREATMENT PLANNING

Before the SBRT treatment planning for the phantom, a feasibility test was conducted by producing a 3-D treatment plan utilising a four-field box approach consisting of two para-opposed fields and two lateral fields with 6 MV photon beams and a dosage prescription of 10 Gy in 5 parts (10 Gy/5). In Figure 3.19, the Eclipse TPS interface depicts the treatment plan for a 90 per cent isodose prescription.

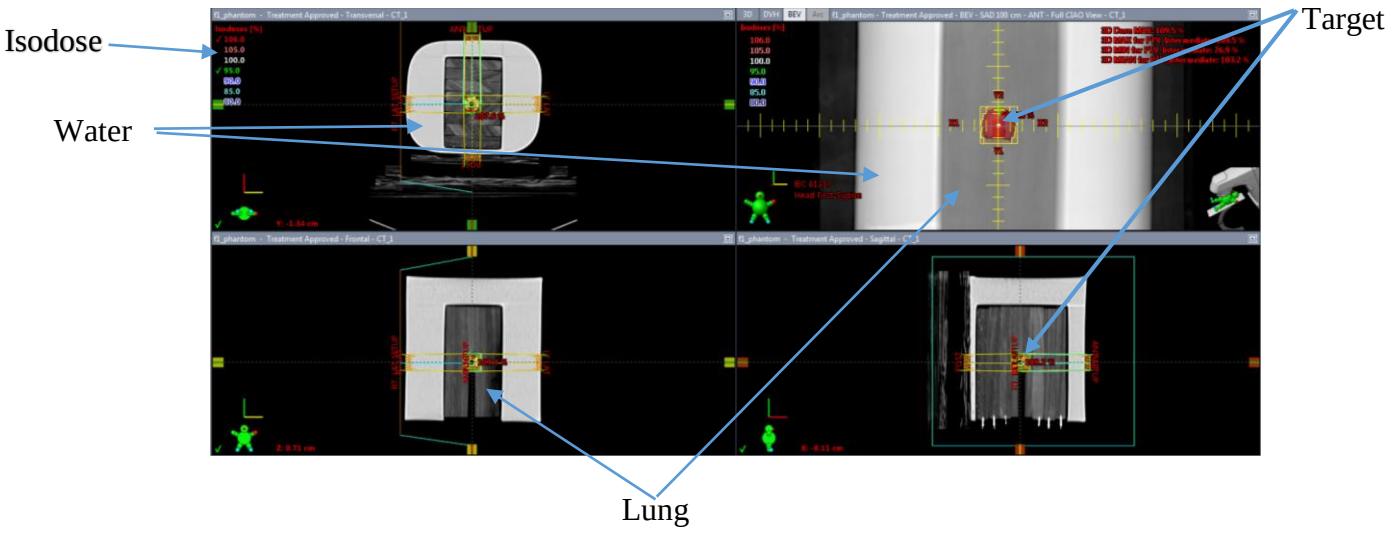

Figure 3.19: Eclipse TPS displaying external beam treatment plan of the fabricated lung phantom

Dose analysis of the dose-volume histogram (DVH) was performed for the plan quality before treatment was delivered.

3.8.2.2 LUNG SBRT TREATMENT PLANNING

3D CRT designs were generated for the phantom to meet target coverage and normal tissue sparing requirements. The treatment dose plans comprised eight (8) non-opposing and coplanar static beams with 6 MV. Several clinical trials have utilised dose prescriptions of 34 Gy in 1 fraction (34 Gy/1), 50 Gy in 5 fractions (50 Gy/5), and 48 Gy in 4 fractions (48 Gy/4) for lung SBRT. In this investigation, a prescribed dose of 50 Gy in 5 portions (50 Gy/5) was employed. Based on the RTOG 0915 (Videtic et al., 2014) and (Osei et al., 2020) studies, dose-volume limits served as a guideline for the three fractionated treatment plans.

The treatment plans were divided into two categories: with and without mobility. These were divided into three subcategories:

- Initially, a static plan based on conventional CT images was supplied to the phantom.

- Secondly, plans were created using slow CT scans that accounted for ITV and were executed on phantoms without motion.
- Thirdly, plans were developed on slow CT images and provided with the phantom in motion.

Figures 3.20, 3.21 and 3.22 show the static beam plan as it appears in the Eclipse TPS. The plan entails 3-D plan beam alignments and dose distribution.

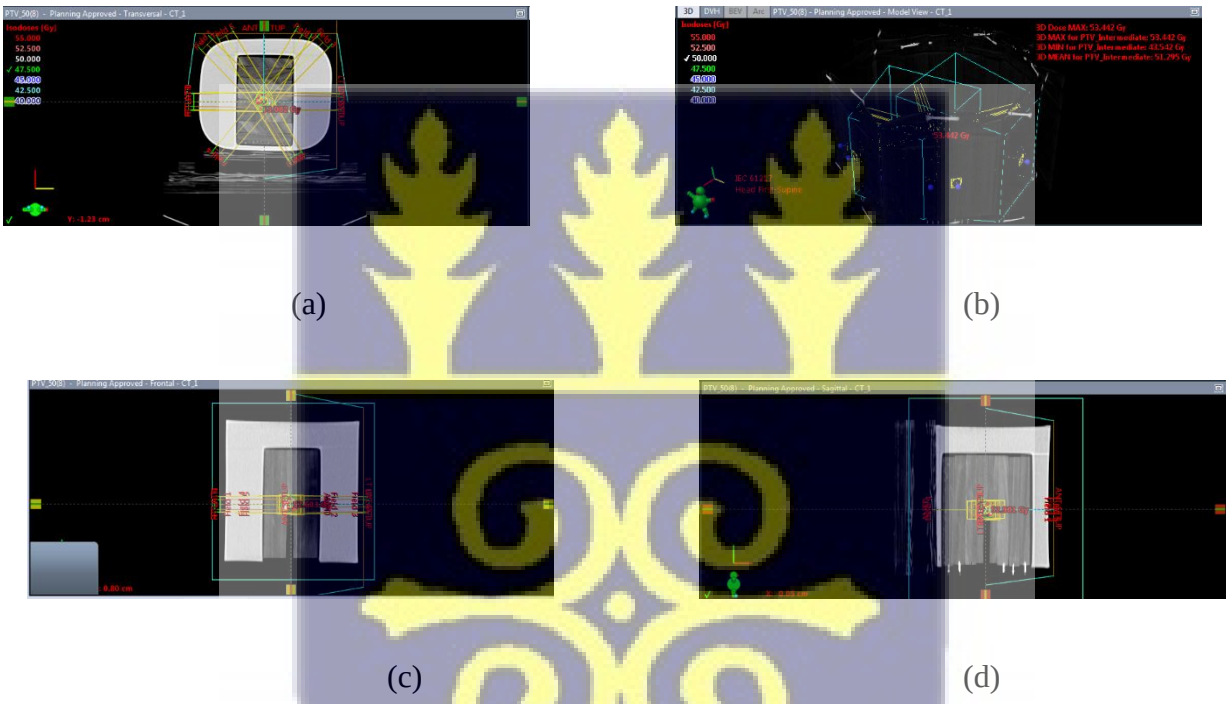

(a) (b)

(c) (d)

Figure 3.20: Static treatment plan with 50 Gy/5 prescription dose; (a) Transverse view, (b) 3D view, (c) Coronal view and (d) Sagittal view.

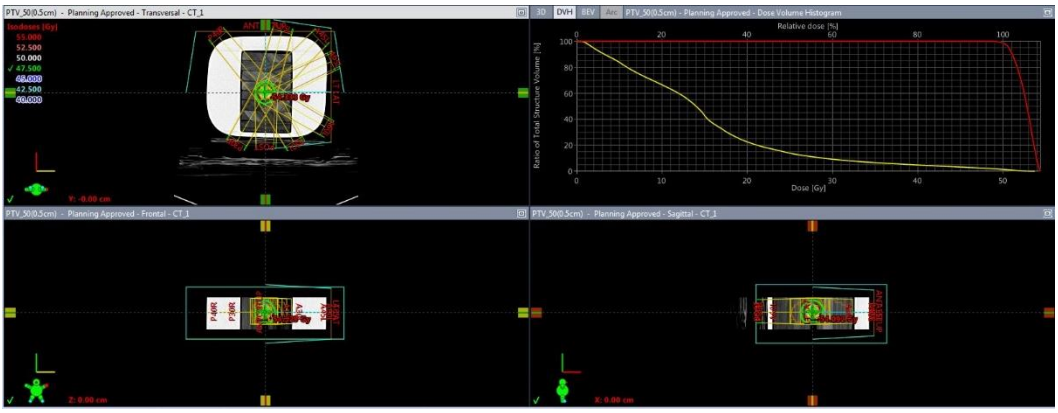

Figure 3.21: Treatment plan with 50 Gy/5 prescription dose for phantom in 0.5 cm motion

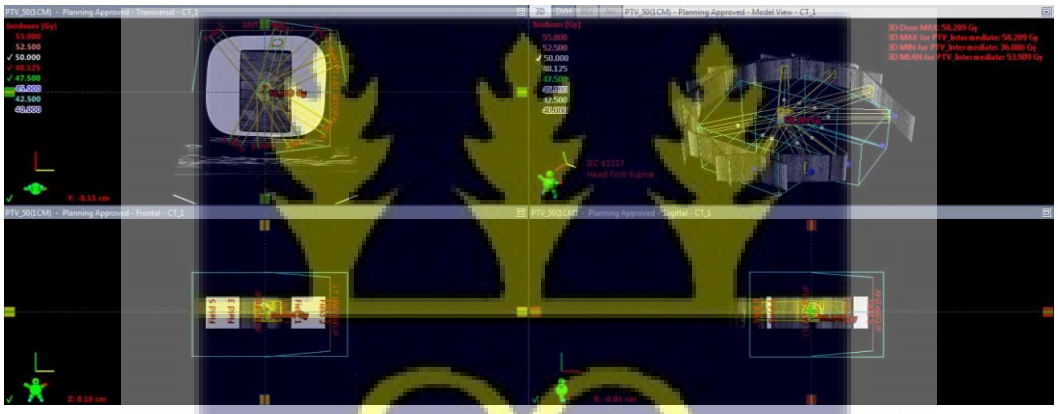

Figure 3.22: Treatment plan with 50 Gy/5 prescription dose for phantom in 1 cm motion

3.8.2.3 LUNG SBRT TREATMENT DELIVERY

The treatment plan was delivered using the Varian Clinac iX treatment machine (Figure 3.23).

Figure 3.23: Varian Clinac iX linear accelerator at Oncology Directorate, KATH (without On-Board Imager)

This same setup for CT image acquisition was used at the time of dose delivery for target localization, as depicted in Figure 3.24, with an Exradin A19 ionisation chamber placed in the centre of the simulated lung region for radiation detection during treatment and coupled to a MAX 400 Plus electrometer that displayed the radiation in charges. Using the formula in the equation, the measured electrometer reading was converted to dose.

$$M = R(C)\ x\ N_{DW}\ x\ P \qquad (3.1)$$

$R = electrometer\ reading\ (\boldsymbol{C})$

$N_{DW} = ionisation\ chamber\ coefficiet = 4.771\ E7\ Gy/C$

$P = perturbation\ factor = K_Q\ x\ K_{T,P}\ x\ K_{pol}\ x\ K_s$

$K_Q =$ *beam quality used for calibration* $Co - 60$

$K_{T,P} =$ *temperature and pressure correction factor*

$K_{pol} =$ *polarity correction factor*

$K_s =$ ion recombination factor

(a) (b) (c)

Figure 3.24: Lung phantom treatment set-up, (b) researcher setting up electrometer and (c) electrometer displaying radiation measurement.

Electronic portal imaging device (EPID) images were obtained for orthogonal fields (Figure 3.25) using the Clinic's gantry to verify the phantom setup. Target localization and phantom repositioning were performed for all treatment sessions, and EPID pictures were matched with planned CT images. During treatment, imaging permits the visualisation of the actual tumour. The availability of respiratory information within the obtained images enables creative anatomical collation. Each tumour position was recorded relative to the initial intended position, allowing the

daily average position to be calculated. To achieve symmetrical dosage distribution, baseline shifts were then rectified by aligning the average position photographs with the target position recorded during planning. Exradin® A19 ionisation chamber and MAX 4000 Plus electrometer were used for the dosimetric measurements and verification of the prescribed and planned doses.

(a) (b)

Figure 3.25: Image verification set up (a) anterior; (b) lateral.

3.8.3 CLINICAL CASE STUDY

The lung phantom only provided information on the dose to the target volume. Hence, a clinical case was simulated to demonstrate exposure to organs at risk (OARs). One patient's CT dataset of a thoracic CT scan demonstrating full lung coverage was located and utilised in a clinical case study for dosimetric analysis of OARs not included in the phantom investigation. At the Oncology Directorate of the Komfo Anokye Teaching Hospital, CT scans were accessed through the Eclipse Treatment planning system. This patient was not diagnosed with lung cancer but with other cancers that required thoracic CT scans.

3.8.3.1 Target and OARs Delineation

SBRT planning incorporates features that are not typically contoured in conventional fractionated plans, which frequently depend on the tumour's location to be treated. Normal OAR structures and targets were defined and contoured per the atlas for OARs in thoracic radiation therapy based on RTOG 0813 and 0915 standards. The OARs consist of the lungs, heart, spinal cord, ribs, bronchial tree, oesophagus, and trachea. For the clinical example, the identified targets and OARs include bilateral lung (right and left), heart, spinal cord, oesophagus, tracheaproximal bronchial tree (left) and ribs. To simulate the phantom scenario and a clinical lung case, respectively, 3 cm and 1 cm tumours were contoured.

3.8.3.2 Lung SBRT Treatment Planning

Using the Eclipse TPS, eight-field 3D treatment plans were developed with 6-MV photon beams and a target prescription dose of 48 Gy in four fractions (48 Gy/4) and 50 Gy in five fractions (Varian Medical Systems, Palo Alto, USA, version 15.6). Analyses were conducted using dosimetric data concerning vital structures. Figures 3.26 and 3.27 depict the beam static plans in the Eclipse TPS used in this investigation for the dose prescription of 50 Gy/5 for 3 cm and 1 cm tumours, respectively. The Figures depict 3-D plan beam alignments and dosage distribution.

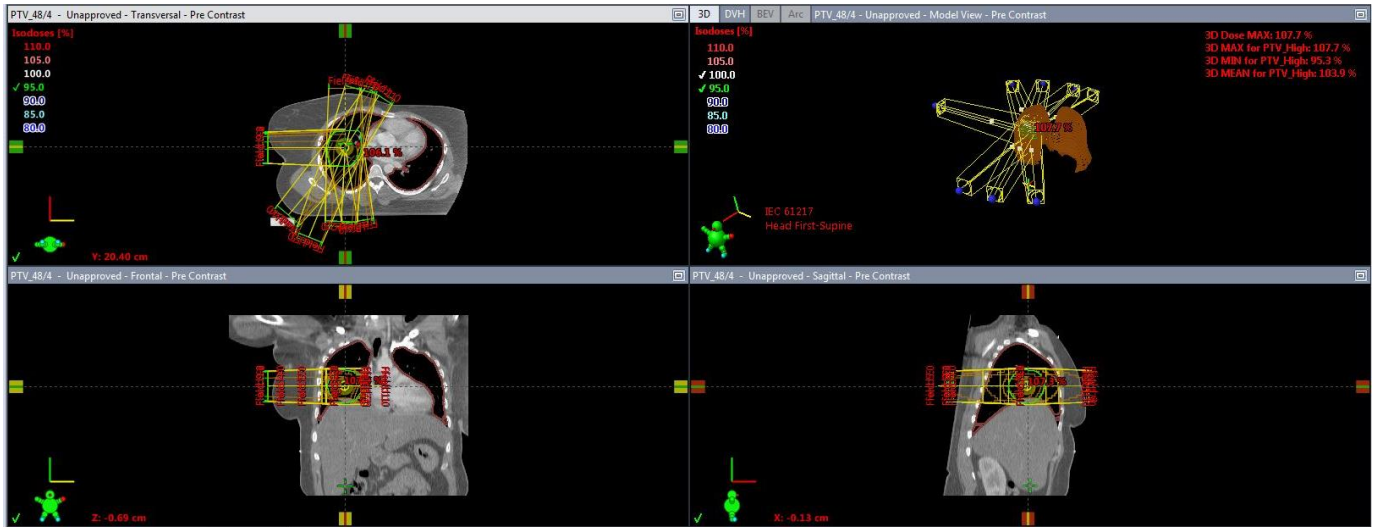

Figure 3.26: Treatment plan with 50 Gy/5 for a 3cm tumour

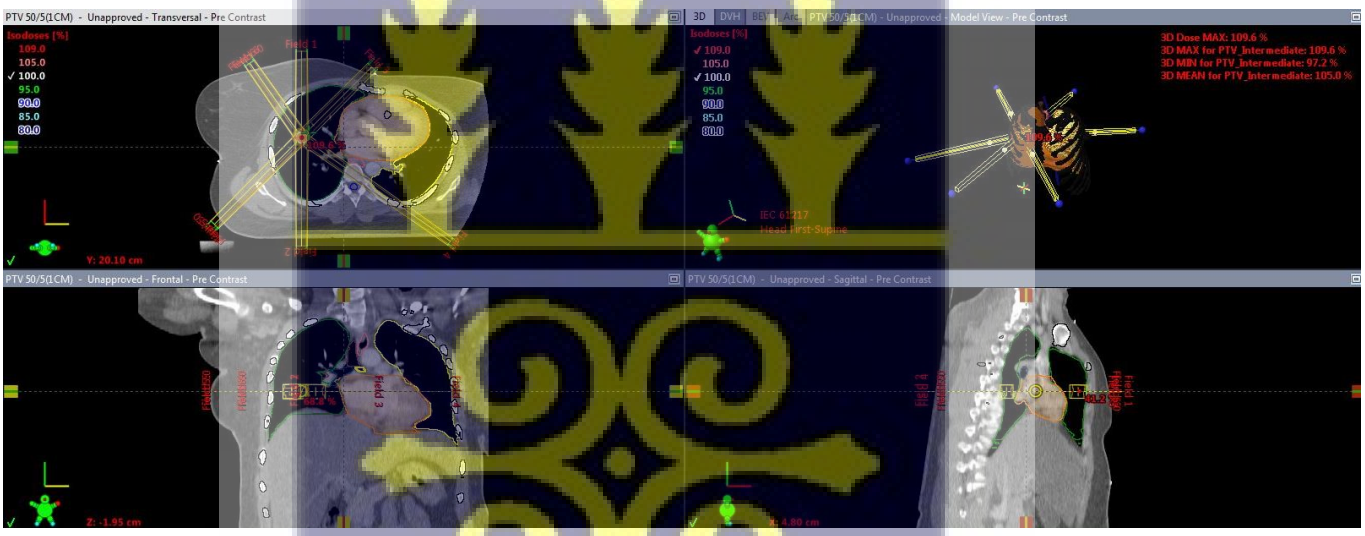

Figure 3.27: Treatment plan with 50 Gy/5 for 1cm tumour

3.9 TREATMENT PLAN EVALUATION

Targets and normal tissue doses of produced treatment regimens were thoroughly examined. Plan quality assessment utilised recommended practical criteria for dosimetry measurements from RTOG 0831 and 0915. Each treatment plan's DVH for the goal and OAR was analysed for the two

prescribed doses. Plans for normal structures were evaluated based on dose statistics comprising minimum, maximum, and mean dose/volume parameters from dose-volume histograms (DVH).

Target coverage, heterogeneity indices, conformance indices, dosage spillage, and gradient index were utilised to evaluate dose distribution objectively. Conformity index (CI) and gradient index were calculated using dose information from the treatment planning system. Homogeneity index (HI) was computed using a ratio of the dose received by 5 per cent of the target volume (D5) to the dose received by 95 per cent of the target volume (D95), as described in equation 3.2.

$$HI_{5/95} = \frac{D_5}{D_{95}} \qquad (3.2)$$

Plan acceptability for target coverage is considered when the maximum dose is within the PTV, at least 99% of the PTV volume is covered by 90% of the prescription dose ($V_{90\%PD}$ > 99%), and the prescription dose covers at least 95% of the PTV volume ($V_{100\%\ PD}$ > 95%). Plan acceptability for OARs is governed by organ dose-volume constraints (Table 3.1).

CHAPTER FOUR

RESULTS AND DISCUSSION

4.1 LUNG AND TUMOUR SIMULATION SAMPLE

CT data of locally available materials sampled to simulate lung tissue and tumour located within the lung were obtained using a Siemens Somatom Perspective CT scanner. Kalef-Ezra et al. (1999) studied the lungs of healthy subjects from entire lung scans and reported mean CT numbers (HU) of -722 and -746 for women and men, respectively. Ohkubo et al. (2016) also studied the lung volume and defined the CT number to be between -950 and -701. Mayer et al. (1998) noted a lung tumour CT number threshold of 13 HU in their study on CT number distribution and its association with local control and as a marker of lung tumour response to radiation. Paul et al. (2017) investigated lung cancer response during radiotherapy and observed substantial changes in the gross tumour volume mean HU between 11 to 48 HU (median 30). From these studies, the HU range of 11 to 48 was used to select suitable materials to simulate tumours.

Table 4.1 presents the CT data of the various samples assessed. Wood samples 2 and 4 were found most suitable with CT numbers comparable to a normal lung and therefore used to develop the lung of the phantom. Comparing the measured HU of the various samples scanned to the reference HU given by literature the following were found suitable: wood samples 1 and 3 for lung tissue equivalent, and acrylic filled roll-on ball. Wood sample one was used for simulating the lung as that was more solid and feasible to work with.

Table 4.1: CT data of samples assessed for the fabrication of lung phantom.

Materials	Hounsfield units Measurements					
	Reference	Measured				
		Number of ROIs	Mean	SD	Minimum	Maximum
Wood sample 1	Lung - 950 to - 701 HU (Kalef-Ezra et al., 1999; Ohkubo et al., 2016)	2	-653.9	51.55	-747.5	-571
Wood sample 2		3	-401.2	94.4	-618	-307
Wood sample 3		3	-657.2	33.1	-701.3	-562
Wood sample 4		3	-403.7	120.6	-653	-16.6
Wood sample 5		3	-431.7	93.9	-635	-296.3
Sawdust plug 1		2	-613.0	37.2	-675	-463
Sawdust plug 2		1	-565.7	38.8	-639	478
Sawdust plug 3		1	-667.7	39.8	-759	-587
Perspex plug 1	11 - 48 HU (Mayer et al., 1998; Paul et al., 2017)	3	111.8	11.4	88	133
Perspex plug 2		3	114.1	11	65	134
Spherical chalk sample		3	856.7	122.4	507	112.1
Flat chalk sample 1		1	574.1	223.5	-108	865
Flat chalk sample 2		2	760.7	163.4	154.5	996.5
Acrylic filled roll-on ball		1	61	8.4	43	79

A lung phantom was fabricated using the selected suitable maerials containing a simulated tumour and lung

4.2 CT ELECTRON DENSITY CALIBRATION

In radiotherapy planning, tissue inhomogeneities are corrected for in the TPS using CT scans of patients. It is therefore essential to achieve the right association between CT number electron densities. The Model 062M Electron density phantom was scanned and regions of interest were drawn to obtain the CT data of the seventeen (17) tissue-equivalent substitutes. The HU for the electron density phantom substitutes and their corresponding relative electron densities specified

on the sample by the manufacturer were entered into the Eclipse TPS (Varian Medical Systems, Palo Alto, CA, USA) and were used to generate the CT scanner calibration curve in Figure 4.1.

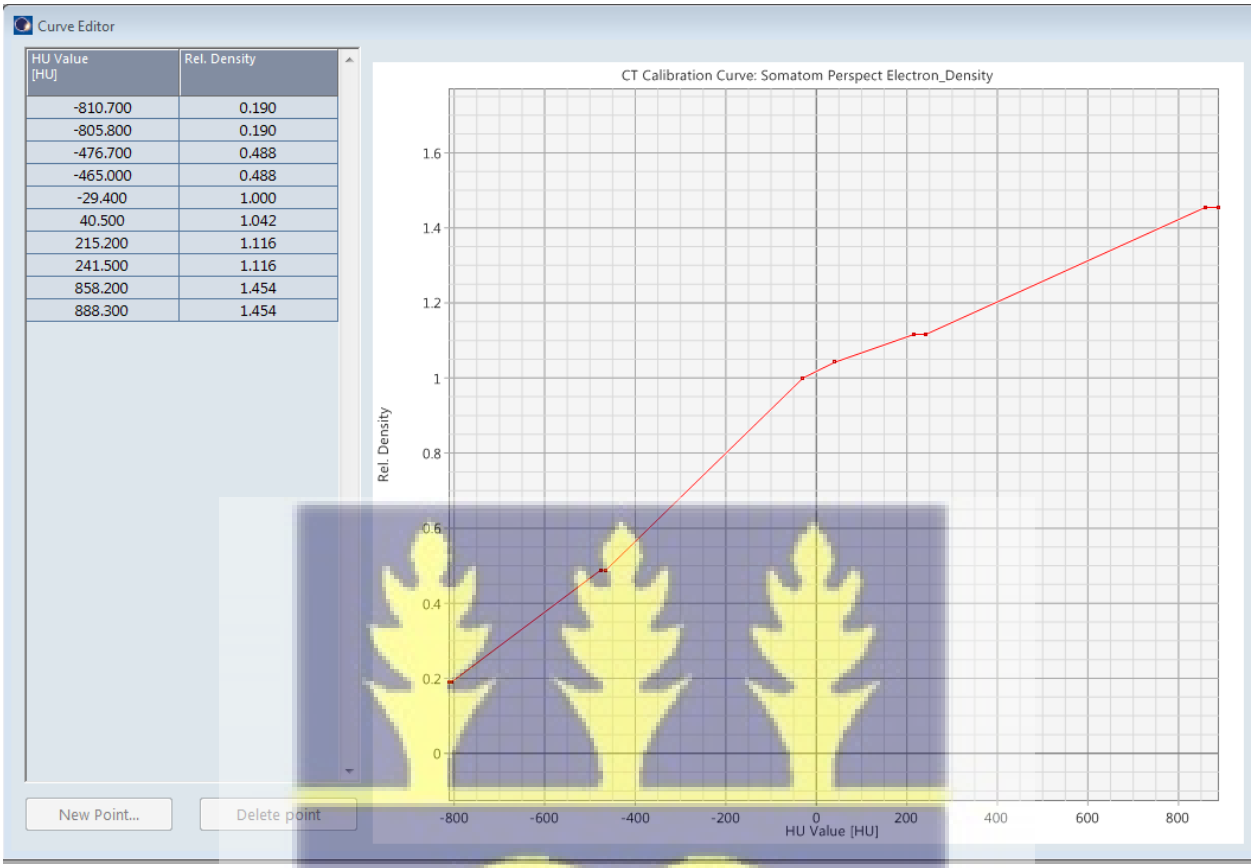

Figure 4.1: The relative electron density (RED) curve of the Siemens Somatom Perspective CT scanner incorporated in the Eclipse TPS.

The dose delivered to a patient treated by a treatment planning system is typically determined using computed tomography data. Multiple tissue categories, including lung, fat, muscle, general organ, cartilage, bone, and tooth, contribute to the complexity and heterogeneity of the natural body. CT number to electron density (CT-ED) calibration is typically accomplished with a calibration phantom containing many tissue substitutes to determine the proper radiation dose for the human body. In an inhomogeneous medium, dosage calculations rely heavily on the precision of CT number to electron density calibration. The CT number, expressed in Hounsfield units (HU),

is a normalised measurement of the linear attenuation coefficient of each voxel (volume pixel) in a CT picture, where the CT number of air is -1000 and that of water is 0. The relationship between HU and ED is often determined using a calibration curve empirically derived from CT scans of a tissue characterization phantom containing inserts of tissue-equivalent materials with a wide range of densities. However, the scanner-dependent calibration curve permits the conversion of CT numbers to densities for use in dosage computation (IAEA, 2008; Mutic et al., 2003).

4.2.1 RESULTS OF FEASIBILITY TEST

One of the key steps in the radiotherapy workflow is plan evaluation. The quality of a treatment plan depends on certain parameters. Plan quality is commonly assessed by evaluating the dose distribution calculated by the treatment planning system. Treatment plan evaluation is generally considered on two levels; the treatment portals and dose distributions. The dose distribution can be analysed using isodose curves in the orthogonal planes, isodose surfaces, dose distribution statistics, and Dose Volume Histograms (DVH). The evaluation of the calculated dose distribution is often based on dose-volume histograms (DVHs). Dose Volume Histograms summarize the dose information in a 3D-dose distribution by excluding detailed positional information about the location of dose levels within a region of interest and are very useful in the initial stages of comparing and evaluating alternative plans in an external beam. There are two types of DVHs.

1. Differential Dose Volume Histogram
2. Cumulative Dose Volume Histogram

Differential Dose Volume Histogram: For a given anatomical structure, the differential DVH describes the fraction of total volume irradiated to the stated dose. It shows volume V(D) plotted against dose, where V(D) is the volume of tissue in which dose ranges between D and (D + dD), where dD is the 'bin width' of the histogram. Bin width is defined using the maximum dose defined

for the plan. Bin width (dD) = Maximum Dose for plan/Number of Bins. You can manually adjust the number of bins to change the histogram resolution. That means if a total of 5000 cGy are prescribed and 50 bins are selected for DVH representation, then DVH will show volume distribution for the doses in the steps (or bin width) of approximately 100 cGy (i.e. 5000/50). The Cumulative Dose Volume Histogram, on the other hand, is an integration of the differential DVH. It describes the fraction of the total volume irradiated to the stated dose or more. In cumulative DVH, the volume (V(D) is plotted against dose (D), where V(D) is the volume of tissue receiving a dose greater than or equal to D. In this thesis all DVHs are presented as cumulative DVH. The cumulative DVHs are used to analyse a patient plan by taking points on the DVH to tell how much volume is covered by a stated dose.

A conventional treatment plan for a feasibility test with a dose prescription of 10 Gy in five parts (10 Gy/5) was administered and measured. The dosimetric characteristics of the treatment plan for the feasibility test were assessed. The conformity index (CI) and gradient index for treatment with a dose prescription of 50 Gy/5 using 3-D CRT technology was derived from the dose statistics on the TPS. Dose coverage of the planned target volume (PTV) and organs at risk (OAR) (lung) was evaluated by analysing dose-volume histograms (DVHs). From the DVH curve of the prescribed dosage of 10 Gy/5 shown in Figure 4.2, the lung phantom target volume, mean, maximum, and minimum doses, as well as the dose received by 95% and 99% of the PTV, were determined.

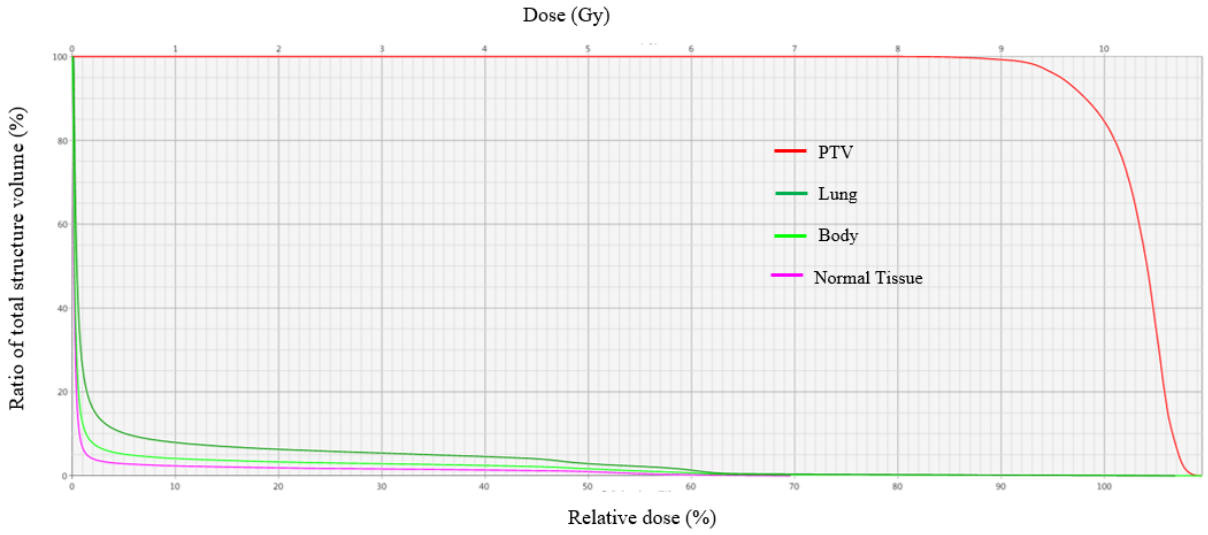

Figure 4.2: Cumulative DVH for a four-field treatment plan with 10 Gy/5 prescription dose.

Then PTV dose coverage D_5 and D_{95} from the DVH were respectively. Heterogeneity and conformity index ($HI_{5/95}$) were 1.12 and 1.06 respectively. Homogeneity characterises the uniformity of the absorbed-dose distribution within the PTV and the "squareness" of the DVH is a measure of the absorbed dose uniformity. An HI value of zero indicates that the absorbed-dose distribution is almost homogeneous.

The conformity index characterises the degree to which the high-dose region conforms to the PTV. The overlap between the isodose surface defining a significantly large absorbed dose and the surface of the PTV give a measure of the conformity.

Dosimetric parameters analysed (PTV volume, maximum, minimum and mean doses, the PTV $V_{100\%}$ and $V_{95\%}$) from the DVH suggest adequate conformal target coverage was achieved for the feasibility test treatment plan with minimal toxicity to the lung (Table 4.2). The data show that for a prescription dose of 10 Gy in 5 fractions to treat the 3cm tumour, the PTV $V_{100\%}$, and $V_{95\%}$ were 85% and 95% respectively. The maximum, minimum and mean PTV doses (%) were 109.5%, 97.6 and 103.2 respectively.

Table 4.2: Planned and reported absorbed dose metrics for lung phantom feasibility treatment planning assessment.

Dose parametre	10 Gy / 5
Maximum PTV Dose (%)	109.5
Minimum PTV dose (%)	97.6
Mean PTV dose (%)	103.2
$V_{100\%}$	85%
$V_{95\%}$	95%
50% PD	1 Gy
CI	1.06
$HI_{5/95}$	1.12
GI	2.15

Outcomes in Table 4.2 show that the PTV volume conformally covered by the prescribed dose was 95% and is acceptable for target coverage, thus the plan was accepted and approved for test delivery. The planned treatment was delivered to the phantom and measured by using the ionisation chamber/electrometer combination. The electrometer was inserted in the middle of the tumour. These measured values were converted to doses to indicate the delivered dose using equation (1). The verification of the dose delivered requires comparisons of measured and calculated dose distributions. The delivered doses were comparable to the clinical treatment planned doses for the target and are presented in Table 4.3. The deviation in Table 4.3 is calculated using equation (4.1).

$$Relative\ deviation = \frac{TPS\ Dose - Measured\ Dose}{TPS\ Dose} \times 100 \qquad (4.1)$$

Table 4.3: Results of fabricated lung phantom dosimetry - planned versus delivered dose.

MU	Measured Dose (Gy)					Average	STD	TPS Calculated Dose (Gy)	Relative Deviation (%)
	1	2	3	4	5				
93	0.52	0.54	0.50	0.48	0.48	0.50	0.02	0.50	0
107	0.46	0.48	0.45	0.44	0.44	0.45	0.02	0.50	10
106	0.47	0.49	0.47	0.46	0.46	0.47	0.01	0.50	6
90	0.53	0.55	0.53	0.51	0.51	0.53	0.02	0.50	- 6
Total	1.99	2.07	1.95	1.88	1.89	1.95	0.07	2.00	10

The ideal and acceptable variation between planned and delivered doses is ± 5% according to ICRU which was achieved for the composite dosimetry. Some reasons for discrepancies between delivered and planned doses for individual fields have been attributed to anatomical changes, geometrical changes, irregular irradiated volume dimensions, variations in beam output (the further drift in beam output during a patient's treatment, and the random day-to-day fluctuations in beam output) and intra- and inter-fractional movements (Bolt et al., 2021; Heukelom et al., 2020). The discrepancies between delivered and planned doses in Table 4.3 could be mainly attributed to the uneven mass distribution within the tumour and set-up uncertainties. However, using a standardised phantom, the variation will be less than 5%.

4.2.2 RESULTS OF PHANTOM STUDY

After designing and assessing the feasibility of dose delivery, the phantom was treated with 50 Gy/5 3D CRT and DVH plots were obtained for dose analysis. The quality of each treatment plan developed for the phantom in static mode and motion was evaluated by analysing the degree to

which each plan satisfied the dosimetric objectives according to the RTOG 0915 standards (Table). The DHVs for the target and lung were analysed. Data are shown as mean SD, median, and range (minimum-maximum) doses to target volumes and OARs for the two treatment approaches and prescription doses.

Riet et al. (1997) based on the study by Saint-Anne, Lariboisiere, and Tenon (SALT) group and Lomax and Scheib defined conformality number as expressed in equation 1, taking into account the volume of healthy tissue irradiated by the prescribed dose. It can better represent dose conformity than other definitions (Cao et al., 2019; Shaw et al., 1993). Dose distribution uniformity was evaluated in the target volume (TV) using the homogeneity index (HI). Feuvret et al. (2006) defined HI as the ratio of the maximum dose (Dmax) to minimum dose (Dmin) or prescription dose (Dp) in PTV. The ideal HI value is 1 indicating that each voxel in the TV receives the same dose (Feuvret et al., 2006b; Shaw et al., 1993). Gradient index (GI) is the volume of 50% prescribed dose to that of the prescribed dose which describes the dose fall-off steepness outside the TV as expressed in equation 3 (Cao et al., 2019; G. G. Zhang et al., 2011). The value of GI is positive, and a lower value means a steeper dose fall-off outside the target and better sparing of normal tissue. For the target coverage, a plan is considered acceptable when at least 95% of the target (PTV) volume is covered by the prescription dose ($V_{100\%} \geq 95\%$), at least 99% of the PTV volume is covered by 90% of the prescription dose (V90%PD > 99%) and the maximum dose is inside the PTV. The plan was acceptable for the organs a risk based on the organ dose-volume constraints (Table 3.1).

Figures 4.3, 4.4 and 4.5 present the DVH plots for the three plans generated for the various scenarios described in chapter 3 and used to assess the quality of each treatment plan by examining the extent to which the target dose coverage and lung dosimetric constraint were achieved.

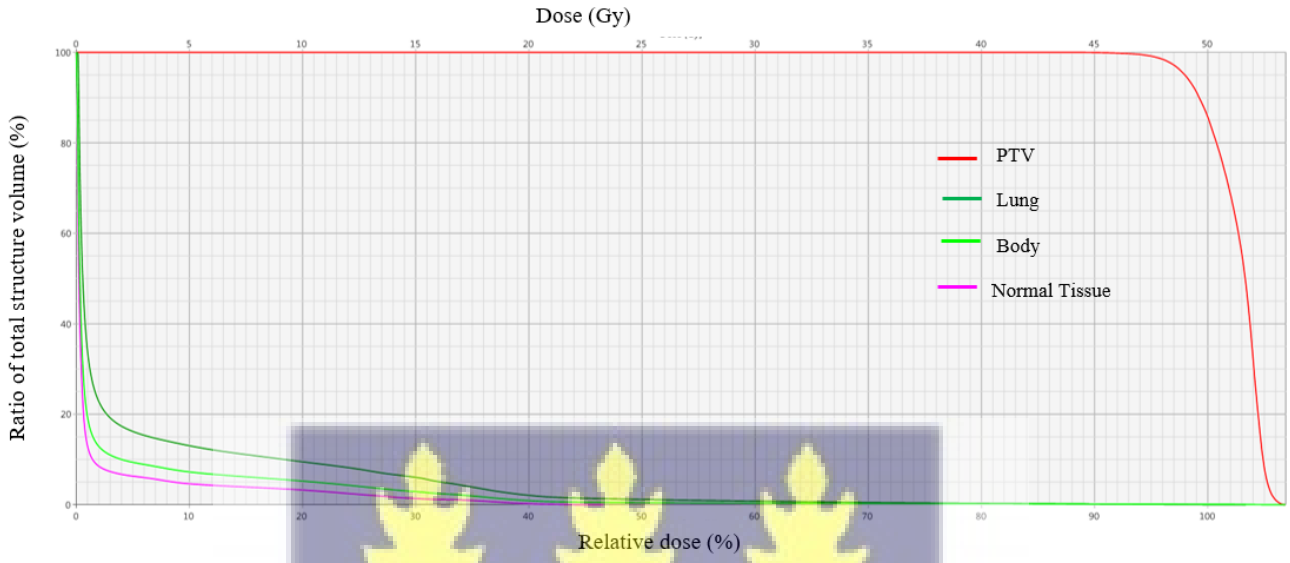

Figure 4.3: Dose-volume histogram (DVH) of the treatment plan with dose prescription of 50 Gy/5.

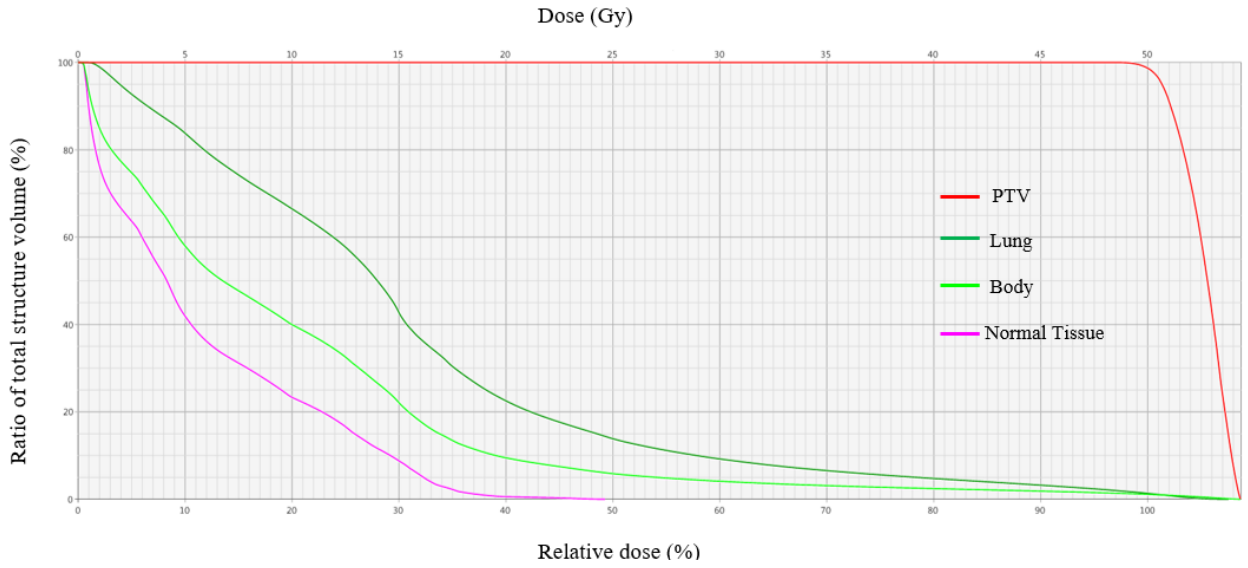

Figure 4.4: Dose-volume histogram (DVH) of the treatment plan with dose prescription of 50 Gy/5 for phantom in 0.5 cm motion.

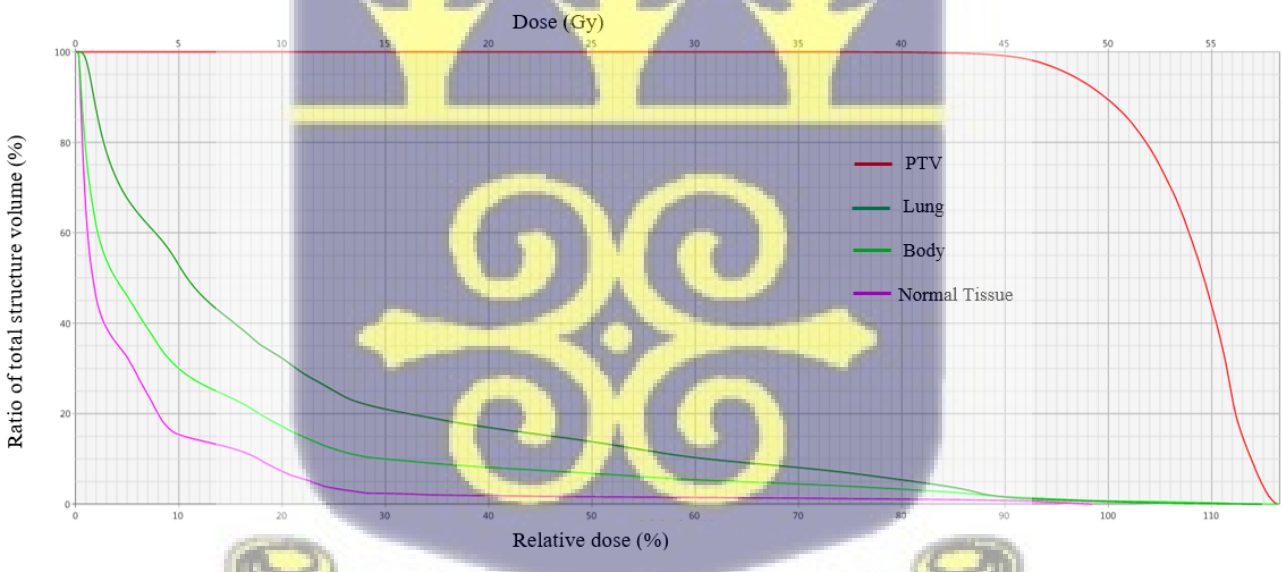

Figure 4.5: Dose-volume histogram (DVH) of the treatment plan with dose prescription of 50 Gy/5 for phantom in 1 cm motion.

Data of the PTV volumes, mean, maximum and minimum doses, the PTV $V_{90\%}$, $V_{95\%}$, and$V_{100\%}$ for all treatment plans for the prescription dose of 50 Gy/5 stratified by phantom in different modes are shown in Tables 4.4. The homogeneity and conformity index extracted from the DVH were 1.07 and 1.04 respectively. Kim et al., (2015) reported a CI of 1·05 ± 0·07 and Weyh et al., (2013) reported a mean CI of 1·36 ± 2·9. Herbert et al., (2013) reported a CI of 1·21 for the 3DCRT plan at a prescription dose of 48 Gy/4. Dose statistics presented in Table 4.5 suggest that sufficient dose conformity to the target was achieved without delivering extreme doses to OARs to reduce toxicity which is the main objective of radiation therapy. Adequate target coverage is associated with tumour control which leads to improved biochemical relapse-free survival, cancer progression-free survival and cancer-specific survival. In analysing the DVH, points are taken on the DVH to know how much volume is covered by a stated dose. The dose gotten from these points is compared to the dose-volume constraints to ensure the dose constraint for the stated target is achieved organ is not exceeded. For instance, in table 4.5, a dose $V_{99\%\ Gy}$ means 99% of the PTV volume should receive more than 90% of the prescription dose and for a prescription dose of 50 Gy/5, 99% of the target volume (PTV) received 91 Gy which is more than 90% of the 50 Gy. Per the requirements of RTOG 0915, the plan is acceptable from the DVH evaluation with maximum target coverage achieved.

Table 4.4: Dose statistics of treatment plan with dose prescription of phantom in motion.

Volume/ OAR	Metric description	50 Gy/5	50 Gy/5 (0.5 cm motion)	50 Gy/5 (1 cm motion)
PTV	$V_{100\%} \geq 95\%$	86.77	98.60	72.71
	$V_{99\%} > 90\%$	91.19	99.61	90.47
	$V_{90\%} \geq 99\%$ maximum dose inside ITV	99.96	100.00	99.65
	D5	52.62	54.10	57.37
	D95	48.98	50.66	48.14
	Maximum dose (Gy)	53.44 (106.9%)	54.36 (108.7%)	58.29 (116.6%)
	Minimum dose (Gy)	43.54 (81.1%)	48.41 (96.8%)	36.09 (72.2%)
	Mean dose (Gy)	51.29 (102.6%)	52.62 (105.2%)	53.91 (107.8%)
	Heterogeneity index ($HI_{5/95}$)	1.07	1.07	1.19
	Conformity Index (CI)	1.04	1.39	1.38
	Gradient Index (GI)	0.93	1.41	1.84
Lung	$V_{5\ Gy}$	13.00	83.69	52.77
	$V_{10\ Gy}$	9.46	66.47	32.23
	$V_{20\ Gy}$	2.07	22.44	16.94
	$V_{30\ Gy}$	0.79	9.22	10.27

The planned treatments were delivered, and the electrometer readings were converted to doses using equation 1. The planned and delivered dose prescription of 50 Gy/5 in different modes were compared yielding the results in Tables 4.5, 4.6 and 4.7. The deviation in the tables is calculated using equation 4.1.

Table 4.5: Comparison of average measure dose to TPS calculated dose for 50 Gy/5 dose fraction in static mode.

MU	Measured Dose (Gy)					Average	STD	TPS Calculated Dose (Gy)	Relative Deviation (%)
	1	2	3	4	5				
210	1.06	1.04	1.16	1.18	1.29	1.15	0.09	1.33	13.55
239	1.14	1.10	1.34	1.39	1.48	1.29	0.15	1.33	2.67
243	1.21	1.15	1.37	1.46	1.56	1.35	0.15	1.33	-1.83
204	0.95	0.93	1.05	1.08	1.18	1.04	0.09	1.06	2.23
191	0.95	0.94	1.17	1.16	1.20	1.09	0.11	1.06	-2.22
205	1.05	1.04	1.23	1.23	1.23	1.16	0.09	1.06	-9.00
147	0.69	0.68	0.82	0.81	0.80	0.76	0.06	0.89	13.96
158	0.78	0.77	0.92	0.91	0.99	0.88	0.09	0.89	0.94
54	0.07	0.07	0.06	0.08	0.15	0.08	0.03	0.27	68.10
57	0.19	0.20	0.23	0.19	0.15	0.19	0.03	0.27	28.20
52	0.08	0.08	0.06	0.07	0.07	0.07	0.01	0.27	72.54
69	0.10	0.09	0.08	0.11	0.12	0.10	0.01	0.27	62.25
Total	8.27	8.10	9.50	9.68	10.23	9.16	0.83	10.00	8.43

Table 4.6: Comparison of average measure dose to TPS calculated dose for 50 Gy/5 prescription dose delivered to phantom with 0.5 cm motion.

MU	Measured Dose (Gy)					Average	STD	TPS Calculated Dose (Gy)	Relative Deviation (%)
	1	2	3	4	5				
185	1.23	1.12	1.26	1.26	1.25	1.22	0.05	1.32	7.16
271	1.79	1.74	1.76	1.79	1.79	1.77	0.02	1.60	-10.76
130	0.88	0.86	0.89	0.90	0.90	0.89	0.02	0.94	5.68
242	1.58	1.55	1.55	1.58	1.58	1.57	0.01	1.41	-11.07
202	1.31	1.29	1.32	1.34	1.34	1.32	0.02	1.22	-7.67
155	1.02	1.00	1.03	1.03	1.03	1.02	0.01	0.94	-8.50
214	1.57	1.49	1.56	1.58	1.58	1.56	0.03	1.43	-8.72
152	1.09	0.97	1.12	1.12	1.11	1.08	0.05	1.13	4.28
Total	10.48	10.02	10.49	10.59	10.57	10.43	0.21	10.00	-4.31

Table 4.7: Comparison of average measure dose to TPS calculated dose for 50 Gy/5 prescription dose delivered to phantom with 1 cm motion.

MU	Measured Dose (Gy)					Average	STD	TPS Calculated Dose (Gy)	Relative Deviation (%)
	1	2	3	4	5				
2	0.02	0.02	0.02	0.02	0.02	0.02	0.00	0.01	-94.19
11	0.07	0.07	0.07	0.07	0.07	0.07	0.00	0.05	-34.95
210	1.31	1.32	1.39	1.27	1.32	1.32	0.04	1.25	-5.90
196	1.16	1.17	1.17	1.16	1.16	1.17	0.00	0.98	-18.90
230	1.37	1.39	1.39	1.38	1.39	1.38	0.01	1.16	-19.23
170	1.04	1.04	1.04	1.04	1.04	1.04	0.00	0.89	-16.61
829	5.61	8.33	7.02	5.62	5.62	6.44	1.09	4.58	-40.61
171	1.15	1.18	1.16	1.15	1.15	1.16	0.01	1.07	-8.36
Total	11.74	14.51	13.25	11.72	11.77	12.60	1.12	10.00	-25.96

The difference observed between planned and delivered doses can be explained by the design of the detector hole precision to fit the specific detector thereby reducing the geometric uncertainty

and the risk of surrounding air gap. The dosimetric variations observed between the planned and the measured dose would be attributed to the uneven mass distribution of acrylic powder within the simulated tumour, set-up uncertainties and style of measurement. However these discrepancies could be reduced by establishing international and/or national guidelines on dose prescription and reporting, volume definitions (e.g. intersection and union of targets and organs at risk), margin status, and volume extension in build-up region and overlapping structures as suggested elsewhere (Das et al., 2008). The dose variation also shows the need to employ motion management techniques as well as image-guided techniques in the planning and treatment delivery of SBRT.

4.2.3 RESULTS OF CLINICAL CASE STUDY

The clinical case study was done to demonstrate dose to critical organs since the phantom only gave dose statistics on the target. Treatment plans were considered acceptable when at least 95% of the PTV volume is covered by the prescription dose (V100%PD > 95%), at least 99% of the PTV volume is covered by 90% of the prescription dose (V90%PD > 99%) for target coverage. Based on the organ dose-volume constraints the plan's acceptability was determined for the OARs (Table 3.1). The DVHs for the various treatment plans on the patient planning CT is displayed in Figures 4.6, 4.7 and 4.8. The DVH plots were used to quantitatively assess the acceptability of each treatment plan by examining the extent to which each plan achieved the target dose coverage and OAR dosimetric constraints.

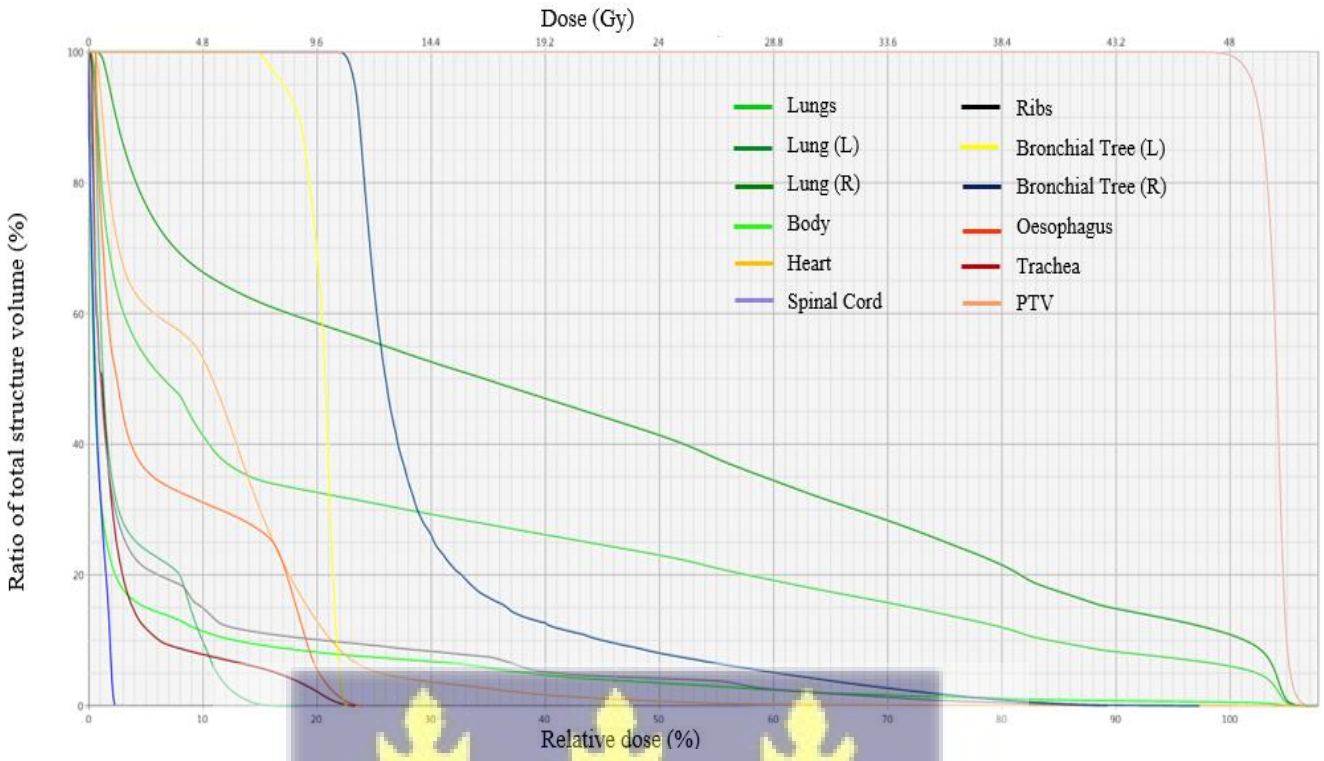

Figure 4.6: DVH of the treatment plan with 48 Gy in 4 fractions for tumour size of 3 cm.

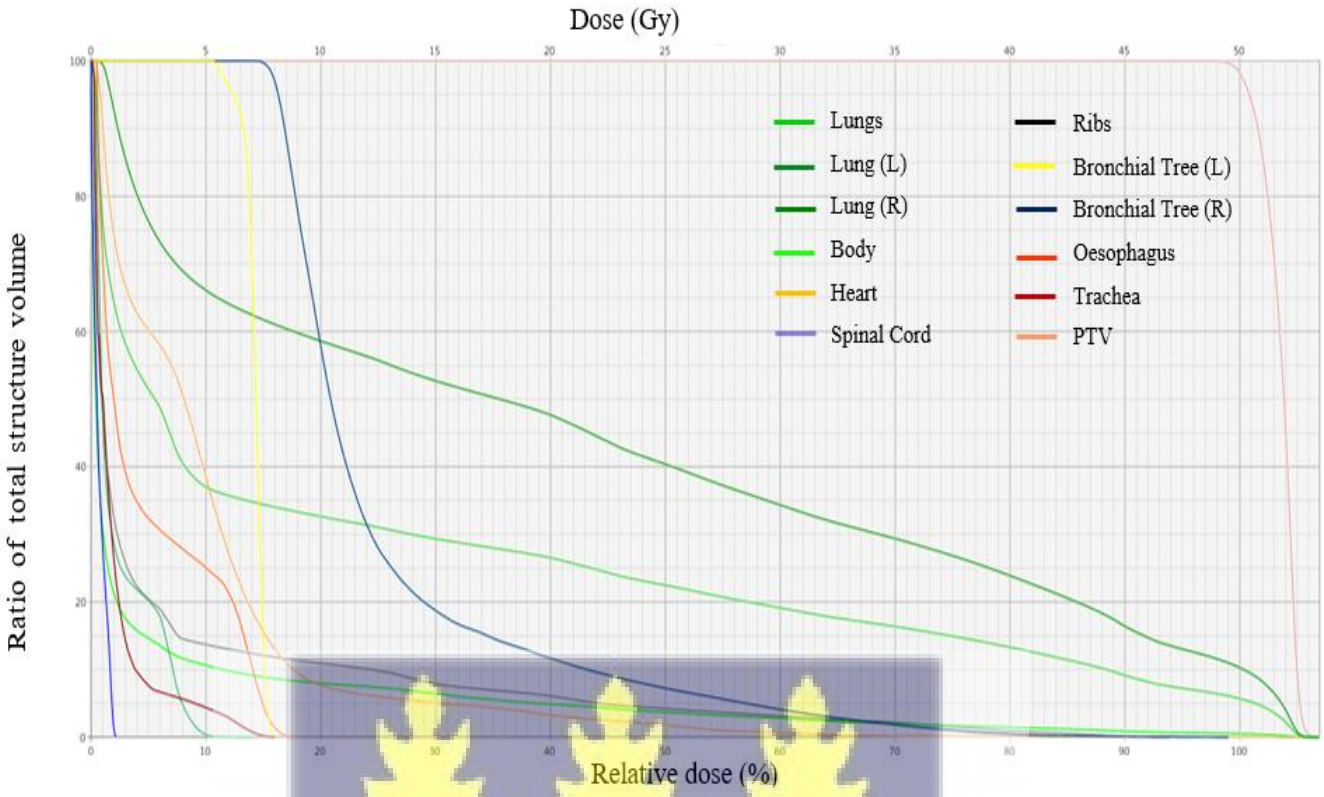

Figure 4.7: DVH of the treatment plan with 50 Gy in 5 fractions for tumour size of 3 cm.

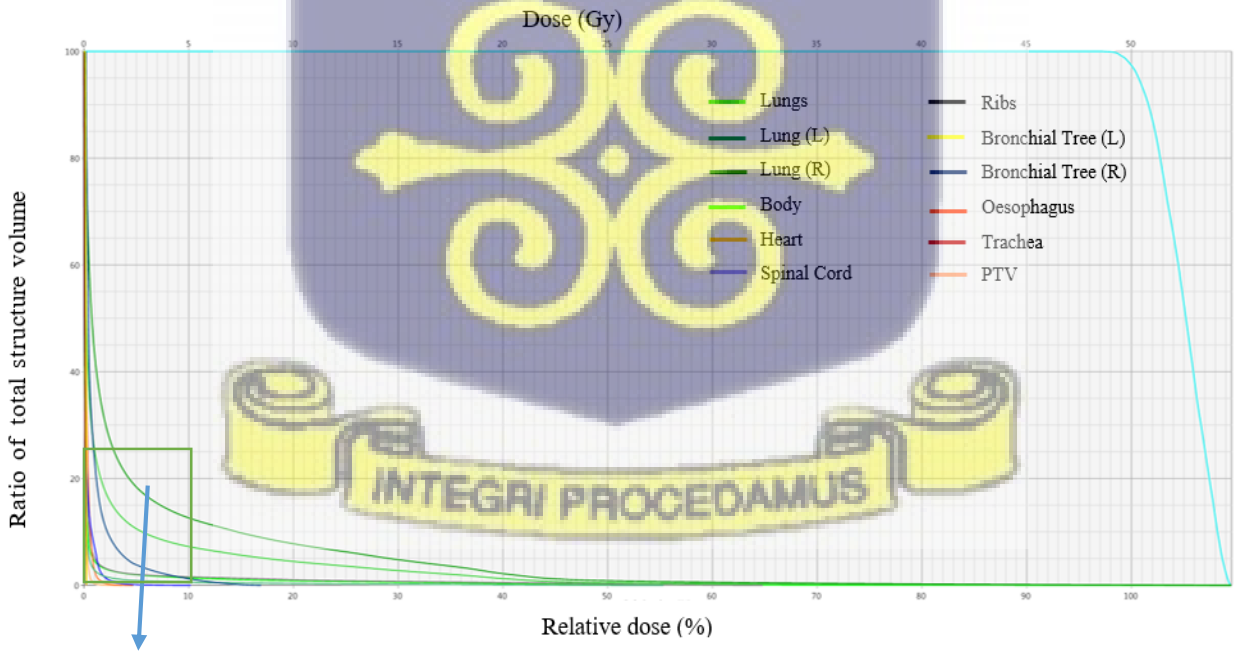

Zoomed part

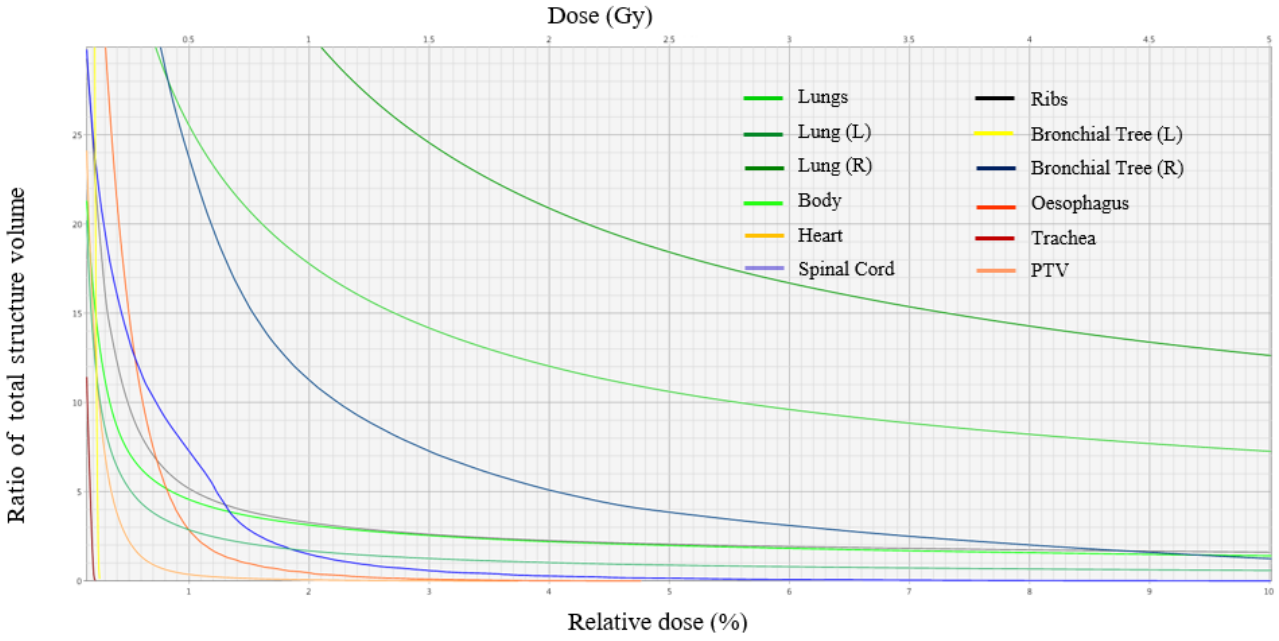

Figure 4.8: DVH of the treatment plan with 50 Gy in 5 fractions for tumour size of 1 cm.

4.2.3.1 DOSE STATISTICS AND DVH EVALUATION OF THE PTV

The quality of treatment plans generated was evaluated by calculating the heterogeneity index ($HI_{5/95}$), but the conformity index (CI) and gradient index were calculated by the treatment planning system. Improved dose conformity to the target is indicated by a conformity index value close to 1.0. $HI_{5/95} < 1{\cdot}2$ is considered ideal or minor deviation for $HI_{5/95} < 1{\cdot}5$ which indicates greater heterogeneity within the target volume. Kim et al., (2015) reported a CI of $1{\cdot}05 \pm 0{\cdot}07$ and Weyh et al., (2013) reported a mean CI of $1{\cdot}36 \pm 2{\cdot}9$. Herbert et al., (2013) reported a CI of 1·21 for the 3DCRT plan at a prescription dose of 48 Gy/4. Data of the PTV volumes, mean, maximum and minimum doses, the PTV V90%, V95%, andV100% for all treatment plans for the prescription dose of 50 Gy/5 and 48 Gy/4 shown in Tables 4.8.

Table 4.8: Dose evaluation indices for prescription doses of 48 Gy/4 and 50 Gy/5 PTV.

Metric description	48 Gy/4	50 Gy/5 (3 cm tumour)	50 Gy/5 (1 cm tumour)
Volume (cm^3)	131.4		
$V_{100\%PD} \geq 95\%$	101.10	98.10	97.36
$V_{99\%} > 90\%$	102.62	99.68	99.19
$V_{90\%PD} \geq 99\%$ maximum dose inside ITV	100.49	100	100
Maximum dose (Gy) (% PD)	51.71 (107.7%)	53.47 (107%)	54.78 (109.6%)
Minimum dose (Gy) (% PD)	45.72 (95.3%)	48.36 (96.7%)	48.59 (97.2%)
Mean dose (Gy) (% PD)	49.88 (103.9%)	51.76 (103.5%)	52.51 (105%)
STD (Gy)	0.49 (3.4%)	0.68 (1.4%)	1.24 (2.5%)
D_5	50.53	52.61	54.33
D_{95}	48.96	50.41	50.34
Heterogeneity index ($HI_{5/95}$)	1.03	1.04	1.08
Conformity Index (CI)	1.24	1.17	1.48
Gradient Index (GI)	2.88	3.06	1.69

Dose fractionation schemes of 48–60 Gy in 4–5 fractions are commonly used for treating stage I primary NSCLC and result in high local control rates and low OARs toxicities (Goldsmith & Gaya, 2012; X. Wang et al., 2018; Y. Zhao et al., 2020). Concerning tumour control, MacHtay et al. (2012) reported that higher radiotherapy doses are associated with improved local-regional control and survival in patients with locally advanced NSCLC that received chemoradiation. Korzets Ceder et al. (2018), Rowe et al. (2012), Verstegen et al. (2015) also treated patient with SBRT and

had about 80% tumour control. Though, pneumonitis and bronchial stenosis were the most frequent side effects.

4.2.3.2 DOSE STATISTICS AND DVH EVALUATION OF THE OARS

Dose to OARs is usually a dose restricting factor for the target dose. Doses to OARs were evaluated from the DVHs of the treatment plans with a prescription dose of 48 Gy in four fractions and 50 Gy in five fractions for tumour sizes of 3 cm and 1 cm. The doses to organs at risk were indexed by the percentage volume of the specified organ receiving 5 Gy ($V_{5\,Gy}$), 10 Gy ($V_{10\,Gy}$), 20 Gy ($V_{20\,Gy}$) and 30 Gy ($V_{30\,Gy}$), minimum, maximum and mean doses. Doses to critical structures are presented in Tables 4.9 to 4.16.

Table 4.9: Dosimetric analysis of the bilateral lung for treatment plans with 48 Gy in four fractions and 50 Gy in 5 fractions.

Dosimetric parameter	48 Gy/4	50 Gy/5 (3 cm)	50 Gy/5 (1 cm)
Volume		2639.1	
Maximum dose (Gy) (% PD)	51.71 Gy (107.7%)	53.48 (107%)	54.78 (109.6%)
Minimum dose (Gy) (% PD)	0.06 (0.1%)	0.04 (0.1%)	0
Mean dose (Gy) (% PD)	11.94 (24.9%)	12.32 (24.6%)	1.39 (2.8%)
STD (Gy)	16.07 (33.5%)	17.03 (34.1%)	4.23 (8.5%)
$V_{5\,Gy}$ (%)	40.20	51.44	10.60
$V_{10\,Gy}$ (%)	32.33	36.98	7.26
$V_{20\,Gy}$ (%)	25.65	32.64	4.47
$V_{30\,Gy}$ (%)	18.28	29.34	2.76

Table 4.10: Dosimetric analysis of the left and right lung for treatment plans with 48 Gy in four fractions and 50 Gy in 5 fractions.

OAR	Dosimetric parameter	48 Gy/4	50 Gy/5 (3 cm)	50 Gy/5 (1 cm)
Left Lung	**Volume (cm^3)**	**1170.4**		
	$V_{5\ Gy}$ (%)	8.03	20.18	0.58
	$V_{10\ Gy}$ (%)	0	0.37	0.35
	$V_{20\ Gy}$ (%)	0	0	0.10
	$V_{30\ Gy}$ (%)	0	0	0
	Maximum dose (Gy) (% PD)	8.90 (18.5%)	7.14 (14.3%)	27.70 (55.4%)
	Minimum dose (Gy) (% PD)	0.06 (0.1%)	0.043 (0.1%)	0
	Mean dose (Gy) (% PD)	1.57 (3.3%)	1.15 (2.3%)	0.16 (0.3%)
	STD (Gy)	1.83 (3.8%)	1.33 (2.6%)	1.12 (2.2%)
Right Lung	Volume (cm^3)	1463.3		
	$V_{5\ Gy}$ (%)	65.80	76.25	12.63
	$V_{10\ Gy}$ (%)	58.02	66.07	7.79
	$V_{20\ Gy}$ (%)	46.06	58.57	2.19
	$V_{30\ Gy}$ (%)	32.82	52.68	0.58
	Maximum dose (Gy) (% PD)	51.70 (107.7%)	53.48 (107%)	54.78 (109.6%)
	Minimum dose (Gy) (% PD)	0.32 (0.7%)	0.31 (0.6%)	0.04 (0.1%)
	Mean dose (Gy) (% PD)	20.2 (42%)	21.21 (42.4%)	2.38 (4.8%)
	STD (Gy)	17.54 (36.5%)	18.48 (37%)	5.39 (10.8%)

Table 4.11: Dosimetric analysis of the heart for treatment plans with 48 Gy in four fractions and 50 Gy in 5 fractions.

Dosimetric parameter	**48 Gy/4**	**50 Gy/5 (3 cm tumour)**	**50 Gy/5 (1 cm tumour)**
Volume	750.9		
Maximum dose (Gy) (% PD)	51.2 (106.7%)	52.71 (105.4%)	1.87 (3.7%)
Minimum dose (Gy) (% PD)	0.22 (0.5%)	0.18 (0.4%)	0
Mean dose (Gy)	5.24 (10.9%)	0.80 (9.6%)	0.06 (0.1%)
STD (Gy)	4.71 (9.8%)	5.38 (10.8%)	0.07 (0.1%)
$V_{5\ Gy}$ (%)	51.54	38.43	0
$V_{10\ Gy}$ (%)	10.83	7.68	0
$V_{20\ Gy}$ (%)	1.46	3.27	0
$V_{30\ Gy}$ (%)	0.17	0.61	0

Table 4.12: Dosimetric analysis of the bronchial tree for treatment plans with 48 Gy in four fractions and 50 Gy in 5 fractions.

OAR	Dosimetric parameter	48 Gy/4	50 Gy/5 (3 cm target)	50 Gy/5 (1 cm target)
Bronchial Tree (Left)	Volume	1.5		
	Maximum dose (Gy)	10.91 (22.7%)	8.04 (16.1%)	0.13 (0.3%)
	Minimum dose (Gy)	7.00 (14.6%)	5.26 (10.5%)	0.05 (0.1%)
	Mean dose (Gy)	9.74 (20.3%)	7.12 (14.2%)	0.10 (0.2%)
	STD (Gy)	0.70 (1.5%)	0.43 (0.9%)	0.01 (0%)
	$V_{5\ Gy}$ (%)	100	100	0
	$V_{10\ Gy}$ (%)	43.90	100	0
	$V_{20\ Gy}$ (%)	0	0	0
	$V_{30\ Gy}$ (%)	0	0	0
Bronchial Tree (Right)	Volume	3.8		
	Maximum dose (Gy)	46.72 (97.3%)	49.56 (99.1%)	8.49 (17%)
	Minimum dose (Gy)	10.44 (21.8%)	7.10 (14.2%)	0.10 (0.2%)
	Mean dose (Gy)	14.70 (30.6%)	12.82 (25.6%)	0.53 (1.1%)
	STD (Gy)	5.70 (11.9%)	6.43 (12.9%)	0.92 (1.8%)
	$V_{5\ Gy}$ (%)	100	100	3.85
	$V_{10\ Gy}$ (%)	100	57.70	1.24
	$V_{20\ Gy}$ (%)	11.57	11.65	0
	$V_{30\ Gy}$ (%)	4.44	4.10	0

Table 4.13: Dosimetric analysis of the oesophagus volume with 48 Gy in four fractions and 50 Gy in 5 fractions.

Dosimetric parameter	48 Gy/4	50 Gy/5 (3 cm)	50 Gy/5 (1 cm)
Volume	26.6		
Maximum dose (Gy)	11.56 (24.1%)	8.72 (17.4%)	2.39 (4.8%)
Minimum dose (Gy)	0.27 (0.6%)	0.23 (0.5%)	0.02 (0%)
Mean dose (Gy)	3.33 (6.9%)	2.48 (5.0%)	0.14 (0.3%)
STD (Gy)	3.64 (7.6%)	2.68 (5.4%)	0.16 (0.3%)
$V_{5\ Gy}$ (%)	30.77	32.31	0
$V_{10\ Gy}$ (%)	3.26	25.00	0
$V_{20\ Gy}$ (%)	0	0	0
$V_{30\ Gy}$ (%)	0	0	0

Table 4.14: Dosimetric analysis for trachea for treatment plans with 48 Gy in four fractions and 50 Gy in 5 fractions.

Dosimetric parameter	48 Gy/4	50 Gy/5 (3 cm)	50 Gy/5 (1 cm)
Volume	15.5		
Maximum dose (Gy)	11.25 (23.4%)	8.05 (16.1 %)	0.11 (0.2%)
Minimum dose (Gy)	0.06 (0.1%)	0.06 (0.1%)	0
Mean dose (Gy)	1.32 (2.7%)	0.96 (1.9%)	0.04 (0.1%)
STD (Gy)	2.22 (4.6%)	1.37 (2.7%)	0.03 (0.1%)
$V_{5\ Gy}$ (%)	7.67	4.36	0
$V_{10\ Gy}$ (%)	1.24	0	0
$V_{20\ Gy}$ (%)	0	0	0
$V_{30\ Gy}$ (%)	0	0	0

Table 4.15: Dosimetric analysis of the spinal cord for treatment plans with 48 Gy in four fractions and 50 Gy in 5 fractions.

Dosimetric parameter	48 Gy/4	50 Gy/5 (3 cm)	50 Gy/5 (1 cm)
Volume	24.7		
Maximum dose (Gy)	1.12 (2.3%)	1.10 (2.2%)	5.14 (10.3%)
Minimum dose (Gy)	0	0	0
Mean dose (Gy)	0.37 (0.8%)	0.34 (0.7%)	0.12 (0.2%)
STD (Gy)	0.32 (0.7%)	0.30 (0.6%)	0.26 (0.5%)
$V_{5\ Gy}$ (%)	0	0	0
$V_{10\ Gy}$ (%)	0	0	0
$V_{20\ Gy}$ (%)	0	0	0
$V_{30\ Gy}$ (%)	0	0	0

Table 4.16: Dosimetric analysis of the ribs for treatment plans with 48 Gy in four fractions and 50 Gy in 5 fractions.

Dosimetric parameter	48 Gy/4	50 Gy/5 (3 cm)	50 Gy/5 (1 cm)
Volume	541.2		
Maximum dose (Gy)	42.84 (89.2%)	46.98 (93.9%)	32.45 (64.9%)
Minimum dose (Gy)	0	0	0
Mean dose (Gy)	3.21 (6.7%)	3.42 (6.8%)	0.35 (0.7%)
STD (Gy)	7.12(15%)	7.99 (16%)	2.19 (4.4%)
$V_{5\ Gy}$ (%)	21.02	20.40	1.60
$V_{10\ Gy}$ (%)	14.92	13.71	1.05
$V_{20\ Gy}$ (%)	10.12	10.94	0.52
$V_{30\ Gy}$ (%)	8.34	7.89	0.03

Critical organ constraints were met for all structures in all three scenarios except the heart in the plan with a 3 cm tumour size, which had a volume dose higher than 34 Gy. This was due to the tumour being close to the heart. Suitable conformal target coverage was achieved for all dose prescriptions which is the primary aim of radiotherapy devoid of extreme doses of OARs to minimise toxicity. Sufficient target coverage is associated with tumour control which leads to improved biochemical relapse-free survival, cancer progression-free survival and cancer-specific survival (Zheng et al., 2014).

CHAPTER FIVE

CONCLUSIONS AND RECOMMENDATIONS

5.1 CONCLUSIONS

In this study, a lung phantom has been fabricated and has been used to investigate the treatment of lung tumours with the SBRT technique without a 4D CT scanner. The study investigated SBRT prescription doses for treating lung tumours according to RTOG 0915. The fabricated lung phantom contained a centrally placed simulated tumour embedded in a tissue-equivalent lung. In this study, the use slow CT scanning for acquiring image dataset for moving targets have been demonstrated to be feasible for achieving greater target dose conformity, rapid dose fall-off from PTV and minimising doses to the organs at risk as done in other.

The study has shown that predefined dose-volume constraints and objectives for SBRT technique can be achieved, resulting in improved dose optimisation and coverage of target volume, reduction in OARs volume receiving high doses and therefore with the potential to reduce the rate of toxicity, decrease pain and improve the quality of life for lung cancer patients in a low resourced setting.

Doses were measured with the phantom in both the static and moving cases using an ionisaiton chamber. Average measured doses were compared to treatment planning calculated doses for the phantom in both the static and moving cases. Dose deviation for treating static mimicked tumour was 8.43%, -4.31% for phantom in 0.5 cm motion, and -25.96% for phantom in 1 cm motion. Phantom dosimetric analysis for PTV $V_{100\%}$, $V_{99\%}$, $V_{90\%}$ at 50 Gy/5 without motion were 86.77%, 91.19% and 99.96%; with 0.5 cm motion were 98.60%, 99.61% and 100%; and with 1 cm motion were 72.72%, 90.47% and 99.65%, respectively. Clinical analysis for PTV $V_{100\%}$, $V_{99\%}$, $V_{90\%}$ at 48 Gy/5 were 101.10%, 102.62% and 100.49%, respectively. For a tumour size of 3 cm at 50 Gy/5

were 98.10%, 99.68% and 100%, respectively; and for 1 cm tumour size were 97.36%, 99.19% and 100 %, respectively.

SBRT treatment planning and treatment delivery protocols have been developed in this study and used to demonstrate that SBRT treatment planning and delivery are feasible at the study site without 4-D CT scanner. The statistics propose that the target was sufficiently covered with the dose for all scenarios, thereby achieving the primary radiotherapy goal without excessively dosing OARs to minimise toxicity. It was demonstrated that sufficient dose conformity to the target in the lung was achieved for all scenarios, thereby fulfilling the radiotherapy goal of maximum tumour control and minimum tissue complication. SBRT treatment planning and delivery are possible to achieve at KATH in the absence of 4D CT based on the results of this study. Thus patients could benefit from highly conformal target coverage for increased tumour control while at the same time minimising dose to surrounding critical structures for minimal treatment-associated toxicities. Recent advances in radiotherapy have enabled safe delivery of SBRT which delivers a high dose per fraction. Although surgery remains the standard of care for operable patients, SBRT offers superior local control and overall survival rates with acceptable toxicity.

5.2 RECOMMENDATIONS

Using 3DCRT for SBRT can be achieved in the study facility. Implementation of the SBRT technique in KATH will ensure adequate target coverage, minimised toxicity to other structures and as a result will prolong patient life. I will therefore recommend the implementation of SBRT at KATH. After the implementation, the technique could be extended to other sites such as the liver and spine. Slow CT scans can be used for acquiring planning CT images of small tumours for treatment planning and delivery. Also, the target range where the tumour can be viewed should be used as ITV during treatment planning. A margin of about 5 mm can be added to the ITV to get

CTV. Then a margin of about 5 mm can be added to the CTV to create the PTV. Planning should be generated on the PTV to ensure the criteria specified by RTOG are fulfilled. Also to further minimise the risk of radiation pneumonitis respiratory gating can be introduced to reduce lung dose.

REFERENCES

Abbas, Z., & Rehman, S. (2018). An Overview of Cancer Treatment Modalities. *Neoplasm*. https://doi.org/10.5772/INTECHOPEN.76558

AFRO UNION Conference. (2011). *Lung Cancer and Tuberculosis Awareness · Welcome to the 18th Conference of The Union*.

Agudo, A., Cayssials, V., Bonet, C., Tjønneland, A., Overvad, K., Boutron-Ruault, M. C., Affret, A., Fagherazzi, G., Katzke, V., Schübel, R., Trichopoulou, A., Karakatsani, A., La Vecchia, C., Palli, D., Grioni, S., Tumino, R., Ricceri, F., Panico, S., Bueno-De-Mesquita, B., … Jakszyn, P. (2018). Inflammatory potential of the diet and risk of gastric cancer in the European Prospective Investigation into Cancer and Nutrition (EPIC) study. *American Journal of Clinical Nutrition*, *107*(4), 607–616. https://doi.org/10.1093/AJCN/NQY002

Akinkuotu, A. C., Maduekwe, U. N., & Hayes-Jordan, A. (2021). Surgical outcomes and survival rates of colon cancer in children and young adults. *American Journal of Surgery*, *221*(4), 718–724. https://doi.org/10.1016/J.AMJSURG.2021.02.010

Akortia, E. (2010). Indoor Radon Gas Levels in Selected Homes in the Greater Accra Region of Ghana Article in. *Research Journal of Applied Sciences, Engineering and Technology*.

Ali, Y. F., Cucinotta, F. A., Ning-Ang, L., & Zhou, G. (2020). Cancer Risk of Low Dose Ionizing Radiation. *Frontiers in Physics*, *8*, 234. https://doi.org/10.3389/FPHY.2020.00234/BIBTEX

Alitalo, A., & Detmar, M. (2011). Interaction of tumor cells and lymphatic vessels in cancer progression. *Oncogene 2012 31:42*, *31*(42), 4499–4508. https://doi.org/10.1038/onc.2011.602

Amadori, D., & Ronconi, S. (2005). Secondary lung tumors in hematological patients. *Seminars in Respiratory and Critical Care Medicine*, *26*(5), 520–526. https://doi.org/10.1055/s-2005-922035

American Cancer Soceity. (2020). *Cancer Staging*.

Amoako, Y. A., Awuah, B., Larsen-Reindorf, R., Awittor, F. K., Kyem, G., Ofori-Boadu, K., Osei-Bonsu, E., & Laryea, D. O. (2019). Malignant tumours in urban Ghana: evidence from the city of Kumasi. *BMC Cancer 2019 19:1*, *19*(1), 1–12. https://doi.org/10.1186/S12885-019-5480-0

Anath, D. S. (2021). *Lung Cancer | Small cell | Non-small cell | Geeky Medics*. https://geekymedics.com/lung-cancer/

Andersson, M., Eckerman, K., & Mattsson, S. (2017). Lifetime attributable risk as an alternative to effective dose to describe the risk of cancer for patients in diagnostic and therapeutic nuclear medicine. *Physics in Medicine & Biology*, *62*(24), 9177. https://doi.org/10.1088/1361-6560/AA959C

Anifah, L., Haryanto, Harimurti, R., Permatasari, Z., Rusimamto, P. W., & Muhamad, A. R. (2018). Cancer lungs detection on CT scan image using artificial neural network backpropagation based gray level coocurrence matrices feature. *2017 International Conference on Advanced Computer Science and Information Systems, ICACSIS 2017*, *2018-*

January, 327–331. https://doi.org/10.1109/ICACSIS.2017.8355054

Ankathil, R. (2010). Tobacco, Genetic Susceptibility and Lung cancer: *Https://Doi.Org/10.4137/TUI.S2819*, *3*, TUI.S2819. https://doi.org/10.4137/TUI.S2819

Aparicio, D. Z., Requejo, O. H., de Julián, M. Á. de la C., Rodríguez, C. R., & Letón, P. F. (2019). Local control rates in stereotactic body radiotherapy (SBRT) of lung metastases associated with the biologically effective dose. *Reports of Practical Oncology and Radiotherapy*, *24*(2), 142. https://doi.org/10.1016/J.RPOR.2019.01.001

Arroyo-Hernández, M., Maldonado, F., Lozano-Ruiz, F., Muñoz-Montaño, W., Nuñez-Baez, M., & Arrieta, O. (2021). Radiation-induced lung injury: current evidence. *BMC Pulmonary Medicine*, *21*(1). https://doi.org/10.1186/S12890-020-01376-4

Atkins, K. M., Chen, Y., Elliott, D. A., Doshi, T. S., Ognjenovic, S., Vachhani, A. S., Kishore, M., Primack, S. L., Fuss, M., Deffebach, M. E., Kubicky, C. D., & Tanyi, J. A. (2015). The impact of anatomic tumor location on inter-fraction tumor motion during lung stereotactic body radiation therapy (SBRT). *Journal of Radiosurgery and SBRT*, *3*(3), 203.

Attfield, M. D., Schleiff, P. L., Lubin, J. H., Blair, A., Stewart, P. A., Vermeulen, R., Coble, J. B., & Silverman, D. T. (2012). The Diesel Exhaust in Miners Study: A Cohort Mortality Study With Emphasis onLung Cancer. *JNCI Journal of the National Cancer Institute*, *104*(11), 869. https://doi.org/10.1093/JNCI/DJS035

Auweter, S. D., Herzen, J., Willner, M., Grandl, S., Scherer, K., Bamberg, F., Reiser, M. F., Pfeiffer, F., & Hellerhoff, K. (2014). X-ray phase-contrast imaging of the breast--advances towards clinical implementation. *The British Journal of Radiology*, *87*(1034). https://doi.org/10.1259/BJR.20130606

Baba, A. I., & Câtoi, C. (2007). *TUMOR CELL MORPHOLOGY*.

Badoe, L. G. (2007). *MEASUREMENT OF RADON GAS LEVEL IN ASHANTI REGION AND DESIGN OF A RADON VULNERABILITY MAP FOR GHANA*. Kwame Nkrumah University of Science and Technology.

Bahig, H., Filion, E., Vu, T., Chalaoui, J., Lambert, L., Roberge, D., Gagnon, M., Fortin, B., Béliveau-Nadeau, D., Mathieu, D., & Campeau, M. (2016). Severe radiation pneumonitis after lung stereotactic ablative radiation therapy in patients with interstitial lung disease. *Practical Radiation Oncology*, *6*(5), 367–374. https://doi.org/10.1016/J.PRRO.2016.01.009

Bandyopadhyay, O., Biswas, A., & Bhattacharya, B. B. (2019). Bone-Cancer Assessment and Destruction Pattern Analysis in Long-Bone X-ray Image. *Journal of Digital Imaging*, *32*(2), 300–313. https://doi.org/10.1007/S10278-018-0145-0

Barta, J. A., Powell, C. A., & Wisnivesky, J. P. (2019). *Global Epidemiology of Lung Cancer*. https://doi.org/10.5334/aogh.2419

Becher, H., & Winkler, V. (2011). Lung cancer mortality in Sub-Saharan Africa. *International Journal of Cancer*, *129*(6), 1537–1540. https://doi.org/10.1002/ijc.25796

Bello, B., Fadahun, O., Kielkowski, D., & Nelson, G. (2011). Trends in lung cancer mortality in South Africa: 1995-2006. *BMC Public Health*, *11*. https://doi.org/10.1186/1471-2458-11-209

Benedict, S., Yenice, K., Followill, D., Galvin, J., Hinson, W., Kavanagh, B., Keall, P., Lovelock, M., Meeks, S., Papiez, L., Purdie, T., Sadagopan, R., Schell, M., Salter, B., Schlesinger, D., Shiu, A., Solberg, T., Song, D., Stieber, V., … Yin, F.-F. (2010). Stereotactic body radiation therapy: the report of AAPM Task Group 101. *Medical Physics*, *37*(8), 4078–4101. https://doi.org/10.1118/1.3438081

Benusiglio, P. R., Fallet, V., Sanchis-Borja, M., Coulet, F., & Cadranel, J. (2021). Lung cancer is also a hereditary disease. *European Respiratory Review*, *30*(162). https://doi.org/10.1183/16000617.0045-2021

Bertuccio, P., Alicandro, G., Rota, M., Pelucchi, C., Bonzi, R., Galeone, C., Bravi, F., Johnson, K. C., Hu, J., Palli, D., Ferraroni, M., López-Carrillo, L., Lunet, N., Ferro, A., Malekzadeh, R., Zaridze, D., Maximovitch, D., Vioque, J., Navarrete-Munoz, E. M., … La Vecchia, C. (2019). Citrus fruit intake and gastric cancer: The stomach cancer pooling (StoP) project consortium. *International Journal of Cancer*, *144*(12), 2936–2944. https://doi.org/10.1002/IJC.32046

Beyer, T., Bidaut, L., Dickson, J., Kachelriess, M., Kiessling, F., Leitgeb, R., Ma, J., Shiyam Sundar, L. K., Theek, B., & Mawlawi, O. (2020). What scans we will read: imaging instrumentation trends in clinical oncology. *Cancer Imaging 2020 20:1*, *20*(1), 1–38. https://doi.org/10.1186/S40644-020-00312-3

Bezjak, A., Bradley, J., Gaspar, L., Timmerman, R., Papiez, L., Gore, E., & Phoenix Kong, F.-M. (2011). *RTOG 0813. SEAMLESS PHASE I/II STUDY OF STEREOTACTIC LUNG RADIOTHERAPY (SBRT) FOR EARLY STAGE, CENTRALLY LOCATED, NON-SMALL CELL LUNG CANCER (NSCLC) IN MEDICALLY INOPERABLE PATIENTS*.

Bissett, R., & McLaughlin, J. (2010). Radon. *Chronic Diseases in Canada*, *29*, 38–50.

Blomgren, H., Lax, I., Göranson, H., Kr\\sgmaelig;pelien, T., Nilsson, B., Näslund, I., Svanström, R., & Tilikidis, A. (2004). Radiosurgery for Tumors in the Body: Clinical Experience Using a New Method. *Journal of Radiosurgery*, *1*(1), 63–74. https://doi.org/10.1023/b:jora.0000010880.40483.c4

Blomgren, H., Lax, I., Näslund, I., & Svanström, R. (2009). Stereotactic High Dose Fraction Radiation Therapy of Extracranial Tumors Using An Accelerator: Clinical experience of the first thirty-one patients. *Http://Dx.Doi.Org/10.3109/02841869509127197*, *34*(6), 861–870. https://doi.org/10.3109/02841869509127197

Bolt, M., Clark, C. H., Nisbet, A., & Chen, T. (2021). Quantification of the uncertainties within the radiotherapy dosimetry chain and their impact on tumour control. *Physics and Imaging in Radiation Oncology*, *19*, 33–38. https://doi.org/10.1016/J.PHRO.2021.06.004

Bray, F., Ferlay, J., Soerjomataram, I., Siegel, R. L., Torre, L. A., & Jemal, A. (2018). 394 CA: A Cancer Journal for Clinicians Global Cancer Statistics 2018: GLOBOCAN Estimates of Incidence and Mortality Worldwide for 36 Cancers in 185 Countries. *CA CANCER J CLIN*, *68*, 394–424. https://doi.org/10.3322/caac.21492

Brierley, J., Gospodarowicz, M., & Wittekind, C. (2017). *TNM Classification of Malignant Tumours. 8th ed. Wiley Blackwell* (J. Brierley, M. Gospodarowicz, C. Wittekind, B. O'ullivan, M. Mason, H. Asamura, A. Lee, E. Van Eycken, L. Denny, M. Amin, & S. Gupta (eds.); 8th ed.). John Wiley & Sons, Ltd.

Brook, I. (2020). Late side effects of radiation treatment for head and neck cancer. *Radiation Oncology Journal*, *38*(2), 84–92. https://doi.org/10.3857/ROJ.2020.00213

Buranaruangrote, S., Sindhu, S., Mayer, D. K., Ratinthorn, A., & Khuhaprema, T. (2014). Factors influencing the stages of breast cancer at the time of diagnosis in Thai women. *Collegian (Royal College of Nursing, Australia)*, *21*(1), 11–20. https://doi.org/10.1016/J.COLEGN.2012.11.005

Burglin, S. A., Hess, S., Høilund-Carlsen, P. F., & Gerke, O. (2017). 18F-FDG PET/CT for detection of the primary tumor in adults with extracervical metastases from cancer of unknown primary: A systematic review and meta-analysis. *Medicine*, *96*(16). https://doi.org/10.1097/MD.0000000000006713

Cady, B. (2007). Regional lymph node metastases; a singular manifestation of the process of clinical metastases in cancer: contemporary animal research and clinical reports suggest unifying concepts. *Annals of Surgical Oncology*, *14*(6), 1790–1800. https://doi.org/10.1245/S10434-006-9234-2

Campos, M. A., & Diaz, A. A. (2018). The Role of Computed Tomography for the Evaluation of Lung Disease in Alpha-1 Antitrypsin Deficiency. *Chest*, *153*(5), 1240. https://doi.org/10.1016/J.CHEST.2017.11.017

Canadian Cancer Society. (2021). *Staging cancer | Canadian Cancer Society*. https://cancer.ca/en/cancer-information/what-is-cancer/stage-and-grade/staging

Cao, T., Dai, Z., Ding, Z., Li, W., & Quan, H. (2019). Analysis of different evaluation indexes for prostate stereotactic body radiation therapy plans: conformity index, homogeneity index and gradient index. *Precision Radiation Oncology*, *3*(3), 72–79. https://doi.org/10.1002/PRO6.1072

Capalbo, E., Kluzer, A., Peli, M., Cosentino, M., Berti, E., & Cariati, M. (2015). Bladder cancer diagnosis: the role of CT urography. *Tumori*, *101*(4), 412–417. https://doi.org/10.5301/TJ.5000331

Cardis, E., Krewski, D., Boniol, M., Drozdovitch, V., Darby, S. C., Gilbert, E. S., Akiba, S., Benichou, J., Ferlay, J., Gandini, S., Hill, C., Howe, G., Kesminiene, A., Moser, M., Sanchez, M., Storm, H., Voisin, L., & Boyle, P. (2006). Estimates of the cancer burden in Europe from radioactive fallout from the Chernobyl accident. *International Journal of Cancer*, *119*(6), 1224–1235. https://doi.org/10.1002/IJC.22037

Chaturvedi, A. K., Pfeiffer, R. M., Chang, L., Goedert, J. J., Biggar, R. J., & Engels, E. A. (2007). Elevated risk of lung cancer among people with AIDS. *AIDS*, *21*(2), 207–213. https://doi.org/10.1097/QAD.0B013E3280118FCA

Chen, G., Dong, B., Shan, G., Zhang, X., Tang, H., Li, Y., Wang, Z., Xu, W., Xu, G., Yan, G., Zhang, F., Hu, X., Yang, J., Xu, Y., Chen, M., & Wang, J. (2019). Choice of immobilization of stereotactic body radiotherapy in lung tumor patient by BMI. *BMC Cancer*, *19*(1), 1–9. https://doi.org/10.1186/S12885-019-5767-1/TABLES/2

Chen, Z., Fillmore, C. M., Hammerman, P. S., Kim, C. F., & Wong, K.-K. (2014). Non-small-cell lung cancers: a heterogeneous set of diseases HHS Public Access. *Nat Rev Cancer*, *14*(8), 535–546. https://doi.org/10.1038/nrc3775

Chinneck, C. D., McJury, M., & Hounsell, A. R. (2010). The potential for undertaking slow CT using a modern CT scanner. *The British Journal of Radiology*, *83*(992), 687. https://doi.org/10.1259/BJR/31551018

Chinniah, C., Aguarin, L., Cheng, P., Decesaris, C., Cutillo, A., Berman, A. T., Frick, M., Levin, W. P., Cengel, K. A., Hahn, S. M., Dorsey, J. F., Kao, G. D., Simone, C. B., Singh, A. K., Gomez Suescun, J. A., Stephans, K. L., Bogart, J. A., Lili, T., Malhotra, H., … Groman, A. (2017). A Phase 2 Randomized Study of 2 Stereotactic Body Radiation Therapy Regimens for Medically Inoperable Patients With Node-Negative, Peripheral Non–Small Cell Lung Cancer. *International Journal of Radiation Oncology, Biology, Physics*, *98*(1), 221–222. https://doi.org/10.1016/J.IJROBP.2017.01.040

Chung, J. P., Seong, Y. M., Kim, T. Y., Choi, Y., Kim, T. H., Choi, H. J., Min, C. H., Benmakhlouf, H., Chun, K. J., & Chung, H. T. (2018). Development of a PMMA phantom as a practical alternative for quality control of gamma knife® dosimetry. *Radiation Oncology*, *13*(1), 1–9. https://doi.org/10.1186/S13014-018-1117-8/TABLES/4

Clark, S. B., & Alsubait, S. (2020). Non Small Cell Lung Cancer. *StatPearls*.

Conrath, S. (2012). *Radon: A Leading Environmental Cause of Cancer Mortality | The EPA Blog*. https://blog.epa.gov/2012/01/24/radon-a-leading-environmental-cause-of-cancer-mortality/

Curran, W. J., Jr, Paulus, R., Langer, C. J., Komaki, R., Lee, J. S., Hauser, S., Movsas, B., Wasserman, T., Rosenthal, S. A., Gore, E., Machtay, M., Sause, W., & Cox, J. D. (2011). Sequential vs Concurrent Chemoradiation for Stage III Non–Small Cell Lung Cancer: Randomized Phase III Trial RTOG 9410. *JNCI Journal of the National Cancer Institute*, *103*(19), 1452. https://doi.org/10.1093/JNCI/DJR325

Dahele, M., Pearson, S., Purdie, T., Bissonnette, J. P., Franks, K., Brade, A., Cho, J., Sun, A., Hope, A., Marshall, A., Higgins, J., & Bezjak, A. (2008). Practical Considerations Arising from the Implementation of Lung Stereotactic Body Radiation Therapy (SBRT) at a Comprehensive Cancer Center. *Journal of Thoracic Oncology*, *3*(11), 1332–1341. https://doi.org/10.1097/JTO.0B013E31818B1771

Das, I. J., Cheng, C. W., Chopra, K. L., Mitra, R. K., Srivastava, S. P., & Glatstein, E. (2008). Intensity-modulated radiation therapy dose prescription, recording, and delivery: Patterns of variability among institutions and treatment planning systems. *Journal of the National Cancer Institute*, *100*(5), 300–307. https://doi.org/10.1093/JNCI/DJN020

de Alencar, V. T. L., Formiga, M. N., & de Lima, V. C. C. (2020). Inherited lung cancer: a review. *Ecancermedicalscience*, *14*. https://doi.org/10.3332/ECANCER.2020.1008

De Flora, S., & La Maestra, S. (2015). Epidemiology of cancers of infectious originand prevention strategies. *Journal of Preventive Medicine and Hygiene*, *56*(1), E15.

Dela Cruz, C. S., Tanoue, L. T., & Matthay, R. A. (2011). Lung Cancer: Epidemiology, Etiology, and Prevention. *Clin Chest Med*, *32*(4). https://doi.org/10.1016/j.ccm.2011.09.001

DeLaney, T. F., Yock, T. I., & Paganetti, H. (2020). Assessing second cancer risk after primary cancer treatment with photon or proton radiotherapy. *Cancer*, *126*(15), 3397–3399. https://doi.org/10.1002/CNCR.32936

Deng, W., Jin, L., Zhuo, H., Vasiliou, V., & Zhang, Y. (2021). Alcohol consumption and risk of stomach cancer: A meta-analysis. *Chemico-Biological Interactions*, *336*, 109365–109365. https://doi.org/10.1016/J.CBI.2021.109365

Dilalla, V., Chaput, G., Williams, T., & Sultanem, K. (2020). Radiotherapy side effects: integrating a survivorship clinical lens to better serve patients. *Current Oncology*, *27*(2), 107. https://doi.org/10.3747/CO.27.6233

Diwanji, T. P., Mohindra, P., Vyfhuis, M., Snider, J. W., Kalavagunta, C., Mossahebi, S., Yu, J., Feigenberg, S., & Badiyan, S. N. (2017). Advances in radiotherapy techniques and delivery for non-small cell lung cancer: Benefits of intensity-modulated radiation therapy, proton therapy, and stereotactic body radiation therapy. In *Translational Lung Cancer Research* (Vol. 6, Issue 2, pp. 131–147). AME Publishing Company. https://doi.org/10.21037/tlcr.2017.04.04

Dodd, M., Miaskowski, C., & Paul, S. (2001). Symptom clusters and their effect on the functional status of patients with cancer. *Oncol Nurs Forum*, *28*, 465–470.

Dong, Y., Skelley, A. M., Merdek, K. D., Sprott, K. M., Jiang, C., Pierceall, W. E., Lin, J., Stocum, M., Carney, W. P., & Smirnov, D. A. (2013). Microfluidics and Circulating Tumor Cells. *The Journal of Molecular Diagnostics*, *15*(2), 149–157. https://doi.org/10.1016/J.JMOLDX.2012.09.004

Dracham, C. B., Shankar, A., & Madan, R. (2018). Radiation induced secondary malignancies: a review article. *Radiation Oncology Journal*, *36*(2), 85. https://doi.org/10.3857/ROJ.2018.00290

Dryden, J. (2016). *Quitting smoking reduces cancer risk - Siteman Cancer Center*. https://siteman.wustl.edu/even-genetic-predisposition-lung-cancer-quitting-smoking-reduces-risk/

Dubin, S., & Griffin, D. (2020). Lung Cancer in Non-Smokers. *Missouri Medicine*, *117*(4), 375.

Duffy, M. J., van Dalen, A., Haglund, C., Hansson, L., Holinski-Feder, E., Klapdor, R., Lamerz, R., Peltomaki, P., Sturgeon, C., & Topolcan, O. (2007). Tumour markers in colorectal cancer: European Group on Tumour Markers (EGTM) guidelines for clinical use. *European Journal of Cancer (Oxford, England : 1990)*, *43*(9), 1348–1360. https://doi.org/10.1016/J.EJCA.2007.03.021

Duffy, Michael J. (2013). Tumor markers in clinical practice: a review focusing on common solid cancers. *Medical Principles and Practice : International Journal of the Kuwait University, Health Science Centre*, *22*(1), 4–11. https://doi.org/10.1159/000338393

Eary, J. F. (1999). Nuclear medicine in cancer diagnosis. *Lancet (London, England)*, *354*(9181), 853–857. https://doi.org/10.1016/S0140-6736(99)80041-5

Edwards, S. (2019). *The Lymphatic System - Sharon Edwards - Lisa's Thermography*. https://lisasthermographyandwellness.com/the-lymphatic-system-sharon-edwards/

Eidy, M., & Tishkowski, K. (2021). Radon Toxicity. *StatPearls*.

Ezer, N., Veluswamy, R., Mhango, G., Rosenzweig, K., Powell, C., & Wisnivesky, J. (2015). Outcomes after Stereotactic Body Radiotherapy versus Limited Resection in Older Patients

with Early-Stage Lung Cancer. *Journal of Thoracic Oncology : Official Publication of the International Association for the Study of Lung Cancer*, *10*(8), 1201–1206. https://doi.org/10.1097/JTO.0000000000000600

Ferlay, J., Soerjomataram, I., Dikshit, R., Eser, S., Mathers, C., Rebelo, M., Parkin, D. M., Forman, D., & Bray, F. (2015). Cancer incidence and mortality worldwide: sources, methods and major patterns in GLOBOCAN 2012. *International Journal of Cancer*, *136*(5), E359–E386. https://doi.org/10.1002/IJC.29210

Feuvret, L., Noël, G., Mazeron, J. J., & Bey, P. (2006a). Conformity index: a review. *International Journal of Radiation Oncology, Biology, Physics*, *64*(2), 333–342. https://doi.org/10.1016/J.IJROBP.2005.09.028

Feuvret, L., Noël, G., Mazeron, J. J., & Bey, P. (2006b). Conformity index: A review. *International Journal of Radiation Oncology, Biology, Physics*, *64*(2), 333–342. https://doi.org/10.1016/J.IJROBP.2005.09.028

Fidler, I. J. (1989). Origin and biology of cancer metastasis. *Cytometry*, *10*(6), 673–680. https://doi.org/10.1002/cyto.990100602

Fidler, M., Reulen, R., Winter, D., Allodji, R., Bagnasco, F., Bardi, E., Bautz, A., Bright, C., Byrne, J., Feijen, E., Garwicz, S., Grabow, D., Gudmundsdottir, T., Guha, J., Haddy, N., Jankovic, M., Kaatsch, P., Kaiser, M., Kuonen, R., … Hawkins, M. (2018). Risk of Subsequent Bone Cancers Among 69 460 Five-Year Survivors of Childhood and Adolescent Cancer in Europe. *Journal of the National Cancer Institute*, *110*(2), 183–194. https://doi.org/10.1093/JNCI/DJX165

Fidler, M., Soerjomataram, I., & Bray, F. (2016). A global view on cancer incidence and national levels of the human development index. *International Journal of Cancer*, *139*(11), 2436–2446. https://doi.org/10.1002/ijc.30382

Ford, E. C., Mageras, G. S., Yorke, E., & Ling, C. C. (2003). Respiration-correlated spiral CT: a method of measuring respiratory-induced anatomic motion for radiation treatment planning. *Medical Physics*, *30*(1), 88–97. https://doi.org/10.1118/1.1531177

Frega, S., Maso, A. D., Pasello, G., Cuppari, L., Bonanno, L., Conte, P., & Evangelista, L. (2020). Novel Nuclear Medicine Imaging Applications in Immuno-Oncology. *Cancers*, *12*(5). https://doi.org/10.3390/CANCERS12051303

Freisling, H., Viallon, V., Lennon, H., Bagnardi, V., Ricci, C., Butterworth, A. S., Sweeting, M., Muller, D., Romieu, I., Bazelle, P., Kvaskoff, M., Arveux, P., Severi, G., Bamia, C., Kühn, T., Kaaks, R., Bergmann, M., Boeing, H., Tjønneland, A., … Ferrari, P. (2020). Lifestyle factors and risk of multimorbidity of cancer and cardiometabolic diseases: A multinational cohort study. *BMC Medicine*, *18*(1), 1–11. https://doi.org/10.1186/S12916-019-1474-7/FIGURES/3

Fukumoto, K., Ito, H., Matsuo, K., Tanaka, H., Yokoi, K., Tajima, K., & Takezaki, T. (2015). Cigarette smoke inhalation and risk of lung cancer: a case-control study in a large Japanese population. *European Journal of Cancer Prevention : The Official Journal of the European Cancer Prevention Organisation (ECP)*, *24*(3), 195–200. https://doi.org/10.1097/CEJ.0000000000000034

Gaafar, R. M., & Aly Eldin, N. H. (2005). Epidemic of mesothelioma in Egypt. *Lung Cancer (Amsterdam, Netherlands)*, *49 Suppl 1*(SUPPL. 1). https://doi.org/10.1016/J.LUNGCAN.2005.03.025

Garcia-Rodriguez, J. A. (2018). Radon gas—the hidden killer: What is the role of family doctors? *Canadian Family Physician*, *64*(7), 496.

Giraud, P., & Houle, A. (2013). Respiratory Gating for Radiotherapy: Main Technical Aspects and Clinical Benefits. *ISRN Pulmonology*, *2013*, 1–13. https://doi.org/10.1155/2013/519602

Giraud, P., Morvan, E., Claude, L., Mornex, F., Le Pechoux, C., Bachaud, J.-M., Boisselier, P., Beckendorf, V., & Morelle, M. (2011). Respiratory Gating Techniques for Optimization of Lung Cancer Radiotherapy. In *JTO Acquisition* (Vol. 6). https://doi.org/10.1097/JTO.0b013e3182307ec2

GLOBOCAN. (2020a). *Ghana Source: Globocan Incidence, Mortality and Prevalence by cancer site*.

GLOBOCAN. (2020b). *World Source: Globocan Incidence, Mortality and Prevalence by cancer site*.

GLOBOCAN, L. S. (2020c). *Lung Source: Globocan 2020 Number of new cases in 2020, both sexes, all ages*.

Goldsmith, C., & Gaya, A. (2012). Stereotactic ablative body radiotherapy (SABR) for primary and secondary lung tumours. *Cancer Imaging*, *12*(2), 351. https://doi.org/10.1102/1470-7330.2012.9015

Grills, I., Mangona, V., Welsh, R., Chmielewski, G., McInerney, E., Martin, S., Wloch, J., Ye, H., & Kestin, L. (2010). Outcomes after stereotactic lung radiotherapy or wedge resection for stage I non-small-cell lung cancer. *Journal of Clinical Oncology : Official Journal of the American Society of Clinical Oncology*, *28*(6), 928–935. https://doi.org/10.1200/JCO.2009.25.0928

Guo, R., Lu, G., Qin, B., & Fei, B. (2018). Ultrasound Imaging Technologies for Breast Cancer Detection and Management: A Review. *Ultrasound in Medicine & Biology*, *44*(1), 37–70. https://doi.org/10.1016/J.ULTRASMEDBIO.2017.09.012

Halvorsen, P., Cirino, C., Das, I., Garrett, J., Yang, J., Yin, F.-F., & Fairobent, L. (2017). AAPM-RSS Medical Physics Practice Guideline 9.a. for SRS-SBRT. *Journal of Applied Clinical Medical Physics*, *18*(5), 10–21. https://doi.org/10.1002/ACM2.12146

Hamdi, Y., Abdeljaoued-Tej, I., Zatchi, A. A., Abdelhak, S., Boubaker, S., Brown, J. S., & Benkahla, A. (2021). Cancer in Africa: The Untold Story. *Frontiers in Oncology*, *11*, 1011. https://doi.org/10.3389/FONC.2021.650117/BIBTEX

Hanahan, D., & Weinberg, R. A. (2000). The Hallmarks of Cancer. *Cell*, *100*(1), 57–70. https://doi.org/10.1016/S0092-8674(00)81683-9

Hanania, A. N., Mainwaring, W., Ghebre, Y., Hanania, N. A., & Ludwig, M. (2019). Radiation-Induced Lung Injury: Assessment and Management. *Chest*, *156*(1), 150–162. https://doi.org/10.1016/J.CHEST.2019.03.033

Hang, B., Mao, J. H., & Snijders, A. M. (2019). Genetic Susceptibility to Thirdhand-Smoke-Induced Lung Cancer Development. *Nicotine & Tobacco Research : Official Journal of the Society for Research on Nicotine and Tobacco*, *21*(9), 1294–1296. https://doi.org/10.1093/NTR/NTY127

Hang, B., Wang, P., Zhao, Y., Chang, H., Mao, J. H., & Snijders, A. M. (2020). Thirdhand smoke: Genotoxicity and carcinogenic potential. *Chronic Diseases and Translational Medicine*, *6*(1), 27–34. https://doi.org/10.1016/J.CDTM.2019.08.002

Hang, B., Wang, Y., Huang, Y., Wang, P., Langley, S. A., Bi, L., Sarker, A. H., Schick, S. F., Havel, C., Jacob, P., Benowitz, N., Destaillats, H., Tang, X., Xia, Y., Jen, K. Y., Gundel, L. A., Mao, J. H., & Snijders, A. M. (2018). Short-term early exposure to thirdhand cigarette smoke increases lung cancer incidence in mice. *Clinical Science (London, England : 1979)*, *132*(4), 475–488. https://doi.org/10.1042/CS20171521

Hanselmann, R. G., & Welter, C. (2022). Origin of Cancer: Cell work is the Key to Understanding Cancer Initiation and Progression. *Frontiers in Cell and Developmental Biology*, *10*. https://doi.org/10.3389/FCELL.2022.787995

Harada, K., Katoh, N., Suzuki, R., Ito, Y. M., Shimizu, S., Onimaru, R., Inoue, T., Miyamoto, N., & Shirato, H. (2016). Evaluation of the motion of lung tumors during stereotactic body radiation therapy (SBRT) with four-dimensional computed tomography (4DCT) using real-time tumor-tracking radiotherapy system (RTRT). *Physica Medica : PM : An International Journal Devoted to the Applications of Physics to Medicine and Biology : Official Journal of the Italian Association of Biomedical Physics (AIFB)*, *32*(2), 305–311. https://doi.org/10.1016/J.EJMP.2015.10.093

Haseltine, J. M., Rimner, A., Gelblum, D. Y., Modh, A., Rosenzweig, K. E., Jackson, A., Yorke, E. D., & Wu, A. J. (2016). Fatal complications after stereotactic body radiation therapy for central lung tumors abutting the proximal bronchial tree. *Practical Radiation Oncology*, *6*(2), e27. https://doi.org/10.1016/J.PRRO.2015.09.012

Hecht, S. S. (1999). Tobacco smoke carcinogens and lung cancer. *Journal of the National Cancer Institute*, *91*(14), 1194–1210. https://doi.org/10.1093/JNCI/91.14.1194

Hecht, S. S. (2012). Lung Carcinogenesis by Tobacco Smoke. *International Journal of Cancer. Journal International Du Cancer*, *131*(12), 2724. https://doi.org/10.1002/IJC.27816

Heinzerling, J. H., Anderson, J. F., Papiez, L., Boike, T., Chien, S., Zhang, G., Abdulrahman, R., & Timmerman, R. (2008). Four-Dimensional Computed Tomography Scan Analysis of Tumor and Organ Motion at Varying Levels of Abdominal Compression During Stereotactic Treatment of Lung and Liver. *International Journal of Radiation Oncology Biology Physics*, *70*(5), 1571–1578. https://doi.org/10.1016/j.ijrobp.2007.12.023

Herbert, C., Kwa, W., Nakano, S., James, K., Moiseenko, V., Wu, J., Schellenberg, D., & Liu, M. (2013). Stereotactic body radiotherapy: volumetric modulated arc therapy versus 3D non-coplanar conformal radiotherapy for the treatment of early stage lung cancer. *Technology in Cancer Research & Treatment*, *12*(6), 511–516. https://doi.org/10.7785/TCRT.2012.500338

Hernando, C. G., Esteban, L., Cañas, T., Van Den Brule, E., & Pastrana, M. (2010). The role of magnetic resonance imaging in oncology. *Clinical & Translational Oncology : Official*

Publication of the Federation of Spanish Oncology Societies and of the National Cancer Institute of Mexico, *12*(9), 606–613. https://doi.org/10.1007/S12094-010-0565-X

Heukelom, J., Kantor, M. E., Mohamed, A. S. R., Elhalawani, H., Kocak-Uzel, E., Lin, T., Yang, J., Aristophanous, M., Rasch, C. R., Fuller, C. D., & Sonke, J. J. (2020). Differences between planned and delivered dose for head and neck cancer, and their consequences for normal tissue complication probability and treatment adaptation. *Radiotherapy and Oncology : Journal of the European Society for Therapeutic Radiology and Oncology*, *142*, 100. https://doi.org/10.1016/J.RADONC.2019.07.034

Hochhegger, B., Alves, G. R. T., Irion, K. L., Fritscher, C. C., Fritscher, L. G., Concatto, N. H., & Marchiori, E. (2015). PET/CT imaging in lung cancer: indications and findings. *Jornal Brasileiro de Pneumologia*, *41*(3), 264–274. https://doi.org/10.1590/S1806-37132015000004479

Hoffman, D., Dragojević, I., Hoisak, J., Hoopes, D., & Manger, R. (2019). Lung Stereotactic Body Radiation Therapy (SBRT) dose gradient and PTV volume: a retrospective multi-center analysis. *Radiation Oncology (London, England)*, *14*(1). https://doi.org/10.1186/S13014-019-1334-9

Holtedahl, K., Borgquist, L., Donker, G. A., Buntinx, F., Weller, D., Campbell, C., Månsson, J., Hammersley, V., Braaten, T., & Parajuli, R. (2021). Symptoms and signs of colorectal cancer, with differences between proximal and distal colon cancer: a prospective cohort study of diagnostic accuracy in primary care. *BMC Family Practice*, *22*(1). https://doi.org/10.1186/S12875-021-01452-6

Holtedahl, K., Hjertholm, P., Borgquist, L., Donker, G. A., Buntinx, F., Weller, D., Braaten, T., Månsson, J., Strandberg, E. L., Campbell, C., Korevaar, J. C., & Parajuli, R. (2018). Abdominal symptoms and cancer in the Abdomen: Prospective cohort study in European primary care. *British Journal of General Practice*, *68*(670), e301–e310. https://doi.org/10.3399/bjgp18X695777

Hoshida, T., Isaka, N., Hagendoorn, J., Di Tomaso, E., Chen, Y. L., Pytowski, B., Fukumura, D., Padera, T. P., & Jain, R. K. (2006). Imaging Steps of Lymphatic Metastasis Reveals That Vascular Endothelial Growth Factor-C Increases Metastasis by Increasing Delivery of Cancer Cells to Lymph Nodes: Therapeutic Implications. *Cancer Research*, *66*(16), 8065–8075. https://doi.org/10.1158/0008-5472.CAN-06-1392

Hu, H. (2016). *Intraoperative pulmonary nodule localization with cone-beam computed tomography and deformable image registration*. University of Toronto.

Huerta, E., & Grey, N. (2007). Cancer Control Opportunities in Low- and Middle-income Countries. *CA: A Cancer Journal for Clinicians*, *57*(2), 72–74. https://doi.org/10.3322/CANJCLIN.57.2.72

Hugo, G. D., & Rosu, M. (2012). Advances in 4D Radiation Therapy for Managing Respiration: Part I – 4D Imaging. *Zeitschrift Fur Medizinische Physik*, *22*(4), 258. https://doi.org/10.1016/J.ZEMEDI.2012.06.009

Hunter, N., Muirhead, C. R., Bochicchio, F., & Haylock, R. G. E. (2015). Calculation of lifetime lung cancer risks associated with radon exposure, based on various models and exposure

scenarios. *Journal of Radiological Protection*, *35*(3), 539. https://doi.org/10.1088/0952-4746/35/3/539

Husband, J. E. (1985). Role of the CT scanner in the management of cancer. *British Medical Journal (Clinical Research Ed.)*, *290*(6467), 527–530. https://doi.org/10.1136/BMJ.290.6467.527

Hutchinson, A., & Bridge, P. (2015). 4DCT radiotherapy for NSCLC: a review of planning methods. *Journal of Radiotherapy in Practice*, *14*(1), 70–79. https://doi.org/10.1017/S1460396914000041

ICRU 50. (1993). *Prescribing, recording, and reporting photon beam therapy. ICRU 50.* .

ICRU 62. (1999). *Prescribing, Recording and Reporting Photon Beam Therapy Supplement to ICRU Report 50 ICRU Report 62*.

ICRU 83. (2010). *International Commission of Radiation Units and Measurements. ICRU report 83: Prescribing, Recording, and Reporting Photon-Beam Intensity-Modulated Radiation Therapy (IMRT)*.

Jacob, L., Freyn, M., Kalder, M., Dinas, K., & Kostev, K. (2018). Impact of tobacco smoking on the risk of developing 25 different cancers in the UK: a retrospective study of 422,010 patients followed for up to 30 years. *Oncotarget*, *9*(25), 17420. https://doi.org/10.18632/ONCOTARGET.24724

Jacob, P., Benowitz, N. L., Destaillats, H., Gundel, L., Hang, B., Martins-Green, M., Matt, G. E., Quintana, P. J. E., Samet, J. M., Schick, S. F., Talbot, P., Aquilina, N. J., Hovell, M. F., Mao, J. H., & Whitehead, T. P. (2017). Thirdhand Smoke: New Evidence, Challenges, and Future Directions. *Chemical Research in Toxicology*, *30*(1), 270. https://doi.org/10.1021/ACS.CHEMRESTOX.6B00343

Jan, N., Hugo, G. D., Mukhopadhyay, N., & Weiss, E. (2015). Respiratory motion variability of primary tumors and lymph nodes during radiotherapy of locally advanced non-small-cell lung cancers. *Radiation Oncology*, *10*(1), 1–8. https://doi.org/10.1186/S13014-015-0435-3/FIGURES/5

Janssen, S., KÄSMANN, L., RUDAT, V., & RADES, D. (2016). Stereotactic Body Radiotherapy Provides Excellent Long-Term Local Control of Very Few Lung Metastases. *In Vivo*, *30*(2).

Jemal, A., Center, M. M., DeSantis, C., & Ward, E. M. (2010). Global Patterns of Cancer Incidence and Mortality Rates and Trends. *Cancer Epidemiology and Prevention Biomarkers*, *19*(8), 1893–1907. https://doi.org/10.1158/1055-9965.EPI-10-0437

Jensen, J. S., Grønhøj, C., Garset-Zamani, M., Westergaard-Nielsen, M., Bjørndal, K., Kiss, K., Charabi, B., von Buchwald, C., & Hjuler, T. (2021). Incidence and survival of salivary gland cancer in children and young adults in Denmark: A nation-wide study for the period 1990-2015. *International Journal of Pediatric Otorhinolaryngology*, *143*. https://doi.org/10.1016/J.IJPORL.2021.110637

Journy, N. M. Y., Lee, C., Harbron, R. W., McHugh, K., Pearce, M. S., & De González, A. B. (2017). Projected cancer risks potentially related to past, current, and future practices in paediatric CT in the United Kingdom, 1990-2020. *British Journal of Cancer*, *116*(1), 109–

116. https://doi.org/10.1038/BJC.2016.351

Kabel, A. M. (2017). Tumor markers of breast cancer: New prospectives. *Journal of Oncological Sciences*, *3*(1), 5–11. https://doi.org/10.1016/J.JONS.2017.01.001

Kalef-Ezra, J., Karantanas, A., & Tsekeris, P. (1999). CT Measurement of Lung Density. *Acta Radiologica*, *40*(3), 333–337. https://doi.org/10.3109/02841859909175564

Kang, K. H., Okoye, C. C., Patel, R. B., Siva, S., Biswas, T., Ellis, R. J., Yao, M., Machtay, M., & Lo, S. S. (2015). Complications from Stereotactic Body Radiotherapy for Lung Cancer. *Cancers*, *7*(2), 981. https://doi.org/10.3390/CANCERS7020820

Kanwal, M., Ding, X. J., & Cao, Y. (2017). Familial risk for lung cancer. *Oncology Letters*, *13*(2), 535. https://doi.org/10.3892/OL.2016.5518

Kapoor, M., & Kasi, A. (2021). PET Scanning. *StatPearls*.

Katzke, V. A., Kaaks, R., & Kühn, T. (2015). Lifestyle and cancer risk. *Cancer Journal (Sudbury, Mass.)*, *21*(2), 104–110. https://doi.org/10.1097/PPO.0000000000000101

Kaufman, E. L., Jacobson, J. S., Hershman, D. L., Desai, M., & Neugut, A. I. (2008). Effect of breast cancer radiotherapy and cigarette smoking on risk of second primary lung cancer. *Journal of Clinical Oncology*, *26*(3), 392–398. https://doi.org/10.1200/JCO.2007.13.3033

Kay, F. U., Kandathil, A., Batra, K., Saboo, S. S., Abbara, S., & Rajiah, P. (2017). Revisions to the Tumor, Node, Metastasis staging of lung cancer (8th edition): Rationale, radiologic findings and clinical implications. *World Journal of Radiology*, *9*(6), 269–279. https://doi.org/10.4329/wjr.v9.i6.269

Keall, P., Balter, J. M., Saint, R. S. E., Center, V. C., Forster, K., Anderson, U. M. D., Princess, D. A. J., Hospital, M., Jiang, S., Low, D. A., Murphy, M. J., Murray, B. R., Van Herk, M. B., Wong, J. W., Hospital, W. B., & Yorke, E. (2006). *Managing Respiratory Motion in Radiation Therapy Managing Respiratory Motion in Radiation Therapy With acknowledgements to fellow TG 76 Task Group Members*.

Keall, P., Mageras, G., Balter, J., Emery, R. S., Forster, K. M., Jiang, S. B., Kapatoes, J. M., Low, D. A., Murphy, M. J., Murray, B. R., Ramsey, C. R., Van Herk, M. B., Sastry Vedam, S., Wong, J. W., & Yorke, E. (2006). *The management of respiratory motion in radiation oncology report of AAPM Task Group 76 a…*. https://doi.org/10.1118/1.2349696

Khan, N., Afaq, F., & Mukhtar, H. (2010). LIFESTYLE AS RISK FACTOR FOR CANCER: EVIDENCE FROM HUMAN STUDIES. *Cancer Letters*, *293*(2), 133. https://doi.org/10.1016/J.CANLET.2009.12.013

Kharsany, A. B. M., & Karim, Q. A. (2016). HIV Infection and AIDS in Sub-Saharan Africa: Current Status, Challenges and Opportunities. *The Open AIDS Journal*, *10*(1), 34–48. https://doi.org/10.2174/1874613601610010034

Khiewvan, B., Atorigian, D., Emamzadehfard, S., Paydary, K., Salavati, A., Houshmand, S., Shamchi, S. P., Werner, T. J., Aydin, A., Roy, S. G., Alavi, A., & Kumar, R. (2016). Update of the role of PET/CT and PET/MRI in the management of patients with cervical cancer. *Hellenic Journal of Nuclear Medicine*, *19*(3), 254–268. https://doi.org/10.1967/S002449910409

Khiewvan, B., Torigian, D. A., Emamzadehfard, S., Paydary, K., Salavati, A., Houshmand, S., Werner, T. J., & Alavi, A. (2017). An update on the role of PET/CT and PET/MRI in ovarian cancer. *European Journal of Nuclear Medicine and Molecular Imaging*, *44*(6), 1079–1091. https://doi.org/10.1007/S00259-017-3638-Z

Kim, A. S., Ko, H. J., Kwon, J. H., & Lee, J. M. (2018). Exposure to Secondhand Smoke and Risk of Cancer in Never Smokers: A Meta-Analysis of Epidemiologic Studies. *International Journal of Environmental Research and Public Health*, *15*(9). https://doi.org/10.3390/IJERPH15091981

Kim, Y. L., Chung, J. B., Kim, J. S., Lee, J. W., Kim, J. Y., Kang, S. W., & Suh, T. S. (2015). Dosimetric comparison of a 6-MV flattening-filter and a flattening-filter-free beam for lung stereotactic ablative radiotherapy treatment. *Journal of the Korean Physical Society 2015 67:9*, *67*(9), 1672–1678. https://doi.org/10.3938/JKPS.67.1672

Kiratli, P. Ö., Tuncel, M., & Bar-Sever, Z. (2016). Nuclear Medicine in Pediatric and Adolescent Tumors. *Seminars in Nuclear Medicine*, *46*(4), 308–323. https://doi.org/10.1053/J.SEMNUCLMED.2016.01.004

Kirk, G. D., Merlo, C., O'Driscoll, P., Mehta, S. H., Galai, N., Vlahov, D., Samet, J., & Engels, E. A. (2007). HIV Infection Is Associated with an Increased Risk for Lung Cancer, Independent of Smoking. *Clinical Infectious Diseases*, *45*(1), 103–110. https://doi.org/10.1086/518606

Kispert, S., & McHowat, J. (2017). Recent insights into cigarette smoking as a lifestyle risk factor for breast cancer. *Breast Cancer: Targets and Therapy*, *9*, 127–132. https://doi.org/10.2147/BCTT.S129746

Kitson-Mills, D., Sovoe, S., Opoku-Ntim, I., Kyei, K. A., Marnotey, S., Anim-Sampong, S., Kwabeng, M. A., Otoo, F., & Baiden, F. (2019). An assessment of indoor radon level in a suburb of Ghana. *Environmental Research Communications*, *1*(6), 061002. https://doi.org/10.1088/2515-7620/AB2AF7

Knudson, A. G. (2002). Cancer genetics. *American Journal of Medical Genetics*, *111*(1), 96–102. https://doi.org/10.1002/AJMG.10320

Koeller, D. R., Chen, R., & Oxnard, G. R. (2018). Hereditary Lung Cancer Risk: Recent Discoveries and Implications for Genetic Counseling and Testing. *Current Genetic Medicine Reports 2018 6:2*, *6*(2), 83–88. https://doi.org/10.1007/S40142-018-0140-2

Korzets Ceder, Y., Fenig, E., Popvtzer, A., Peled, N., Kramer, M. R., Saute, M., Bragilovsky, D., Schochat, T., & Allen, A. M. (2018). Stereotactic body radiotherapy for central lung tumors, yes we can! *Radiation Oncology (London, England)*, *13*(1), 77. https://doi.org/10.1186/S13014-018-1017-Y/FIGURES/3

Kourou, K., Exarchos, T. P., Exarchos, K. P., Karamouzis, M. V., & Fotiadis, D. I. (2015). Machine learning applications in cancer prognosis and prediction. *Computational and Structural Biotechnology Journal*, *13*, 8–17. https://doi.org/10.1016/J.CSBJ.2014.11.005

Kraus, K. M., Oechsner, M., Wilkens, J. J., Kessel, K. A., Münch, S., & Combs, S. E. (2021). Patient individual phase gating for stereotactic radiation therapy of early stage non-small cell lung cancer (NSCLC). *Scientific Reports 2021 11:1*, *11*(1), 1–10. https://doi.org/10.1038/s41598-021-85031-w

Kuchenbaecker, K., Hopper, J., Barnes, D., Phillips, K., Mooij, T., Roos-Blom, M., S, J., FE, van L., RL, M., N, A., DE, G., MB, T., MA, R., DF, E., AC, A., L, M., DG, E., D, B., D, F., … H, O. (2017). Risks of Breast, Ovarian, and Contralateral Breast Cancer for BRCA1 and BRCA2 Mutation Carriers. *JAMA*, *317*(23), 2402–2416. https://doi.org/10.1001/JAMA.2017.7112

Kumar, S. S., Higgins, K. A., & McGarry, R. C. (2017). Emerging Therapies for Stage III Non-Small Cell Lung Cancer: Stereotactic Body Radiation Therapy and Immunotherapy. *Frontiers in Oncology*, *0*(SEP), 197. https://doi.org/10.3389/FONC.2017.00197

Lagerwaard, F. J., Haasbeek, C. J. A., Smit, E. F., Slotman, B. J., & Senan, S. (2008). Outcomes of Risk-Adapted Fractionated Stereotactic Radiotherapy for Stage I Non-Small-Cell Lung Cancer. *International Journal of Radiation Oncology Biology Physics*, *70*(3), 685–692. https://doi.org/10.1016/j.ijrobp.2007.10.053

Lagerwaard, F. J., Van Sornsen de Koste, J. R., Nijssen-Visser, M. R. J., Schuchhard-Schipper, R. H., Oei, S. S., Munne, A., & Senan, S. (2001). Multiple 'slow' CT scans for incorporating lung tumor mobility in radiotherapy planning. *International Journal of Radiation Oncology, Biology, Physics*, *51*(4), 932–937. https://doi.org/10.1016/S0360-3016(01)01716-3

Laird, B. J. A., Scott, A. C., Colvin, L. A., McKeon, A. L., Murray, G. D., Fearon, K. C. H., & Fallon, M. T. (2011). Pain, Depression, and Fatigue as a Symptom Cluster in Advanced Cancer. *Journal of Pain and Symptom Management*, *42*(1), 1–11. https://doi.org/10.1016/J.JPAINSYMMAN.2010.10.261

Lambert, A. W., Pattabiraman, D. R., & Weinberg, R. A. (2017). Emerging Biological Principles of Metastasis. *Cell*, *168*(4), 670–691. https://doi.org/10.1016/J.CELL.2016.11.037

Lambrecht, M., Clementel, E., Sonke, J. J., Nestle, U., Adebahr, S., Guckenberger, M., Andratschke, N., Weber, D. C., Verheij, M., & Hurkmans, C. W. (2019). Radiotherapy quality assurance of SBRT for patients with centrally located lung tumours within the multicentre phase II EORTC Lungtech trial: Benchmark case results. *Radiotherapy and Oncology*, *132*, 63–69. https://doi.org/10.1016/J.RADONC.2018.10.025

Land, C. E., Bouville, A., Apostoaei, I., & Simon, S. L. (2010). PROJECTED LIFETIME CANCER RISKS FROM EXPOSURE TO REGIONAL RADIOACTIVE FALLOUT IN THE MARSHALL ISLANDS. *Health Physics*, *99*(2), 201. https://doi.org/10.1097/HP.0B013E3181DC4E84

Langen, K. M., & Jones, D. T. L. (2001). Organ motion and its management. *International Journal of Radiation Oncology, Biology, Physics*, *50*(1), 265–278. https://doi.org/10.1016/S0360-3016(01)01453-5

Laryea, D. O., Awuah, B., Amoako, Y. A., Osei-Bonsu, E., Dogbe, J., Larsen-Reindorf, R., Ansong, D., Yeboah-Awudzi, K., Oppong, J. K., Konney, T. O., Boadu, K. O., Nguah, S. B., Titiloye, N. A., Frimpong, N. O., Awittor, F. K., & Martin, I. K. (2014). Cancer incidence in Ghana, 2012: Evidence from a population-based cancer registry. *BMC Cancer*, *14*(1). https://doi.org/10.1186/1471-2407-14-362

Latimer, K. (2018). Lung Cancer: Clinical Presentation and Diagnosis. *FP Essentials*, *464*, 23–26.

Laughlin, J. M. (2012). An historical overview of radon and its progeny: applications and health

effects. *Radiation Protection Dosimetry*, *152*(1–3), 2–8. https://doi.org/10.1093/RPD/NCS189

Lax, I., Blomgren, H., Larson, D., & Näslund, I. (1998). Extracranial Stereotactic Radiosurgery of Localized Targets. *Journal of Radiosurgery*, *1*(2), 135–148.

Lee, P., Loo, B. W., Biswas, T., Ding, G. X., El Naqa, I. M., Jackson, A., Kong, F. M., LaCouture, T., Miften, M., Solberg, T., Tome, W. A., Tai, A., Yorke, E., & Li, X. A. (2021). Local Control After Stereotactic Body Radiation Therapy for Stage I Non-Small Cell Lung Cancer. *International Journal of Radiation Oncology, Biology, Physics*, *110*(1), 160–171. https://doi.org/10.1016/J.IJROBP.2019.03.045

Lemjabbar-Alaoui, H., Hassan, O., Yang, Y.-W., & Buchanan, P. (2015). Lung cancer: biology and treatment options. *Biochimica et Biophysica Acta*, *1856*(2), 189–210. https://doi.org/10.1016/j.bbcan.2015.08.002

Leong, S. P. L., Nakakura, E. K., Pollock, R., Choti, M. A., Morton, D. L., Henner, W. D., Lal, A., Pillai, R., Clark, O. H., & Cady, B. (2011). Unique patterns of metastases in common and rare types of malignancy. *Journal of Surgical Oncology*, *103*(6), 607–614. https://doi.org/10.1002/JSO.21841

Li, W., Tse, L. A., Au, J. S. K., Wang, F., Qiu, H., & Yu, I. T. S. (2016). Secondhand Smoke Enhances Lung Cancer Risk in Male Smokers: An Interaction. *Nicotine & Tobacco Research : Official Journal of the Society for Research on Nicotine and Tobacco*, *18*(11), 2057–2064. https://doi.org/10.1093/NTR/NTW115

Lindberg, K., Nyman, J., Riesenfeld Källskog, V., Hoyer, M., Lund, J. A., Lax, I., Wersäll, P., Karlsson, K., Friesland, S., & Lewensohn, R. (2015). Long-term results of a prospective phase II trial of medically inoperable stage i NSCLC treated with SBRT - The Nordic experience. *Acta Oncologica*, *54*(8), 1096–1104. https://doi.org/10.3109/0284186X.2015.1020966/SUPPL_FILE/IONC_A_1020966_SM1404.PDF

Linet, M. S., Slovis, T. L., Miller, D. L., Kleinerman, R., Lee, C., Rajaraman, P., & Gonzalez, A. B. de. (2012). Cancer Risks Associated with External Radiation From Diagnostic Imaging Procedures. *CA: A Cancer Journal for Clinicians*, *62*(2), 75. https://doi.org/10.3322/CAAC.21132

Liu, H. H., Balter, P., Tutt, T., Choi, B., Zhang, J., Wang, C., Chi, M., Luo, D., Pan, T., Hunjan, S., Starkschall, G., Rosen, I., Prado, K., Liao, Z., Chang, J., Komaki, R., Cox, J. D., Mohan, R., & Dong, L. (2007). Assessing respiration-induced tumor motion and internal target volume using four-dimensional computed tomography for radiotherapy of lung cancer. *International Journal of Radiation Oncology, Biology, Physics*, *68*(2), 531–540. https://doi.org/10.1016/J.IJROBP.2006.12.066

Lloyd, C., & McHugh, K. (2010). The role of radiology in head and neck tumours in children. *Cancer Imaging : The Official Publication of the International Cancer Imaging Society*, *10*(1), 49–61. https://doi.org/10.1102/1470-7330.2010.0003

Lorenzo-González, M., Torres-Durán, M., Barbosa-Lorenzo, R., Provencio-Pulla, M., Barros-Dios, J. M., & Ruano-Ravina, A. (2019). Radon exposure: a major cause of lung cancer.

Expert Review of Respiratory Medicine, *13*(9), 839–850. https://doi.org/10.1080/17476348.2019.1645599

Luining, W. I., Cysouw, M. C. F., Meijer, D., Hendrikse, N. H., Boellaard, R., Vis, A. N., & Oprea-Lager, D. E. (2022). Targeting PSMA Revolutionizes the Role of Nuclear Medicine in Diagnosis and Treatment of Prostate Cancer. *Cancers*, *14*(5). https://doi.org/10.3390/CANCERS14051169

LUNGEVITY. (2021). *How Lung Cancer Develops | LUNGevity Foundation*. https://www.lungevity.org/for-patients-caregivers/lung-cancer-101/how-lung-cancer-develops

Lupo, P. J., Schraw, J. M., Desrosiers, T. A., Nembhard, W. N., Langlois, P. H., Canfield, M. A., Copeland, G., Meyer, R. E., Brown, A. L., Chambers, T. M., Sok, P., Danysh, H. E., Carozza, S. E., Sisoudiya, S. D., Hilsenbeck, S. G., Janitz, A. E., Oster, M. E., Scheuerle, A. E., Schiffman, J. D., … Plon, S. E. (2019). Association Between Birth Defects and Cancer Risk Among Children and Adolescents in a Population-Based Assessment of 10 Million Live Births. *JAMA Oncology*, *5*(8), 1. https://doi.org/10.1001/JAMAONCOL.2019.1215

Lupo, P. J., & Spector, L. G. (2020). Cancer Progress and Priorities: Childhood Cancer. *Cancer Epidemiology and Prevention Biomarkers*, *29*(6), 1081–1094. https://doi.org/10.1158/1055-9965.EPI-19-0941

MacHtay, M., Bae, K., Movsas, B., Paulus, R., Gore, E. M., Komaki, R., Albain, K., Sause, W. T., & Curran, W. J. (2012). Higher biologically effective dose of radiotherapy is associated with improved outcomes for locally advanced non-small cell lung carcinoma treated with chemoradiation: an analysis of the Radiation Therapy Oncology Group. *International Journal of Radiation Oncology, Biology, Physics*, *82*(1), 425–434. https://doi.org/10.1016/J.IJROBP.2010.09.004

Mageras, G. S., Pevsner, A., Yorke, E. D., Rosenzweig, K. E., Ford, E. C., Hertanto, A., Larson, S. M., Lovelock, D. M., Erdi, Y. E., Nehmeh, S. A., Humm, J. L., & Ling, C. C. (2004). Measurement of lung tumor motion using respiration-correlated CT. *International Journal of Radiation Oncology Biology Physics*, *60*(3), 933–941. https://doi.org/10.1016/j.ijrobp.2004.06.021

Mahadevan, A., Blanck, O., Lanciano, R., Peddada, A., Sundararaman, S., D'Ambrosio, D., Sharma, S., Perry, D., Kolker, J., & Davis, J. (2018). Stereotactic Body Radiotherapy (SBRT) for liver metastasis - clinical outcomes from the international multi-institutional RSSearch® Patient Registry. *Radiation Oncology*, *13*(1), 1–11. https://doi.org/10.1186/S13014-018-0969-2/TABLES/2

Majeed, H., & Gupta, V. (2021). Adverse Effects Of Radiation Therapy. *StatPearls*.

Malhotra, J., Malvezzi, M., Negri, E., La Vecchia, C., & Boffetta, P. (2016). Risk factors for lung cancer worldwide. *The European Respiratory Journal*, *48*(3), 889–902. https://doi.org/10.1183/13993003.00359-2016

Martinelli, C., Pucci, C., & Ciofani, G. (2019). Nanostructured carriers as innovative tools for cancer diagnosis and therapy. *APL Bioengineering*, *3*(1). https://doi.org/10.1063/1.5079943

Mayer, R., Stanton, K., Kleinberg, L., Chakravarthy, A., & Fishman, E. (1998). *CT number*

distribution and its association with local control and as a marker of lung tumor response to radiation - Mayer - 1998 - Radiation Oncology Investigations - Wiley Online Library. https://onlinelibrary.wiley.com/doi/10.1002/(SICI)1520-6823(1998)6:6%3C281::AID-ROI6%3E3.0.CO;2-H

Mayo Clinic. (2020). *Early Detection of Lung Cancer Using Nano-Nose - A Review*. https://benthamopen.com/FULLTEXT/TOBEJ-9-228/FIGURE/F1/

McCarten, K. M., Nadel, H. R., Shulkin, B. L., & Cho, S. Y. (2019). Imaging for diagnosis, staging and response assessment of Hodgkin lymphoma and non-Hodgkin lymphoma. *Pediatric Radiology*, *49*(11), 1545–1564. https://doi.org/10.1007/S00247-019-04529-8

McKenzie, F., Biessy, C., Ferrari, P., Freisling, H., Rinaldi, S., Chajes, V., Dahm, C. C., Overvad, K., Dossus, L., Lagiou, P., Trichopoulos, D., Trichopoulou, A., Bas Bueno-De-Mesquita, H., May, A., Peeters, P. H., Weiderpass, E., Sanchez, M. J., Navarro, C., Ardanaz, E., … Romieu, I. (2016). Healthy lifestyle and risk of cancer in the European prospective investigation into cancer and nutrition cohort study. *Medicine (United States)*, *95*(16). https://doi.org/10.1097/MD.0000000000002850

MedicineNet, I. (2010). *Lung Cancer vs. Pneumonia: Symptoms, Signs & Causes*. https://www.emedicinehealth.com/lung_cancer_vs_pneumonia_symptoms_and_signs/article_em.htm

Melin-Johansson, C., Axelsson, B., Gaston-Johansson, F., & Danielson, E. (2010). Significant improvement in quality of life of patients with incurable cancer after designation to a palliative homecare team. *European Journal of Cancer Care*, *19*(2), 243–250. https://doi.org/10.1111/J.1365-2354.2008.01017.X

Mendhiratta, N., Taneja, S. S., & Rosenkrantz, A. B. (2016). The role of MRI in prostate cancer diagnosis and management. *Future Oncology (London, England)*, *12*(21), 2431–2443. https://doi.org/10.2217/FON-2016-0169

Mendiratta, G., Ke, E., Aziz, M., Liarakos, D., Tong, M., & Stites, E. C. (2021). Cancer gene mutation frequencies for the U.S. population. *Nature Communications*, *12*(1). https://doi.org/10.1038/S41467-021-26213-Y

Mensah, K. B., & Mensah, A. B. B. (2020). Cancer control in Ghana: A narrative review in global context. In *Heliyon* (Vol. 6, Issue 8). Elsevier Ltd. https://doi.org/10.1016/j.heliyon.2020.e04564

Miyakawa, A., Shibamoto, Y., Baba, F., Manabe, Y., Murai, T., Sugie, C., Yanagi, T., & Takaoka, T. (2017). Stereotactic body radiotherapy for stage I non-small-cell lung cancer using higher doses for larger tumors: results of the second study. *Radiation Oncology (London, England)*, *12*(1). https://doi.org/10.1186/S13014-017-0888-7

Modh, A., Rimner, A., Williams, E., Foster, A., Mihir, S. M., Shi, W., Zhang, Z., Gelblum, D. Y., Rosenzweig, K. E., Yorke, E. D., Jackson, A., & Wu, A. J. (2014). Local Control and Toxicity in a Large Cohort of Central Lung Tumors Treated With Stereotactic Body Radiotherapy. *International Journal of Radiation Oncology, Biology, Physics*, *90*(5), 1168. https://doi.org/10.1016/J.IJROBP.2014.08.008

Molitoris, J. K., Diwanji, T., Snider, J. W., Mossahebi, S., Samanta, S., Onyeuku, N., Mohindra,

P., Isabelle Choi, J., & Simone, C. B. (2019). Optimizing immobilization, margins, and imaging for lung stereotactic body radiation therapy. *Translational Lung Cancer Research*, *8*(1), 24. https://doi.org/10.21037/TLCR.2018.09.25

Moustakis, C., Ebrahimi Tazehmahalleh, F., Elsayad, K., Fezeu, F., & Scobioala, S. (2020). A novel approach to SBRT patient quality assurance using EPID-based real-time transit dosimetry: A step to QA with in vivo EPID dosimetry. *Strahlentherapie Und Onkologie*, *196*(2), 182–192. https://doi.org/10.1007/S00066-019-01549-Z

Naeem, Z. (2015). Second-hand smoke – ignored implications. *International Journal of Health Sciences*, *9*(2), V.

Nagata, Y., & Kimura, T. (2018). Stereotactic body radiotherapy (SBRT) for Stage I lung cancer. In *Japanese Journal of Clinical Oncology* (Vol. 48, Issue 5, pp. 405–409). Oxford University Press. https://doi.org/10.1093/jjco/hyy034

Nakamura, H., & Maeda, H. (2022). Cancer Chemotherapy. *Fundamentals of Pharmaceutical Nanoscience*, 401–427. https://doi.org/10.1007/978-1-4614-9164-4_15

National Cancer Institute. (2015). *Cancer Staging*. https://www.cancer.gov/about-cancer/diagnosis-staging/staging

Navarro-Martin, A., Aso, S., Cacicedo, J., Arnaiz, M., Navarro, V., Rosales, S., De Blas, R., Ramos, R., & Guedea, F. (2016). Phase II Trial of SBRT for Stage I NSCLC: Survival, Local Control, and Lung Function at 36 Months. *Journal of Thoracic Oncology : Official Publication of the International Association for the Study of Lung Cancer*, *11*(7), 1101–1111. https://doi.org/10.1016/J.JTHO.2016.03.021

NCCN. (2021). *NCCN Guidelines for Patients®: Lung Cancer—Early and Locally Advanced—Non-Small Cell Lung Cancer*.

NCI. (2021). *Risk Factors: Age - National Cancer Institute*. https://www.cancer.gov/about-cancer/causes-prevention/risk/age

Negoro, Y., Nagata, Y., Aoki, T., Mizowaki, T., Araki, N., Takayama, K., Kokubo, M., Yano, S., Koga, S., Sasai, K., Shibamoto, Y., & Hiraoka, M. (2001). The effectiveness of an immobilization device in conformal radiotherapy for lung tumor: reduction of respiratory tumor movement and evaluation of the daily setup accuracy. *International Journal of Radiation Oncology, Biology, Physics*, *50*(4), 889–898. https://doi.org/10.1016/S0360-3016(01)01516-4

Newman, N. B., Sherry, A. D., Byrne, D. W., & Osmundson, E. C. (2019). *Stereotactic body radiotherapy versus conventional radiotherapy for early-stage small cell lung cancer*. https://doi.org/10.1007/s13566-019-00395-x

Nishio, T., Shirato, H., Ishikawa, M., Miyabe, Y., Kito, S., Narita, Y., Onimaru, R., Ishikura, S., Ito, Y., & Hiraoka, M. (2014). Design, development of water tank-type lung phantom and dosimetric verification in institutions participating in a phase I study of stereotactic body radiation therapy in patients with T2N0M0 non-small cell lung cancer: Japan Clinical Oncology Group trial. *Journal of Radiation Research*, *55*(3), 600. https://doi.org/10.1093/JRR/RRT135

Nottelmann, L., Groenvold, M., Vejlgaard, T. B., Petersen, M. A., & Jensen, L. H. (2021). Early, integrated palliative rehabilitation improves quality of life of patients with newly diagnosed advanced cancer: The Pal-Rehab randomized controlled trial. *Palliative Medicine*, *35*(7), 1344–1355. https://doi.org/10.1177/02692163211015574

Nyman, J., Hallqvist, A., Lund, J.-Å., Brustugun, O.-T., Bergman, B., Bergström, P., Friesland, S., Lewensohn, R., Holmberg, E., & Lax, I. (2016a). *A phase II trial of Stereotactic Body Radiation Therapy (SBRT) in the treatment of patients with medically inoperable stage I/II non-small cell lung cancer, RTOG 0236,2004*. *121*(1), 1–6. https://doi.org/10.1016/j.radonc.2016.08.015

Nyman, J., Hallqvist, A., Lund, J. Å., Brustugun, O. T., Bergman, B., Bergström, P., Friesland, S., Lewensohn, R., Holmberg, E., & Lax, I. (2016b). SPACE – A randomized study of SBRT vs conventional fractionated radiotherapy in medically inoperable stage I NSCLC. *Radiotherapy and Oncology*, *121*(1), 1–8. https://doi.org/10.1016/J.RADONC.2016.08.015

O'Keeffe, L. M., Taylor, G., Huxley, R. R., Mitchell, P., Woodward, M., & Peters, S. A. E. (2018). Smoking as a risk factor for lung cancer in women and men: a systematic review and meta-analysis. *BMJ Open*, *8*(10), e021611. https://doi.org/10.1136/BMJOPEN-2018-021611

Ohkubo, H., Kanemitsu, Y., Uemura, T., Takakuwa, O., Takemura, M., Maeno, K., Ito, Y., Oguri, T., Kazawa, N., Mikami, R., & Niimi, A. (2016). Normal Lung Quantification in Usual Interstitial Pneumonia Pattern: The Impact of Threshold-based Volumetric CT Analysis for the Staging of Idiopathic Pulmonary Fibrosis. *PLoS ONE*, *11*(3). https://doi.org/10.1371/JOURNAL.PONE.0152505

Ohshima, H., & Bartsch, H. (1994). Chronic infections and inflammatory processes as cancer risk factors: possible role of nitric oxide in carcinogenesis. *Mutation Research*, *305*(2), 253–264. https://doi.org/10.1016/0027-5107(94)90245-3

Osann, K. E. (1991). Lung Cancer in Women: The Importance of Smoking, Family History of Cancer, and Medical History of Respiratory Disease. *Cancer Research*, *51*(18).

Osei, E., Darko, J., Swanson, S., Fleming, K., Snelgrove, R., Bhangu, A., & Gopaul, D. (2020). Dosimetric evaluation of SBRT treatment plans of non-central lung tumours: Clinical experience. *Journal of Radiotherapy in Practice*. https://doi.org/10.1017/S146039692000103X

Otoni, J. C., Noschang, J., Okamoto, T. Y., Vieira, D. R., Petry, M. S. M., de Araujo Ramos, L., Barbosa, P. N. V. P., Bitencourt, A. G. V., & Chojniak, R. (2017). Role of computed tomography at a cancer center emergency department. *Emergency Radiology*, *24*(2), 113–117. https://doi.org/10.1007/S10140-016-1449-3

Padera, T. P., Meijer, E. F. J., & Munn, L. L. (2016). The Lymphatic System in Disease Processes and Cancer Progression. *Annual Review of Biomedical Engineering*, *18*, 125–158. https://doi.org/10.1146/ANNUREV-BIOENG-112315-031200

Pakela, J. M., Knopf, A., Dong, L., Rucinski, A., & Zou, W. (2022). Management of Motion and Anatomical Variations in Charged Particle Therapy: Past, Present, and Into the Future. *Frontiers in Oncology*, *12*, 629. https://doi.org/10.3389/FONC.2022.806153/BIBTEX

Pallonen, T. A.-S., Lempiäinen, S. M. M., Joutsiniemi, T. K., Aaltonen, R. I., Pohjola, P. E., &

Kankuri-Tammilehto, M. K. (2022). Genetic, clinic and histopathologic characterization of BRCA-associated hereditary breast and ovarian cancer in southwestern Finland. *Scientific Reports*, *12*(1), 6704. https://doi.org/10.1038/s41598-022-10519-y

Parker, M. (2019). *Risk Factors for Lung Cancer | Thoracic Key*. https://thoracickey.com/risk-factors-for-lung-cancer/

Paul, J., Yang, C., Wu, H., Tai, A., Dalah, E., Zheng, C., Johnstone, C., Kong, F. M., Gore, E., & Li, X. A. (2017). Early Assessment of Treatment Responses During Radiation Therapy for Lung Cancer Using Quantitative Analysis of Daily Computed Tomography. *International Journal of Radiation Oncology, Biology, Physics*, *98*(2), 463–472. https://doi.org/10.1016/J.IJROBP.2017.02.032

Paydary, K., Seraj, S. M., Zadeh, M. Z., Emamzadehfard, S., Shamchi, S. P., Gholami, S., Werner, T. J., & Alavi, A. (2019). The Evolving Role of FDG-PET/CT in the Diagnosis, Staging, and Treatment of Breast Cancer. *Molecular Imaging and Biology*, *21*(1). https://doi.org/10.1007/S11307-018-1181-3

Plaks, V., Koopman, C. D., & Werb, Z. (2013). Circulating tumor cells. *Science*, *341*(6151), 1186–1188. https://doi.org/10.1126/SCIENCE.1235226/ASSET/73EA0127-0FF8-4B5C-8DE8-88D072125A81/ASSETS/GRAPHIC/341_1186_F1.JPEG

Postmus, P. E., Kerr, K. M., Oudkerk, M., Senan, S., Waller, D. A., Vansteenkiste, J., Escriu, C., & Peters, S. (2017). Early and locally advanced non-small-cell lung cancer (NSCLC): ESMO Clinical Practice Guidelines for diagnosis, treatment and follow-up. *Annals of Oncology*, *28*, iv1–iv21. https://doi.org/10.1093/ANNONC/MDX222

Prado, C. M. M., Birdsell, L. A., & Baracos, V. E. (2009). The emerging role of computerized tomography in assessing cancer cachexia. *Current Opinion in Supportive and Palliative Care*, *3*(4), 269–275. https://doi.org/10.1097/SPC.0B013E328331124A

Priedigkeit, N., Ding, K., Horne, W., Kolls, J. K., Du, T., Lucas, P. C., Blohmer, J. U., Denkert, C., Machleidt, A., Ingold-Heppner, B., Oesterreich, S., & Lee, A. V. (2021). Acquired mutations and transcriptional remodeling in long-term estrogen-deprived locoregional breast cancer recurrences. *Breast Cancer Research : BCR*, *23*(1). https://doi.org/10.1186/S13058-020-01379-3

Pucci, C., Martinelli, C., & Ciofani, G. (2019). Innovative approaches for cancer treatment: current perspectives and new challenges. *Ecancermedicalscience*, *13*. https://doi.org/10.3332/ECANCER.2019.961

Qi, Y., Li, J., Zhang, Y., Shao, Q., Liu, X., Li, F., Wang, J., Li, Z., & Wang, W. (2021). Effect of abdominal compression on target movement and extension of the external boundary of peripheral lung tumours treated with stereotactic radiotherapy based on four-dimensional computed tomography. *Radiation Oncology*, *16*(1), 1–8. https://doi.org/10.1186/S13014-021-01889-0/TABLES/2

Rahi, M. S., Parekh, J., Pednekar, P., Parmar, G., Abraham, S., Nasir, S., Subramaniyam, R., Jeyashanmugaraja, G. P., & Gunasekaran, K. (2021). Radiation-Induced Lung Injury-Current Perspectives and Management. *Clinics and Practice*, *11*(3), 410–429. https://doi.org/10.3390/CLINPRACT11030056

Rakha, E. A., Reis-Filho, J. S., Baehner, F., Dabbs, D. J., Decker, T., Eusebi, V., Fox, S. B., Ichihara, S., Jacquemier, J., Lakhani, S. R., Palacios, J., Richardson, A. L., Schnitt, S. J., Schmitt, F. C., Tan, P. H., Tse, G. M., Badve, S., & Ellis, I. O. (2010). Breast cancer prognostic classification in the molecular era: The role of histological grade. *Breast Cancer Research*, *12*(4), 1–12. https://doi.org/10.1186/BCR2607/TABLES/2

Rao, Y. J., & Grigsby, P. W. (2018). The Role of PET Imaging in Gynecologic Radiation Oncology. *PET Clinics*, *13*(2), 225–237. https://doi.org/10.1016/J.CPET.2017.11.007

Ricardi, U., Filippi, A. R., Guarneri, A., Giglioli, F. R., Ciammella, P., Franco, P., Mantovani, C., Borasio, P., Scagliotti, G. V., & Ragona, R. (2010). Stereotactic body radiation therapy for early stage non-small cell lung cancer: results of a prospective trial. *Lung Cancer (Amsterdam, Netherlands)*, *68*(1), 72–77. https://doi.org/10.1016/J.LUNGCAN.2009.05.007

Riet, A. V. t., Mak, A. C. A., Moerland, M. A., Elders, L. H., & Van Der Zee, W. (1997). A conformation number to quantify the degree of conformality in brachytherapy and external beam irradiation: Application to the prostate. *International Journal of Radiation Oncology, Biology, Physics*, *37*(3), 731–736. https://doi.org/10.1016/S0360-3016(96)00601-3

Rix, A., Lederle, W., Theek, B., Lammers, T., Moonen, C., Schmitz, G., & Kiessling, F. (2018). Advanced Ultrasound Technologies for Diagnosis and Therapy. *Journal of Nuclear Medicine : Official Publication, Society of Nuclear Medicine*, *59*(5), 740–746. https://doi.org/10.2967/JNUMED.117.200030

Rizwan Khan, M., Naushad, M., & Abdullah Alothman, Z. (2017). Presence of heterocyclic amine carcinogens in home-cooked and fast-food camel meat burgers commonly consumed in Saudi Arabia. *Scientific Reports 2017 7:1*, *7*(1), 1–7. https://doi.org/10.1038/s41598-017-01968-x

Rogotti, N. (2022). *Benefits and consequences of smoking cessation - UpToDate*. https://www.uptodate.com/contents/benefits-and-consequences-of-smoking-cessation#H30936515

Rowe, B. P., Boffa, D. J., Wilson, L. D., Kim, A. W., Detterbeck, F. C., & Decker, R. H. (2012). Stereotactic body radiotherapy for central lung tumors. *Journal of Thoracic Oncology : Official Publication of the International Association for the Study of Lung Cancer*, *7*(9), 1394–1399. https://doi.org/10.1097/JTO.0B013E3182614BF3

Roy, J. S., Chatterjee, D., Das, N., & Giri, A. K. (2018). Substantial Evidences Indicate That Inorganic Arsenic Is a Genotoxic Carcinogen: a Review. *Toxicological Research*, *34*(4), 311. https://doi.org/10.5487/TR.2018.34.4.311

Ruano-Raviña, A., Provencio, M., Calvo De Juan, V., Carcereny, E., Moran, T., Rodriguez-Abreu, D., López-Castro, R., Cuadrado Albite, E., Guirado, M., Gómez González, L., Massutí, B., Ortega Granados, A. L., Blasco, A., Cobo, M., Garcia-Campelo, R., Bosch, J., Trigo, J., Juan, Ó., Aguado De La Rosa, C., … Cerezo, S. (2020). Lung cancer symptoms at diagnosis: results of a nationwide registry study. *ESMO Open*, *5*(6). https://doi.org/10.1136/ESMOOPEN-2020-001021

Saito, T., Matsuyama, T., Toya, R., Fukugawa, Y., Toyofuku, T., Semba, A., & Oya, N. (2014). Respiratory Gating during Stereotactic Body Radiotherapy for Lung Cancer Reduces Tumor Position Variability. *PLOS ONE*, *9*(11), e112824.

https://doi.org/10.1371/JOURNAL.PONE.0112824

Salmanoglu, E. (2021). The role of [18F]FDG PET/CT for gastric cancer management. *Nuclear Medicine Review. Central & Eastern Europe*, *24*(2), 99–103. https://doi.org/10.5603/NMR.2021.0021

Samet, J. M., Humble, C. G., & Pathak, D. R. (1986). Personal and family history of respiratory disease and lung cancer risk. *The American Review of Respiratory Disease*, *134*(3), 466–470. https://doi.org/10.1164/ARRD.1986.134.3.466

Samet, Jonathan M., Avila-Tang, E., Boffetta, P., Hannan, L. M., Olivo-Marston, S., Thun, M. J., & Rudin, C. M. (2009). LUNG CANCER IN NEVER SMOKERS: CLINICAL EPIDEMIOLOGY AND ENVIRONMENTAL RISK FACTORS. *Clinical Cancer Research : An Official Journal of the American Association for Cancer Research*, *15*(18), 5626. https://doi.org/10.1158/1078-0432.CCR-09-0376

Sarker, A. H., Trego, K. S., Zhang, W., Jacob, P., Snijders, A. M., Mao, J. H., Schick, S. F., Cooper, P. K., & Hang, B. (2020). Thirdhand smoke exposure causes replication stress and impaired transcription in human lung cells. *Environmental and Molecular Mutagenesis*, *61*(6), 635–646. https://doi.org/10.1002/EM.22372

Sarudis, S., Hauer, K. A., Nyman, J., & Bäck, A. (2017). Systematic evaluation of lung tumor motion using four-dimensional computed tomography. *Acta Oncologica (Stockholm, Sweden)*, *56*(4), 525–530. https://doi.org/10.1080/0284186X.2016.1274049

Schonfeld, S. J., Merino, D. M., Curtis, R. E., de Gonzalez, A. B., Herr, M. M., Kleinerman, R. A., Savage, S. A., Tucker, M. A., & Morton, L. M. (2019). Risk of Second Primary Bone and Soft–Tissue Sarcomas Among Young Adulthood Cancer Survivors. *JNCI Cancer Spectrum*, *3*(3). https://doi.org/10.1093/JNCICS/PKZ043

Seike, Y., Kawagishi, Y., Bando, A., Kimoto, K., Hongo, M., & Takeda, S. (2021). Development of second primary small-cell lung cancer within the irradiated field after chemoradiotherapy: a report of two cases. *Respirology Case Reports*, *9*(6), e00767. https://doi.org/10.1002/rcr2.767

Seppenwoolde, Y., Shirato, H., Kitamura, K., Shimizu, S., Van Herk, M., Lebesque, J. V., & Miyasaka, K. (2002). Precise and real-time measurement of 3D tumor motion in lung due to breathing and heartbeat, measured during radiotherapy. *International Journal of Radiation Oncology, Biology, Physics*, *53*(4), 822–834. https://doi.org/10.1016/S0360-3016(02)02803-1

Serrano, O. K., Chaudhry, M. A., & Leach, S. D. (2010). The role of PET scanning in pancreatic cancer. *Advances in Surgery*, *44*(1), 313–325. https://doi.org/10.1016/J.YASU.2010.05.007

Shaverdian, N., Wang, P.-C., Steinberg, M., & Lee, P. (2015). The patient's perspective on stereotactic body radiation therapy (SBRT) vs. surgery for treatment of early stage non-small cell lung cancer (NSCLC). *Lung Cancer (Amsterdam, Netherlands)*, *90*(2), 230–233. https://doi.org/10.1016/J.LUNGCAN.2015.07.009

Shaw, E., Kline, R., Gillin, M., Souhami, L., Hirschfeld, A., Dinapoli, R., & Martin, L. (1993). Radiation therapy oncology group: Radiosurgery quality assurance guidelines. *International Journal of Radiation Oncology, Biology, Physics*, *27*(5), 1231–1239.

https://doi.org/10.1016/0360-3016(93)90548-A

Sheng, L., Tu, J. W., Tian, J. H., Chen, H. J., Pan, C. L., & Zhou, R. Z. (2018). A meta-analysis of the relationship between environmental tobacco smoke and lung cancer risk of nonsmoker in China. *Medicine (United States)*, *97*(28). https://doi.org/10.1097/MD.0000000000011389

Shibamoto, Y., Hashizume, C., Baba, F., Ayakawa, S., Miyakawa, A., Murai, T., Takaoka, T., Hattori, Y., & Asai, R. (2015). Stereotactic body radiotherapy using a radiobiology-based regimen for stage I non-small-cell lung cancer: five-year mature results. *Journal of Thoracic Oncology : Official Publication of the International Association for the Study of Lung Cancer*, *10*(6), 960–964. https://doi.org/10.1097/JTO.0000000000000525

Shiels, M. S., Cole, S. R., Mehta, S. H., & Kirk, G. D. (2010). Lung cancer incidence and mortality among HIV-infected and HIV-uninfected injection drug users. *Journal of Acquired Immune Deficiency Syndromes*, *55*(4), 510–515. https://doi.org/10.1097/QAI.0B013E3181F53783

Shimizu, S., Shirato, H., Ogura, S., Akita-Dosaka, H., Kitamura, K., Nishioka, T., Kagei, K., Nishimura, M., & Miyasaka, K. (2001). Detection of lung tumor movement in real-time tumor-tracking radiotherapy. *International Journal of Radiation Oncology Biology Physics*, *51*(2), 304–310. https://doi.org/10.1016/S0360-3016(01)01641-8

Shirato, H., Seppenwoolde, Y., Kitamura, K., Onimura, R., & Shimizu, S. (2004). Intrafractional tumor motion: lung and liver. *Seminars in Radiation Oncology*, *14*(1), 10–18. https://doi.org/10.1053/J.SEMRADONC.2003.10.008

Siddiqui, F., Vaqar, S., & Siddiqui, A. H. (2021). Lung Cancer. *Cambridge Handbook of Psychology, Health and Medicine, Second Edition*, 605–606. https://doi.org/10.1017/CBO9780511543579.138

Siegel, R. L., Miller, K. D., Fuchs, H. E., & Jemal, A. (2021). Cancer Statistics, 2021. *CA: A Cancer Journal for Clinicians*, *71*(1), 7–33. https://doi.org/10.3322/CAAC.21654

Sigel, K., Makinson, A., & Thaler, J. (2017). Lung Cancer in Persons with HIV. *Current Opinion in HIV and AIDS*, *12*(1), 31. https://doi.org/10.1097/COH.0000000000000326

Sigel, K., Wisnivesky, J., Gordon, K., Dubrow, R., Justice, A., Brown, S. T., Goulet, J., Butt, A. A., Crystal, S., Rimland, D., Rodriguez-Barradas, M., Gibert, C., Park, L. S., & Crothers, K. (2012). HIV as an independent risk factor for incident lung cancer. *AIDS*, *26*(8), 1017–1025. https://doi.org/10.1097/QAD.0B013E328352D1AD

Silverman, D., Samanic, C., Lubin, J., Blair, A., Stewart, P., Vermeulen, R., Coble, J., Rothman, N., Schleiff, P., Travis, W., Ziegler, R., Wacholder, S., & Attfield, M. (2012). The Diesel Exhaust in Miners study: a nested case-control study of lung cancer and diesel exhaust. *Journal of the National Cancer Institute*, *104*(11), 855–868. https://doi.org/10.1093/JNCI/DJS034

Singh, D., Chen, Y., Bergsma, D. P., Usuki, K. Y., Dhakal, S., Hare, M. Z., Joyce, N., Smudzin, T., Rosenzweig, D., Schell, M. C., & Milano, M. T. (2015). Local control rates with five fractions of stereotactic body radiotherapy for primary lung tumors: a single institution experience of 153 consecutive patients. *Translational Cancer Research*, *4*(4), 332–339. https://doi.org/10.21037/4956

Singh, D., Chen, Y., Hare, M. Z., Usuki, K. Y., Zhang, H., Lundquist, T., Joyce, N., Schell, M. C., & Milano, M. T. (2014). Local control rates with five-fraction stereotactic body radiotherapy for oligometastatic cancer to the lung. *Journal of Thoracic Disease*, *6*(4), 369–374. https://doi.org/10.3978/J.ISSN.2072-1439.2013.12.03

SMETANA, K., LACINA, L., SZABO, P., DVOŘÁNKOVÁ, B., BROŽ, P., & ŠEDO, A. (2016). Ageing as an Important Risk Factor for Cancer. *Anticancer Research*, *36*(10).

Society, A. C. (2019). *Lung Cancer*.

Solberg, T. D., Balter, J. M., Benedict, S. H., Fraass, B. A., Kavanagh, B., Miyamoto, C., Pawlicki, T., Potters, L., & Yamada, Y. (2012). Quality and safety considerations in stereotactic radiosurgery and stereotactic body radiation therapy: Executive summary. *Practical Radiation Oncology*, *2*(1), 2–9. https://doi.org/10.1016/J.PRRO.2011.06.014/ATTACHMENT/0E73D26C-E283-4766-B41A-1CB607259A33/MMC1.PDF

St. Stamford Modern Cancer Hospital Guangzhou. (2019). *Lung Cancer Staging | St. Stamford Modern Cancer Hospital Guangzhou*. https://www.moderncancerhospital.com.cn/cancer-staging/lung-cancer-staging/

Stumpf, P. K., Jones, B., Jain, S. K., Amini, A., Thornton, D. A., Dzingle, W., & Schefter, T. E. (2016). Stereotactic body radiation therapy for pancreatic cancer: Assessing motion with and without abdominal compression. *Https://Doi.Org/10.1200/Jco.2016.34.4_suppl.234*, *34*(4_suppl), 234–234. https://doi.org/10.1200/JCO.2016.34.4_SUPPL.234

Sun, Y. Q., Chen, Y., Langhammer, A., Skorpen, F., Wu, C., & Mai, X. M. (2017). Passive smoking in relation to lung cancer incidence and histologic types in Norwegian adults: the HUNT study. *European Respiratory Journal*, *50*(4). https://doi.org/10.1183/13993003.00824-2017

Sureshkumar, A., Hansen, B., & Ersahin, D. (2020). Role of Nuclear Medicine in Imaging. *Seminars in Ultrasound, CT, and MR*, *41*(1), 10–19. https://doi.org/10.1053/J.SULT.2019.10.005

Tedesco, G., Sarno, A., Rizzo, G., Grecchi, A., Testa, I., Giannotti, G., & D'onofrio, M. (2019). Clinical use of contrast-enhanced ultrasound beyond the liver: a focus on renal, splenic, and pancreatic applications. *Ultrasonography (Seoul, Korea)*, *38*(4), 278–288. https://doi.org/10.14366/USG.18061

Thomas, J. L., Hecht, S. S., Luo, X., Ming, X., Ahluwalia, J. S., & Carmella, S. G. (2014). Thirdhand Tobacco Smoke: A Tobacco-Specific Lung Carcinogen on Surfaces in Smokers' Homes. *Nicotine & Tobacco Research*, *16*(1), 26. https://doi.org/10.1093/NTR/NTT110

Thompson, M., & Rosenzweig, K. E. (2019). The evolving toxicity profile of SBRT for lung cancer. *Translational Lung Cancer Research*, *8*(1), 48. https://doi.org/10.21037/TLCR.2018.10.06

Timmerman, R, Hu, C., Michalski, J., Straube, W., Galvin, J., Johnstone, D., Bradley, J., Barriger, R., Bezjak, A., Videtic, G. M., Nedzi, L., Werner-Wasik, M., Chen, Y., Komaki, R. U., Choy, H., Shaikh, F., Foster, A., Zhang, Z., Woo, K., … Rimner, A. (2014). Long-term Results of RTOG 0236: A Phase II Trial of Stereotactic Body Radiation Therapy (SBRT) in the

Treatment of Patients with Medically Inoperable Stage I Non-Small Cell Lung Cancer. *International Journal of Radiation Oncology, Biology, Physics*, *90*(1), S30. https://doi.org/10.1016/J.IJROBP.2014.05.135

Timmerman, Robert, Papiez, L., McGarry, R., Likes, L., DesRosiers, C., Frost, S., & Williams, M. (2003). Extracranial Stereotactic Radioablation: Results of a Phase I Study in Medically Inoperable Stage I Non-small Cell Lung Cancer. *Chest*, *124*(5), 1946–1955. https://doi.org/10.1378/CHEST.124.5.1946

Timmerman, Robert, Paulus, R., Galvin, J., Michalski, J., Straube, W., Bradley, J., Fakiris, A., Bezjak, A., Videtic, G., Johnstone, D., Fowler, J., Gore, E., & Choy, H. (2010). Stereotactic body radiation therapy for inoperable early stage lung cancer. *JAMA - Journal of the American Medical Association*, *303*(11), 1070–1076. https://doi.org/10.1001/jama.2010.261

Toh, C.-K., & Tan, D. (2017). *Lung Cancer in Never-Smokers: An Epidemiologic Perspective | IASLC*. International Association for the Study of Lung Cancer. https://www.iaslc.org/iaslc-news/ilcn/lung-cancer-never-smokers-epidemiologic-perspective

Tomasetti, C., Marchionni, L., Nowak, M. A., Parmigiani, G., & Vogelstein, B. (2015). Only three driver gene mutations are required for the development of lung and colorectal cancers. *Proceedings of the National Academy of Sciences of the United States of America*, *112*(1), 118–123. https://doi.org/10.1073/PNAS.1421839112

Torre, L. A., Siegel, R. L., & Jemal, A. (2016). Lung Cancer Statistics. *Advances in Experimental Medicine and Biology*, *893*, 1–19. https://doi.org/10.1007/978-3-319-24223-1_1

Torre, L., Bray, F., RL, S., J, F., J, L.-T., & A, J. (2015). Global cancer statistics, 2012. *CA: A Cancer Journal for Clinicians*, *65*(2), 87–108. https://doi.org/10.3322/CAAC.21262

Torshabi, A. E., & Dastyar, S. A. R. (2017). Motion Challenge of Thoracic Tumors at Radiotherapy by Introducing an Available Compensation Strategy. In *Radiotherapy*. InTech. https://doi.org/10.5772/67444

U.S. Department of Health and Human Services. (2020). *Smoking Cessation: A Report of the Surgeon General (Executive Summary)*.

Uematsu, M., Shioda, A., Fukul, T., Yamamoto, F., Tsumatori, G., Ozekl, Y., Aoki, T., Watanabe, M., & Kusano, S. (1997). *Focal, High Dose, and Fractionated Modified Stereotactic Radiation Therapy for Lung Carcinoma Patients A Preliminary Experience BACKGROUND. Stereotactic radiation therapy is highly effective in the treatment*.

UICC, I. U. A. C. (2016). *TNM Classification of Malignant Tumours*. 138–141.

UNSCEAR. (2006). *UNSCEAR. Effects of Ionizing Radiation: UNSCEAR 2006 Report to the General Assembly, with Scientific Annexes. Volume I. Effects of Ionizing Radiation*.

Urman, A., Josyula, S., Rosenberg, A., Lounsbury, D., Rohan, T., Dean Hosgood, H., & Hosgood, D. (2016). Burden of Lung Cancer and Associated Risk Factors in Africa by Region. *J Pulm Respir Med*, *6*(3), 340. https://doi.org/10.4172/2161-105X.1000340

Van Cott, C. (2020). Cancer Genetics. *The Surgical Clinics of North America*, *100*(3), 483–498. https://doi.org/10.1016/J.SUC.2020.02.012

van Dooijeweert, C., Baas, I. O., Deckers, I. A. G., Siesling, S., van Diest, P. J., & van der Wall, E. (2021). The increasing importance of histologic grading in tailoring adjuvant systemic therapy in 30,843 breast cancer patients. *Breast Cancer Research and Treatment*, *187*(2), 577–586. https://doi.org/10.1007/S10549-021-06098-7/TABLES/4

Van Gelder, R., Wong, S., Le, A., Podreka, A., Briggs, A., Haddad, C., & Hardcastle, N. (2018). Experience with an abdominal compression band for radiotherapy of upper abdominal tumours. *J Med Radiat Sci*, *65*, 48–54. https://doi.org/10.1002/jmrs.254

Van Sörnsen De Koste, J. R., Lagerwaard, F. J., De Boer, H. C. J., Nijssen-Visser, M. R. J., & Senan, S. (2003). Are multiple CT scans required for planning curative radiotherapy in lung tumors of the lower lobe? *International Journal of Radiation Oncology, Biology, Physics*, *55*(5), 1394–1399. https://doi.org/10.1016/S0360-3016(02)04602-3

Van Sörnsen De Koste, J. R., Lagerwaard, F. J., Schuchhard-Schipper, R. H., Nijssen-Visser, M. R. J., Voet, P. W. J., Oei, S. S., & Senan, S. (2001). Dosimetric consequences of tumor mobility in radiotherapy of stage I non-small cell lung cancer--an analysis of data generated using 'slow' CT scans. *Radiotherapy and Oncology : Journal of the European Society for Therapeutic Radiology and Oncology*, *61*(1), 93–99. https://doi.org/10.1016/S0167-8140(01)00373-5

Vedam, S. S., Keall, P. J., Kini, V. R., Mostafavi, H., Shukla, H. P., & Mohan, R. (2003). Acquiring a four-dimensional computed tomography dataset using an external respiratory signal. *Physics in Medicine and Biology*, *48*(1), 45–62. https://doi.org/10.1088/0031-9155/48/1/304

Verstegen, N. E., Lagerwaard, F. J., Hashemi, S. M. S., Dahele, M., Slotman, B. J., & Senan, S. (2015). Patterns of Disease Recurrence after SABR for Early Stage Non–Small-Cell Lung Cancer: Optimizing Follow-Up Schedules for Salvage Therapy. *Journal of Thoracic Oncology*, *10*(8), 1195–1200. https://doi.org/10.1097/JTO.0000000000000576

Videtic, G., Donington, J., Giuliani, M., Heinzerling, J., Karas, T. Z., Kelsey, C. R., Lally, B. E., Latzka, K., Lo, S. S., Moghanaki, D., Movsas, B., Rimner, A., Roach, M., Rodrigues, G., Shirvani, S. M., Simone, C. B., Timmerman, R., & Daly, M. E. (2017). Stereotactic body radiation therapy for early-stage non-small cell lung cancer: Executive Summary of an ASTRO Evidence-Based Guideline. *Practical Radiation Oncology*, *7*(5), 295–301. https://doi.org/10.1016/j.prro.2017.04.014

Videtic, G., Hu, C., Singh, A. K., Chang, J. Y., Parker, W., Olivier, K. R., Schild, S. E., Komaki, R., Urbanic, J. J., & Choy, H. (2015). NRG Oncology RTOG 0915 (NCCTG N0927): A Randomized Phase II Study Comparing 2 Stereotactic Body Radiation Therapy (SBRT) Schedules for Medically Inoperable Patients with Stage I Peripheral Non-Small Cell Lung Cancer. *International Journal of Radiation Oncology, Biology, Physics*, *93*(4), 757. https://doi.org/10.1016/J.IJROBP.2015.07.2260

Videtic, G., Paulus, R., Singh, A. K., Chang, J. Y., Parker, W., Olivier, K. R., Timmerman, R. D., Komaki, R. R., Urbanic, J. J., Stephans, K. L., Yom, S. S., Robinson, C. G., Belani, C. P., Iyengar, P., Ajlouni, M. I., Gopaul, D. D., Gomez Suescun, J. B., McGarry, R. C., Choy, H., & Bradley, J. D. (2019). Long term follow-up on NRG Oncology RTOG 0915 (NCCTG N0927): A randomized phase II study comparing 2 stereotactic body radiation therapy schedules for medically inoperable patients with stage I peripheral non-small cell lung cancer.

International Journal of Radiation Oncology, Biology, Physics, *103*(5), 1077. https://doi.org/10.1016/J.IJROBP.2018.11.051

Videtic, G., Singh, A. K., Chang, J. Y., Le, Q.-T., Parker, W., Olivier, K. R., Schild, S. E., & Hu, C. (2014). *RTOG 0915. A RANDOMIZED PHASE II STUDY COMPARING 2 STEREOTACTIC BODY RADIATION THERAPY (SBRT) SCHEDULES FOR MEDICALLY INOPERABLE PATIENTS WITH STAGE I PERIPHERAL NON-SMALL CELL LUNG CANCER.*

von Reibnitz, D., Shaikh, F., Wu, A. J., Treharne, G. C., Dick-Godfrey, R., Foster, A., Woo, K. M., Shi, W., Zhang, Z., Din, S. U., Gelblum, D. Y., Yorke, E. D., Rosenzweig, K. E., & Rimner, A. (2018). Stereotactic body radiation therapy (SBRT) improves local control and overall survival compared to conventionally fractionated radiation for stage I non-small cell lung cancer (NSCLC). *Acta Oncologica*, *57*(11), 1567–1573. https://doi.org/10.1080/0284186X.2018.1481292/SUPPL_FILE/IONC_A_1481292_SM3527.ZIP

Wakelee, H. A., Chang, E. T., Gomez, S. L., Keegan, T. H., Feskanich, D., Clarke, C. A., Holmberg, L., Yong, L. C., Kolonel, L. N., Gould, M. K., & West, D. W. (2016). Lung Cancer Incidence in Never Smokers. *Https://Doi.Org/10.1200/JCO.2006.07.2983*, *25*(5), 472–478. https://doi.org/10.1200/JCO.2006.07.2983

Walsh, L., Zhang, W., Shore, R. E., Auvinen, A., Laurier, D., Wakeford, R., Jacob, P., Gent, N., Anspaugh, L. R., Schüz, J., Kesminiene, A., Van Deventer, E., Tritscher, A., & Del Rosarion Pérez, M. (2014). A Framework for Estimating Radiation-Related Cancer Risks in Japan from the 2011 Fukushima Nuclear Accident. *Https://Doi.Org/10.1667/RR13779.1*, *182*(5), 556–572. https://doi.org/10.1667/RR13779.1

Wang, K., Newman, J., Lee, C.-S., & Seetharamu, N. (2021). Epidemiology and clinicopathological features of lung cancer in patients with prior history of breast cancer. *SAGE Open Medicine*, *9*, 20503121211017756. https://doi.org/10.1177/20503121211017757

Wang, S. Y., Tsai, C. M., Chen, B. C., Lin, C. H., & Lin, C. C. (2008). Symptom clusters and relationships to symptom interference with daily life in Taiwanese lung cancer patients. *J Pain Symptom Manage*, *35*, 258–266.

Wang, W. J., Chiou, J. F., & Huang, Y. (2018). Treatment of Liver Metastases Using an Internal Target Volume Method for Stereotactic Body Radiotherapy. *Journal of Visualized Experiments : JoVE*, *2018*(135), 57050. https://doi.org/10.3791/57050

Wang, X., Zamdborg, L., Ye, H., Grills, I. S., & Yan, D. (2018). A matched-pair analysis of stereotactic body radiotherapy (SBRT) for oligometastatic lung tumors from colorectal cancer versus early stage non-small cell lung cancer. *BMC Cancer*, *18*(1). https://doi.org/10.1186/S12885-018-4865-9

Wang, Z., Gao, S., Xue, Q., Guo, X., Wang, L., Yu, X., Yang, Y., & Mu, J. (2018). Surgery of primary non-small cell lung cancer with oligometastasis: analysis of 172 cases. *Journal of Thoracic Disease*, *10*(12), 6540–6546. https://doi.org/10.21037/JTD.2018.11.125

Ward, E., DeSantis, C., Robbins, A., Kohler, B., & Jemal, A. (2014). Childhood and adolescent cancer statistics, 2014. *CA: A Cancer Journal for Clinicians*, *64*(2), 83–103.

https://doi.org/10.3322/CAAC.21219

Wennstig, A.-K., Wadsten, C., Garmo, H., Johansson, M., Fredriksson, I., Blomqvist, C., Holmberg, L., Nilsson, G., & Sund, M. (2021). Risk of primary lung cancer after adjuvant radiotherapy in breast cancer-a large population-based study. *NPJ Breast Cancer*, *7*(1), 71. https://doi.org/10.1038/s41523-021-00280-2

Weyh, A., Konski, A., Nalichowski, A., Maier, J., & Lack, D. (2013). Lung SBRT: dosimetric and delivery comparison of RapidArc, TomoTherapy, and IMRT. *Journal of Applied Clinical Medical Physics*, *14*(4), 3. https://doi.org/10.1120/JACMP.V14I4.4065

White, M. C., Holman, D. M., Boehm, J. E., Peipins, L. A., Grossman, M., & Jane Henley, S. (2014). Age and Cancer Risk: A Potentially Modifiable Relationship. *American Journal of Preventive Medicine*, *46*(3 0 1), S7. https://doi.org/10.1016/J.AMEPRE.2013.10.029

WHO. (2020a). *Assessing national capacity for the prevention and control of noncommunicable diseases: Report of he 2019 global survey*.

WHO. (2020b). *Ghana - World Health Organization Cancer Country Profile 2020*.

Winstone, T., Man, S., M, H., JS, M., & DD, S. (2013). Epidemic of lung cancer in patients with HIV infection. *Chest*, *143*(2), 305–314. https://doi.org/10.1378/CHEST.12-1699

Wolthaus, J. W. H., Sonke, J.-J., Herk, M. van, Belderbos, J. S. A., Rossi, M. M. G., Lebesque, J. V., & Damen, E. M. F. (2008). Comparison of Different Strategies to Use Four-Dimensional Computed Tomography in Treatment Planning for Lung Cancer Patients. *International Journal of Radiation Oncology, Biology, Physics*, *70*(4), 1229–1238. https://doi.org/10.1016/J.IJROBP.2007.11.042

Wu, R. C., Lebastchi, A. H., Hadaschik, B. A., Emberton, M., Moore, C., Laguna, P., Fütterer, J. J., & George, A. K. (2021). Role of MRI for the detection of prostate cancer. *World Journal of Urology*, *39*(3), 637–649. https://doi.org/10.1007/S00345-020-03530-3

Wurstbauer, K., Deutschmann, H., Kopp, P., & Sedlmayer, F. (2005). Radiotherapy planning for lung cancer: slow CTs allow the drawing of tighter margins. *Radiotherapy and Oncology : Journal of the European Society for Therapeutic Radiology and Oncology*, *75*(2), 165–170. https://doi.org/10.1016/J.RADONC.2005.02.003

Xia, Y., Adamson, J., Zlateva, Y., & Giles, W. (2020). Application of TG-218 action limits to SRS and SBRT pre-treatment patient specific QA. *Journal of Radiosurgery and SBRT*, *7*(2), 135.

Yamamoto, T., Jingu, K., Shirata, Y., Koto, M., Matsushita, H., Sugawara, T., Kubozono, M., Umezawa, R., Abe, K., Kadoya, N., Ishikawa, Y., Kozumi, M., Takahashi, N., Takeda, K., & Takai, Y. (2014). Outcomes after stereotactic body radiotherapy for lung tumors, with emphasis on comparison of primary lung cancer and metastatic lung tumors. *BMC Cancer 2014 14:1*, *14*(1), 1–10. https://doi.org/10.1186/1471-2407-14-464

Yamashita, H., Takahashi, W., Haga, A., & Nakagawa, K. (2014). Radiation pneumonitis after stereotactic radiation therapy for lung cancer. *World Journal of Radiology*, *6*(9), 708. https://doi.org/10.4329/WJR.V6.I9.708

Yan, S., Gan, Y., Song, X., Chen, Y., Liao, N., Chen, S., & Lv, C. (2018). Association between refrigerator use and the risk of gastric cancer: A systematic review and meta-analysis of

observational studies. *PLOS ONE*, *13*(8), e0203120. https://doi.org/10.1371/JOURNAL.PONE.0203120

Yang, I. A., Holloway, J. W., & Fong, K. M. (2013). Genetic susceptibility to lung cancer and co-morbidities. *Journal of Thoracic Disease*, *5*(Suppl 5), S454. https://doi.org/10.3978/J.ISSN.2072-1439.2013.08.06

Yang, S., Zhang, Z., & Wang, Q. (2019). Emerging therapies for small cell lung cancer. *Journal of Hematology and Oncology*, *12*(1), 47. https://doi.org/10.1186/s13045-019-0736-3

Yarbro, J. W. (1992). Oncogenes and cancer suppressor genes. *Seminars in Oncology Nursing*, *8*(1), 30–39. https://doi.org/10.1016/0749-2081(92)90006-O

Yeung, R., Hamm, J., Liu, M., & Schellenberg, D. (2017). Institutional analysis of stereotactic body radiotherapy (SBRT) for oligometastatic lymph node metastases. *Radiation Oncology 2017 12:1*, *12*(1), 1–8. https://doi.org/10.1186/S13014-017-0820-1

Yoganathan, S. A., Maria Das, K. J., Subramanian, V. S., Raj, D. G., Agarwal, A., & Kumar, S. (2017). Investigating different computed tomography techniques for internal target volume definition. *Journal of Cancer Research and Therapeutics*, *13*(6), 994. https://doi.org/10.4103/0973-1482.220353

Yoganathan, S., Maria Das, K., Agarwal, A., & Kumar, S. (2017). Magnitude, Impact, and Management of Respiration-induced Target Motion in Radiotherapy Treatment: A Comprehensive Review. *Journal of Medical Physics*, *42*(3), 101–115. https://doi.org/10.4103/JMP.JMP_22_17

Yoo, H., Jeong, B. H., Chung, M. J., Lee, K. S., Kwon, O. J., & Chung, M. P. (2019). Risk factors and clinical characteristics of lung cancer in idiopathic pulmonary fibrosis: a retrospective cohort study. *BMC Pulmonary Medicine*, *19*(1). https://doi.org/10.1186/S12890-019-0905-8

Yu, Z. H., Lin, S. H., Balter, P., Zhang, L., & Dong, L. (2012). A comparison of tumor motion characteristics between early stage and locally advanced stage lung cancers. *Radiotherapy and Oncology*, *104*(1), 33–38. https://doi.org/10.1016/j.radonc.2012.04.010

Zappa, C., & Mousa, S. A. (2016). Non-small cell lung cancer: Current treatment and future advances. *Translational Lung Cancer Research*, *5*(3), 288–300. https://doi.org/10.21037/tlcr.2016.06.07

Zaucha, J. M., Chauvie, S., Zaucha, R., Biggii, A., & Gallamini, A. (2019). The role of PET/CT in the modern treatment of Hodgkin lymphoma. *Cancer Treatment Reviews*, *77*, 44–56. https://doi.org/10.1016/J.CTRV.2019.06.002

Zhang, G. G., Ku, L., Dilling, T. J., Stevens, C. W., Zhang, R. R., Li, W., & Feygelman, V. (2011). Volumetric modulated arc planning for lung stereotactic body radiotherapy using conventional and unflattened photon beams: a dosimetric comparison with 3D technique. *Radiation Oncology (London, England)*, *6*(1), 152. https://doi.org/10.1186/1748-717X-6-152

Zhang, Y., & Yu, J. (2020). The role of MRI in the diagnosis and treatment of gastric cancer. *Diagnostic and Interventional Radiology (Ankara, Turkey)*, *26*(3), 176–182. https://doi.org/10.5152/DIR.2019.19375

Zhao, H., Ren, D., Liu, H., & Chen, J. (2018). Comparison and discussion of the treatment

guidelines for small cell lung cancer. *Thoracic Cancer*, *9*(7), 769–774. https://doi.org/10.1111/1759-7714.12765

Zhao, Y., Khawandanh, E., Thomas, S., Zhang, S., Dunne, E. M., Liu, M., & Schellenberg, D. (2020). Outcomes of stereotactic body radiotherapy 60 Gy in 8 fractions when prioritizing organs at risk for central and ultracentral lung tumors. *Radiation Oncology*, *15*(1), 1–13. https://doi.org/10.1186/S13014-020-01491-W/TABLES/3

Zheng, X., Schipper, M., Kidwell, K., Lin, J., Reddy, R., Ren, Y., Chang, A., Lv, F., Orringer, M., & Spring Kong, F. M. (2014). Survival outcome after stereotactic body radiation therapy and surgery for stage i non-small cell lung cancer: A meta-analysis. *International Journal of Radiation Oncology Biology Physics*, *90*(3), 603–611. https://doi.org/10.1016/J.IJROBP.2014.05.055/ATTACHMENT/6CD8B4C7-55C4-4A45-B251-C89736709BE7/MMC1.DOC

Zhong, H., Adams, J., Glide-Hurst, C., Zhang, H., Li, H., & Chetty, I. (2016). Development of a deformable dosimetric phantom to verify dose accumulation algorithms for adaptive radiotherapy. *Journal of Medical Physics*, *41*(2), 106–114. https://doi.org/10.4103/0971-6203.181641

Zhou, H., Lei, P. J., & Padera, T. P. (2021). Progression of Metastasis through Lymphatic System. *Cells*, *10*(3), 1–23. https://doi.org/10.3390/CELLS10030627

Zhou, Q., & Xi, S. (2018). A review on arsenic carcinogenesis: Epidemiology, metabolism, genotoxicity and epigenetic changes. *Regulatory Toxicology and Pharmacology*, *99*, 78–88. https://doi.org/10.1016/J.YRTPH.2018.09.010

Zingde, S. M. (1993). Cancer genes. *Western Journal of Medicine*, *158*(3), 273. https://doi.org/10.1007/978-1-59259-125-1_3

APPENDICES

APPENDIX A

UNIVERSITY OF GHANA
ETHICS COMMITTEE FOR BASIC AND APPLIED SCIENCES (ECBAS)

P. O. Box LG 1195, Legon, Accra, Ghana

Ref. No: ECBAS 051/20-21

8th September, 2021.

Ms. Abigail Naa Momoede Quaye
Department of Medical Physics
University of Ghana
Legon, Accra

Dear Ms. Quaye,

ECBAS 051/20-21: CLINICAL IMPLEMENTATION OF LUNG STEREOTACTIC BODY RADIATION THERAPY (SBRT)

This is to inform you that the above referenced study has been presented to the Ethics Committee for Basic and Applied Sciences for a full board review and the following actions taken subject to the conditions and explanation provided below:

Expiry Date:	30/09/2022
On Agenda for:	Initial Submission
Date of Submission:	31/05/2021
ECBAS Action:	Approved
Reporting:	Annually

Please accept my congratulations.

Yours sincerely,

Professor Daniel Bruce Sarpong

APPENDIX B

KOMFO ANOKYE TEACHING HOSPITAL

P. O. Box 1934
Kumasi - Ghana
Tel: +233 - 3200-22301 - 4
Fax: +233 - 3220-24654 / 24621
Website: www.kathhsp.org

Our Ref. No.: *KATH IRB/AP/095/21*

Your Ref... No:.....

Komfo Anokye Teaching Hospital Institutional Review Board

23rd August 2021

Miss. Abigail Naa Momoede Quaye
School of Nuclear and Allied Sciences
Medical Physics Department,
University of Ghana,
Legon-Accra.

Dear Miss. Quaye,

Ethics Approval

Protocol title:	Clinical Implementation of Lung Stereotactic Body Radiation Therapy (SBRT)
Study site:	Oncology Directorate of the Komfo Anokye Teaching Hospital
Sponsor:	Self-funded

We write in response to your correspondence of 19th July 2021 requesting the Komfo Anokye Teaching Hospital Institutional Review Board (KATH IRB) to review the research study referenced above.

The proposed research study went through expedited review and we are pleased to inform you that KATH IRB has given approval for the following study documents:

- *Protocol version 1.0 last updated 19th July 2021*

Approval for the study is in effect until **22nd** August **2022** and it is the responsibility of the Principal Investigator to maintain the study in good standing at the Komfo Anokye Teaching Hospital. The Board anticipates to be notified of the actual start date of your project.

Prior to the expiration of the study approval, you must submit to the KATH IRB an "Application for Continuing Review" along with provision of "Annual Report" when the study is ongoing, or a "Termination Report" if the research has been completed.
You must hastily report to the KATH IRB should a modification to the research be proposed, and without delay if an unanticipated development occurs before the next required review. Regulations do not permit you to modify conduct of the study in its present form prior to ethics approval; except where urgent action is required to eliminate an apparent immediate hazard to a study subject or other person. It is of utmost importance data generated from this study must be used for the intended purpose only.

A Centre of Excellence

Page 1 of 2

Thank you.

Sincerely,

Prof. Kwabena Antwi Dansoa, BSc, MB ChB, FWACS, FGCS, FACOG
Chairman, KATH IRB

INTEGRI PROCEDAMUS